

GROUNDWATER DYNAMICS IN DEGRADING, DISCONTINUOUS PERMAFROST

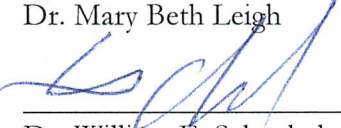
By

Michelle L. Barnes

RECOMMENDED:



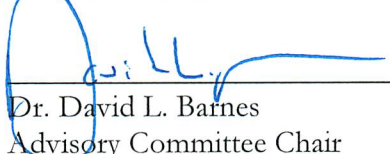
Dr. Mary Beth Leigh




Dr. William E. Schnabel



Dr. Yuri L. Shur

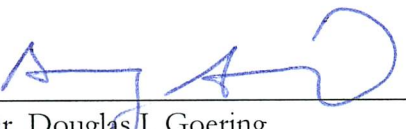


Dr. David L. Barnes
Advisory Committee Chair

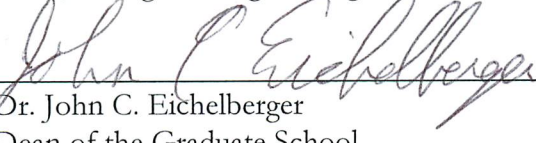


Dr. Robert A. Perkins
Chair, Department of Civil and Environmental Engineering

APPROVED:



Dr. Douglas J. Goering
Dean, College of Engineering and Mines



Dr. John C. Eichelberger
Dean of the Graduate School



Date

GROUNDWATER DYNAMICS IN DEGRADING, DISCONTINUOUS PERMAFROST

A
THESIS

Presented to the Faculty
of the University of Alaska Fairbanks

in Partial Fulfillment of the Requirements
for the Degree of

MASTER OF SCIENCE

By

Michelle L. Barnes, B.S.

Fairbanks, Alaska

December 2014

ABSTRACT

In regions impacted by permafrost, discontinuities are areas of possible connection between the supra- and sub-permafrost portions of an aquifer. Permafrost discontinuities influence the transport of contaminants in an aquifer, necessitating delineation of these discontinuities and their influence on groundwater flow. Means of identifying the locations of permafrost discontinuities have previously been limited to geophysical methods and the evaluation of well logs. In this study we use groundwater elevation trends and environmental tracers (e.g., stable isotopes and temperature) to evaluate the dynamics in a sulfolane-contaminated aquifer located in a region of discontinuous permafrost in the Interior of Alaska. Using tracers to identify areas of discontinuities in the permafrost should help us locate thawed through-taliks and may also improve our understanding of the interaction between the supra- and sub-permafrost groundwater in discontinuous permafrost. With this approach we identified at least three discontinuities within the study area. The locations of these discontinuities coincide with transport of the contaminant found in this aquifer. The primary source of recharge for this aquifer is the Tanana River, a major tributary to the Yukon River. The source of water for the Tanana River is glacial melt in the summer and groundwater during the winter. Through the isotopic composition of the supra-permafrost groundwater we show the occurrence of additional recharge to the supra-permafrost groundwater from sub-permafrost groundwater and precipitation. Understanding these dynamics is paramount to characterizing the contaminant transport in permafrost impacted aquifers.

TABLE OF CONTENTS

	Page
Signature Page	i
Title Page.....	iii
Abstract	v
Table of Contents	vii
List of Figures.....	xi
List of Tables	xiii
List of Appendices	xv
Acknowledgments.....	xvii
1 Introduction.....	1
1.1 Thesis Objectives	4
2 Site Description.....	7
2.1.1 Sulfolane Contamination	7
2.1.1.1 Contaminant Characteristics	7
2.1.1.2 Groundwater Contamination.....	7
2.1.2 Climate, Land Use and Land Cover.....	10
2.1.3 Geology and Permafrost.....	10
2.1.4 Hydrology.....	13
2.1.4.1 Aquifer Recharge and Properties	14
2.1.4.2 Tanana River	15
2.1.4.3 Chena River	16

2.1.4.4	Moose Creek Dam.....	17
2.1.4.5	Sloughs.....	17
2.1.4.6	C-ditch and Gravel Pits.....	17
3	Natural Tracers and Trends in Groundwater Elevations.....	19
3.1	Groundwater Elevations.....	19
3.2	Groundwater Temperatures.....	20
3.3	Stable Isotopes.....	21
4	Methods.....	23
4.1	Data Collection.....	23
4.1.1	Groundwater Elevations.....	23
4.1.2	Groundwater Temperatures.....	23
4.1.3	Stable Isotopes.....	25
4.2	Data Analysis Procedure.....	27
4.2.1	Groundwater Elevation Trends.....	27
4.2.2	Groundwater Temperature Profile Trends.....	28
4.2.3	Stable Isotope Classifications.....	29
5	Results.....	31
5.1	Groundwater Elevation Trends.....	31
5.2	Groundwater Temperature Profile Trends.....	34
5.3	Stable Isotope Classifications and Trends.....	37
5.3.1	Monitoring well.....	37
5.3.2	Private Sub-permafrost Wells.....	40

5.4	Combined Spatial Analysis.....	43
6	Discussion.....	45
6.1	Indicators of Discontinuities	45
6.2	Locations of Discontinuities.....	46
6.3	Ground Penetrating Radar.....	49
6.4	Differences in Isotopic Signatures.....	50
6.5	Improved Understanding of Aquifer Dynamics.....	52
6.5.1	Spring 2013	53
6.5.2	Late Summer 2013.....	53
6.5.3	Fall 2013	54
6.5.4	Supra-permafrost Groundwater Recharge	54
6.6	Contaminant Transport.....	55
6.7	Other Applications.....	57
6.8	Groundwater Temperature Profiles Used for Indicators of Taliks	58
6.9	Future Work.....	59
7	Conclusion.....	61
	References.....	63
	Appendix.....	69

LIST OF FIGURES

	Page
Figure 1. Conceptual model of groundwater movement in permafrost discontinuities.	3
Figure 2. Monitoring well network for characterizing and monitoring groundwater contamination. ..	9
Figure 3. Depth to permafrost from monitoring well drill logs.....	12
Figure 4. Surface water features relevant to the study area.....	13
Figure 5. Tanana River stage for 2011 through 2013 (USGS, 2014a).....	16
Figure 6. Approximate surface water sample locations for the summer of 2013.....	26
Figure 7. Comparison of MW-326-20 (SWI, 2013) to the Tanana River stage (USGS, 2014a).....	28
Figure 8. Groundwater elevations grouped by similarities between monitoring wells.....	32
Figure 9. Groundwater elevation trend classifications represented spatially.	33
Figure 10. Examples of groundwater temperature profiles.....	34
Figure 11. Groundwater temperature profile trends represent spatial similarities.	36
Figure 12. Groundwater stable isotope classifications and trends for three 2013 sampling events. ...	38
Figure 13. Groundwater stable isotope classifications represented spatially.	39
Figure 14. Groundwater isotopic composition for private sub-permafrost wells.....	42
Figure 15. Increasing-temperatures-with-depth and associated stable isotope classifications.	44
Figure 16. Monitoring wells that exhibit characteristics of discontinuities.	48
Figure F-1. Time series of groundwater temperatures at the water table.....	85
Figure F-2. Groundwater temperature contours at the water table recorded by data loggers	86
Figure H-1. Groundwater isotopic composition relative to screen-depth.	90
Figure H-2. Groundwater isotopic composition relative to groundwater temperature.	91
Figure H-3. Groundwater isotopic composition for all four monitoring well sampling periods.	92
Figure H-4. Groundwater stable isotope trends for all four monitoring well sampling periods.	93

Figure H-5. Groundwater isotopic composition represented spatially for all for sampling events.....94

Figure I-1. Stable isotope trends for the extended study area, at and below the water table.95

Figure I-2. Temperature profiles for the extended study area.96

LIST OF TABLES

	Page
Table 1. Classification units of permafrost depths and general locations within the study area.....	11
Table 2. Summary of groundwater samples collected for study.	25
Table 3. Summary of surface water samples collected for stable isotope analysis.	26
Table 4. Stable isotope classifications for purpose of this study.	29
Table 5. Figure legend for Figure 12.....	37
Table B-1. Monitoring wells with HOBO U20 Water Level Data Loggers.....	73
Table B-2. Wells with HOBO TidbiT v2 Temperature Data Loggers	73
Table C-1. Comparison of temperature measurement accuracy and resolution from user manuals. .	75
Table D-1. TC/EA conditions.	78
Table E-1. Summary of monitoring well samples collected for stable isotope analysis.	79
Table E-2. Summary of private subpermafrost well samples collected for stable isotope analysis.	83
Table G-1. Stable isotope data for the Tanana and Chena Rivers and the Chena Slough.....	87

LIST OF APPENDICES

Appendix A. Sulfolane concentration maps.69

Appendix B. List of monitoring wells with data loggers.....73

Appendix C. Comparison of data logger temperature accuracy and resolution.....75

Appendix D. Stable isotope laboratory procedure and collection procedure.....77

Appendix E. Sample logs for stable isotopes.79

Appendix F. Groundwater temperatures at the water table.85

Appendix G. Summary of surface water stable isotopic composition.....87

Appendix H. Supplemental stable isotope plots.89

Appendix I. Extended study area figures for temperature profiles and stable isotopes.....95

ACKNOWLEDGMENTS

I was fortunate that my graduate research was part of a current event that directly impacts lives in the community and incorporated collaboration between state regulatory agency, private industry, and multiple university departments. I had opportunity to witness how all the moving parts smoothly progress when different entities work together and how things stop during conflict. This project gave me motivation to complete my research and fueled my enthusiasm.

Each of my four committee members also contributed to my academic and professional growth as well as to the writing process. The work completed as part of my master's thesis was made possible by guidance and support from my advisor, Dr. David Barnes. I am grateful for the many hours spent answering questions, interpreting results, and discussing the implications. The writing course taught by Dr. Bill Schnabel provided me the opportunity to draft my thesis and get valuable feedback through the review process. Dr. Mary Beth Leigh's interest and ability to ask questions and request further explanation helped me gain confidence in my results as I learned to better explain them. The permafrost expertise provided by Dr. Yuri Shur was invaluable for this investigation of a permafrost-impacted aquifer.

The work completed for this thesis was made possible by the collaboration and work of others. I would like to thank the State of Alaska, Department of Environmental Conservation, Contaminated Sites Program (DEC) and their consultants ERM Group, Inc. (ERM). DEC staff, Ann Farris and Tamara Cardona, deserves acknowledgment for all their hard work as Project Managers. I truly admire their dedication to ensuring the health and welfare of the public. I appreciate the support and interest throughout my research. I am also grateful for funding provided by the DEC to complete the research presented in this thesis. ERM staff provided valuable feedback in interpretation of

results. ERM field crews were also responsible for collecting the surface water samples for stable isotope analysis.

I would additionally like to thank Flint Hills Resources and their consultants Arcadis, Barr Engineering, Geomega, and Shannon and Wilson, Inc. I am especially grateful for the approval from Flint Hills Resources that allowed me to work directly with staff from Shannon and Wilson, Inc., on many fronts. More specifically, Kristen Freiburger, for scheduling fieldwork to accommodate our sample requests; the field crews, for collecting hundreds of water samples for stable isotope analysis; and Shandra Miller and Andrew Frick, for their patience and assistance in the field while deploying and downloading data loggers.

As much as I loved graduate school, it was a struggle; but I survived because of the support from my family and friends as well as from numerous Thai food and ice cream breaks.

1 INTRODUCTION

Maintenance of drinking water sources is always a concern, one that is especially important in arctic and subarctic regions, where groundwater is a primary drinking water source. With so many people relying on this water supply, maintaining groundwater resources is crucial. Even if communities use surface water as their primary drinking water source, the groundwater contribution to the surface water source during winter months is likely significant. Water quality, storage and capacity, and longevity of the aquifer are all parameters that need to be considered for maintenance or development of a groundwater source. Groundwater contamination and climate change are important parameters that can negatively influence water resource maintenance.

The implications of groundwater contamination are obvious, however the impacts of climate change are not so intuitive. Increased air temperatures in the arctic and subarctic (Hinzman, Bettez, et al., 2005) have stimulated recession of glaciers and degradation of permafrost (Osterkamp and Romanovsky, 1999; Jorgenson et al., 2001; Hinzman, Jones, et al., 2005; Jorgenson et al., 2006; Osterkamp, 2007; Shur and Jorgenson, 2007). The implications of retreating glaciers and degrading permafrost have spurred numerous studies on arctic and subarctic water resources (Rouse et al., 1997; Jorgenson et al., 2001; Prowse et al., 2006; Osterkamp et al., 2009; Evengard, et al., 2011; Green et al., 2011; Haldorsen et al., 2011; Muskett and Romanovsky, 2011). Interactions between sub-permafrost groundwater and surface water have become increasingly important (Williams and van Everdingen, 1973; Callegary et al., 2013), especially with regard to changes in those interactions due to degrading permafrost (Kane and Slaughter, 1973; Yoshikawa and Hinzman, 2003; Hinzman, Jones, et al., 2005; Walvoord and Striegl, 2007; Roach et al., 2011). Glacial recession will change the contribution of meltwater into stream systems (Wada et al., 2011). While groundwater has always been a component in climate-related studies, few of these studies have evaluated groundwater dynamics (Yoshikawa and Hinzman, 2003; Woo et al., 2008; Bense et al., 2009; Walvoord et al.,

2012). A greater understanding of how climate change affects water resources may be gained by looking at groundwater dynamics and seasonality of aquifers to infer source contributions throughout the year and extrapolate how these contributions will change with continued climate change.

Groundwater flow regimes are complex in discontinuous permafrost aquifers as the result of heterogeneous permafrost distribution and the presence of “through-taliks”. Through-taliks (referred to as discontinuities in later sections) are areas of thawed permafrost that form under various conditions (French, 2007; Wellman et al., 2013). One way that through-taliks can form is under large lakes and rivers due to the hydrothermal properties of water. In discontinuous permafrost aquifers a connection exists between the groundwater below the permafrost layer (sub-permafrost groundwater) and the groundwater above the permafrost layer (supra-permafrost groundwater) by means of through-taliks. The presence of these discontinuities or permafrost controls subarctic hydrology (Bolton, 2006).

Discontinuities can influence groundwater flow in two ways. First, supra-permafrost groundwater can flow downward into the sub-permafrost portion of the aquifer (Figure 1a). Movement of the supra-permafrost groundwater can occur from downward trending flow, a result of either a pressure head such as river stage or density driven flow. Downward flow is likely to occur where lateral groundwater movement through an area of discontinuous permafrost intersects a permafrost mass. Second, sub-permafrost groundwater can flow upward through discontinuities due to pressure gradients (Figure 1b). These pressure-gradients originate from either recharge of the sub-permafrost groundwater at elevations greater than that of the discontinuity or when groundwater is forced to flow beneath the permafrost (Figure 1a). Groundwater introduced into the sub-permafrost portion of the aquifer by either of these mechanisms is under confining pressure, similar to a confined

aquifer. Once the sub-permafrost groundwater reaches a down-gradient talik, the flow is directed upward through the talik caused by the pressure differential. Due to upward flow, the hydraulic head in regions of discontinuities is generally greater than the hydraulic head of the surrounding area. The difference in hydraulic head can develop a localized gradient that differs from the regional gradient, redirecting the flow.

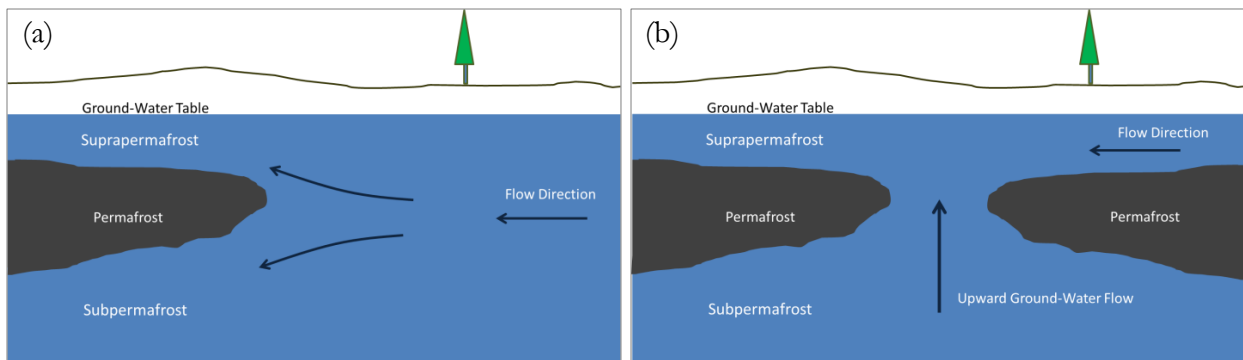


Figure 1. Conceptual model of groundwater movement in permafrost discontinuities.

Knowledge of groundwater dynamics in permafrost regions comes from contaminant transport studies (Deprez et al., 1999; Hinzman, Johnson, et al., 2000; Iwakun et al., 2008; Carlson and Barnes, 2011). From these studies the complex flow path of groundwater becomes at least partially evident by treating the contaminant as a non-conservative tracer. However, the investigations of groundwater flow paths conducted by Deprez et al. (1999), Hinzman, Johnson, et al. (2000), Iwakun et al. (2008), and Carlson and Barnes (2011) required extensive monitoring well network systems, which in most cases are not possible.

Groundwater contamination in permafrost regions is inevitable with natural resource development (e.g., mineral and oil extraction, processing, and transport activities) and other industrial and human activities. Predicting contaminant transport in permafrost aquifers is complex and requires a thorough understanding of aquifer dynamics. Hinzman, Johnson, et al. (2000) first found that permafrost can cause channelization of contaminated groundwater, which was further supported by

Carlson and Barnes (2011). While delineating contaminant distributions in continuous permafrost regions are complex, these challenges are more complicated in regions of discontinuous permafrost. Carlson and Barnes (2011) found that upward flow of sub-permafrost water through discontinuities can redirect contaminate plumes. Discontinuities serve as contaminant transport pathways, allowing contaminated groundwater to migrate into uncontaminated portions of the aquifer. However, there is a lack of understanding in regards to the interaction between the supra- and sub-permafrost groundwater.

Dissolved-phase plumes in the Interior of Alaska are ideal for studying groundwater dynamics in degrading, discontinuous permafrost. At a large contaminated site in Interior Alaska, others have extensively characterized the distribution of sulfolane concentrations (Barr, 2012). This contaminant plume was unique in many ways related to the presence of permafrost discontinuous. Most importantly to this study, the plume appeared to have a unique configuration, suggesting that the mechanisms discussed previously were influencing the transport of contaminant. Furthermore, the large, braided river that bounds one edge of the plume is a source of aquifer recharge. The slough that bounds the other edge was initially believed to be a sink for supra-permafrost groundwater; however, the contaminant concentrations were non-detect in the area of the slough suggesting a different flow scenario. Finally, contamination was detected in the sub-permafrost groundwater indicating that there was a yet to be discovered pathway for the contaminant to migrate below permafrost.

1.1 Thesis Objectives

The primary goal of the work presented in this thesis was to use groundwater characteristics to qualitatively evaluate the dynamics of contaminated groundwater in degrading, discontinuous permafrost. Selected physical (i.e., groundwater temperatures and groundwater elevations) and

chemical (i.e., stable isotopes) groundwater characteristics were evaluated for spatial and temporal trends to better understand groundwater dynamics. The discussion focuses on the influence of groundwater dynamics in relation to: (1) identification of locations of discontinuities, (2) dynamics at locations of discontinuities, and (3) seasonality of the aquifer. The findings of this thesis further our understanding of groundwater dynamics in degrading, discontinuous permafrost aquifers as well as aid regulators in decision-making processes related to groundwater contamination.

2 SITE DESCRIPTION

2.1.1 Sulfolane Contamination

2.1.1.1 Contaminant Characteristics

Sulfolane is used as an industrial solvent in both natural gas and oil refinery processes. Sulfolane is a slightly polar, highly water-soluble compound with very low sorption. The physical and chemical characteristics of sulfolane allow it to act as a conservative tracer, identifying groundwater movement and/or flow paths within the aquifer. Currently, there are only a few studied sulfolane-contaminated sites in the world. At this time, the long-term health effects of sulfolane are unknown, but they are being studied more as sulfolane is considered an emerging contaminant.

2.1.1.2 Groundwater Contamination

At the North Pole Refinery, sulfolane is used in the liquid-liquid extraction process (Geomega, 2013). Potential sources of sulfolane leaks were investigated when sulfolane was first found beyond the boundaries of the North Pole Refinery in 2009. Since then, sulfolane has been detected in over 300 private drinking-water wells, with concentrations ranging from 3.2 µg/L to greater than 500 µg/L (Arcadis, 2013). An extensive monitoring network (Figure 2) was developed for the sampling and data collection necessary for characterizing and monitoring the sulfolane plume. Monitoring-well concentrations off of the refinery property range from less than 6.2 µg/L to more than 200 µg/L (Arcadis, 2013). Concentrations of sulfolane on the refinery property are as high as 6,520 µg/L (Arcadis, 2013).

The sulfolane plume has many unique characteristics that indicate the influence of permafrost on contaminant transport. Maps of the sulfolane plume are included in Appendix A (Arcadis, 2014; DEC, 2014). The lateral extent of the supra-permafrost plume is approximately 2.5 miles wide by 3 miles long. The aspect ratio (length : width) of the lateral extent is approaching unity (~1:1). The

vertical extent of the sub-permafrost plume is up to 305 feet below ground surface (bgs). Sulfolane detected throughout the supra- and sub-permafrost groundwater indicates migration of contaminated groundwater into the sub-permafrost groundwater through a discontinuity.

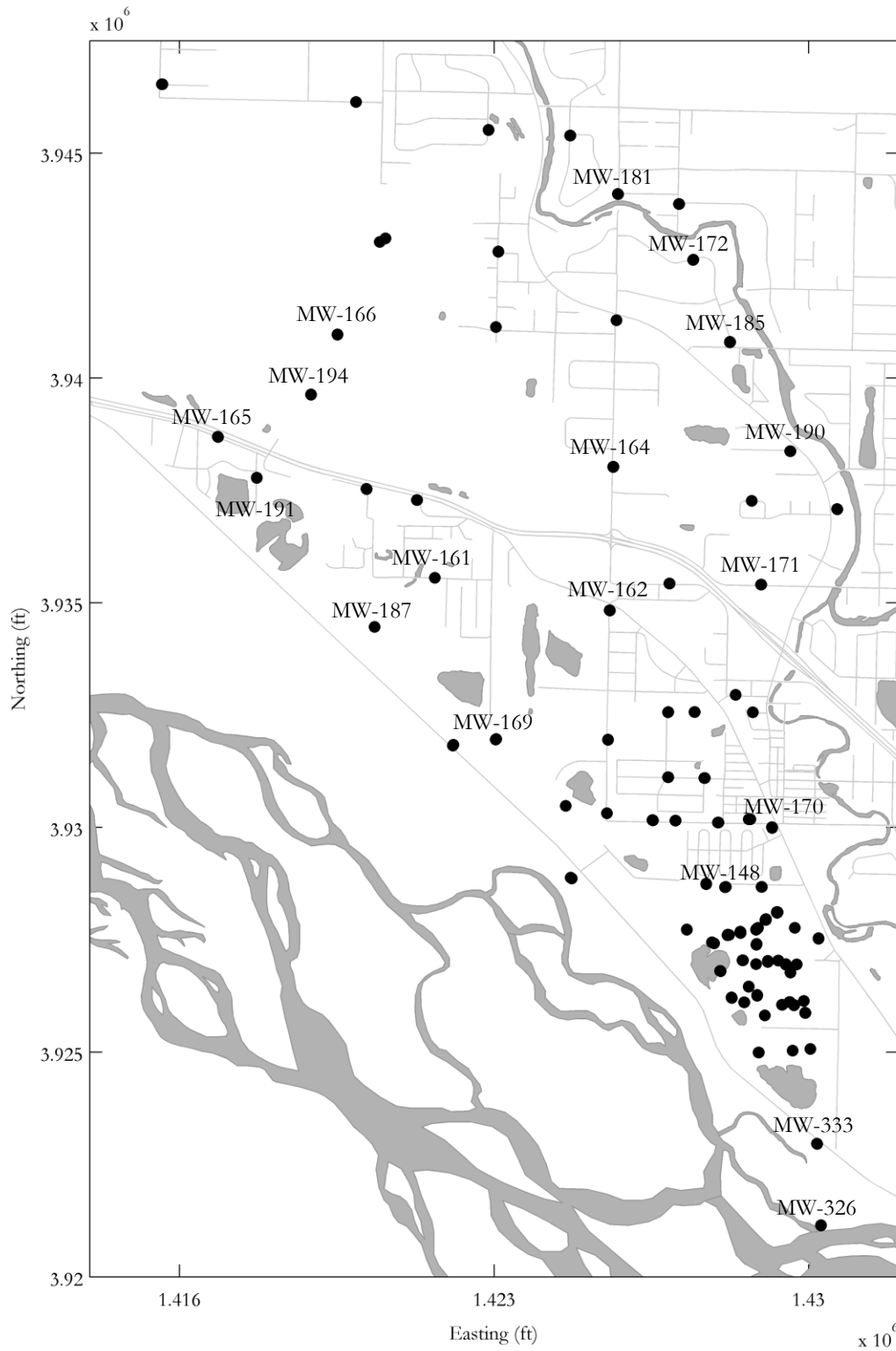


Figure 2. Monitoring well network for characterizing and monitoring groundwater contamination. Additional monitoring wells exist beyond the study area boundaries.

2.1.2 Climate, Land Use and Land Cover

The study area is situated in the Tanana River floodplain in Interior Alaska. The approximate elevation of the study area is 480 feet above mean sea level (amsl). Consistent with a continental climate, the area has large daily and annual temperature ranges, low humidity and relatively light and irregular precipitation (Alaska Climate Research Center, 2014).

The study area is a rural to urban area, where developed land is used for residential or light commercial applications. Large areas of undeveloped land have vegetation consistent with that of boreal forest floodplains of Interior Alaska. The dominant tree species are typically black spruce (*Picea mariana*) and aspen (*Populus tremuloides*) (Anderson, 1970; Chapin et al., 2006). Shrubs such as alders (e.g., *Alnus incana*) and willow (e.g., *Salix alaxensis*) are expected in floodplains near streams and river (Boggs et al, 2012). The bogs and fens within the floodplains are typically more diverse than adjacent forested regions (Chapin et al., 2006).

2.1.3 Geology and Permafrost

The study area is classified as discontinuous permafrost (Ferrians, 1965), which is defined as lowland areas generally underlain by numerous isolated permafrost masses (Anderson, 1970). The geology is classified as flood-plain alluvium with low ice content and well-stratified to lenticular silt, sand, and gravel (Anderson, 1970). Péwé et al. (1976) classified the majority of North Pole as “Chena Alluvium, well-stratified layers and lenses of unconsolidated sand rounded river gravel overlain by as much as 15 feet of gray silt.” In the region classified as Chena Alluvium, permafrost thickness can range between 5 and 275 feet with discontinuities occurring in many areas, especially under lakes and rivers and creeks (Péwé and Bell, 1975a). Private sub-permafrost well logs indicate that the thickness of permafrost varies from approximately 50 to 100 feet (Arcadis, 2012). Strings of swale and slough deposits consisting of “poorly stratified lenses and layers of unconsolidated stream-laid silt and silty

sand” (Péwé et al., 1976) are distributed throughout the study area. Young swale and slough deposits with intermittent streams generally have no underlying permafrost (Péwé and Bell, 1975a).

For the purpose of this thesis, depth to permafrost was separated into three classification units: shallow, mid-range, and deep. Data from available drill logs provide the basis for this classification summarized in Table 1. Figure 3 shows the depth to permafrost information obtained from monitoring well drill logs. Depth to permafrost is greatest in the southern region and along the Chena Slough. Depth to permafrost decreases to shallow and mid-range away from these areas.

Table 1. Classification units of permafrost depths and general locations within the study area.

Classification	Depth to Permafrost	General Locations
Shallow Permafrost	Less than 60 feet bgs	Central and Northwest Regions
Mid-range Permafrost	60 – 100 feet bgs	Central and Northwest Regions
Deep Permafrost	Greater than 100 feet bgs	Southern Region & along Chena Slough

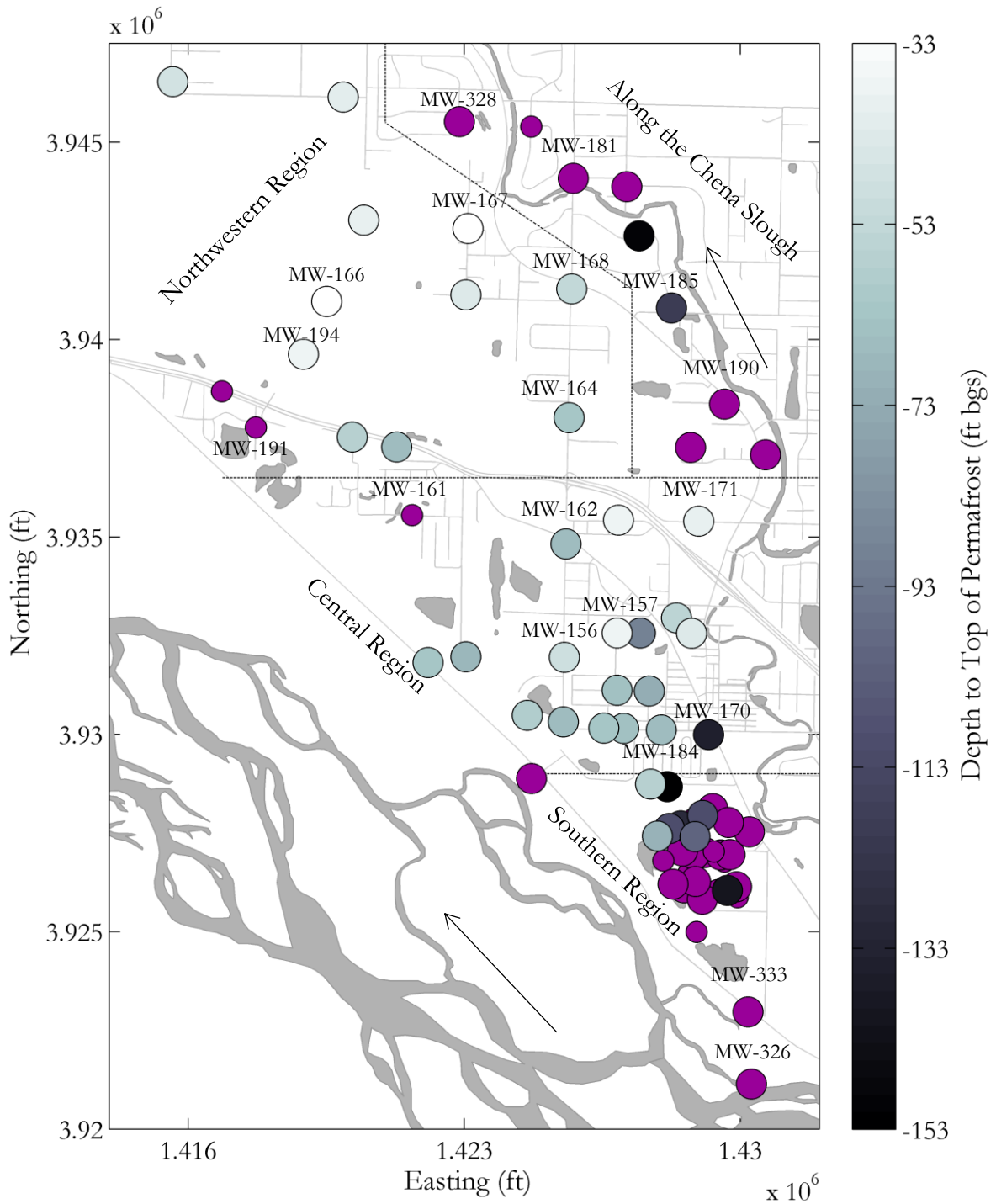


Figure 3. Depth to permafrost from monitoring well drill logs. Gray scale circles identify where permafrost was found; large maroon circles indicate where permafrost was not found at a depths greater than 100 feet bgs; small maroon circles indicate where permafrost was not found at a depth of 60–100 feet bgs.

2.1.4 Hydrology

Surface water interaction with groundwater is a controlling factor in the flow of supra-permafrost groundwater and at least the upper portion of the sub-permafrost groundwater. A number of water bodies exist within and around the study area (Figure 4). The two largest surface water features are the Tanana and Chena Rivers. The study area has sloughs and gravel pits of varying size distributed throughout. The Moose Creek Dam and associated spillway are other notable water-related features. A number of dikes and levees are also present.

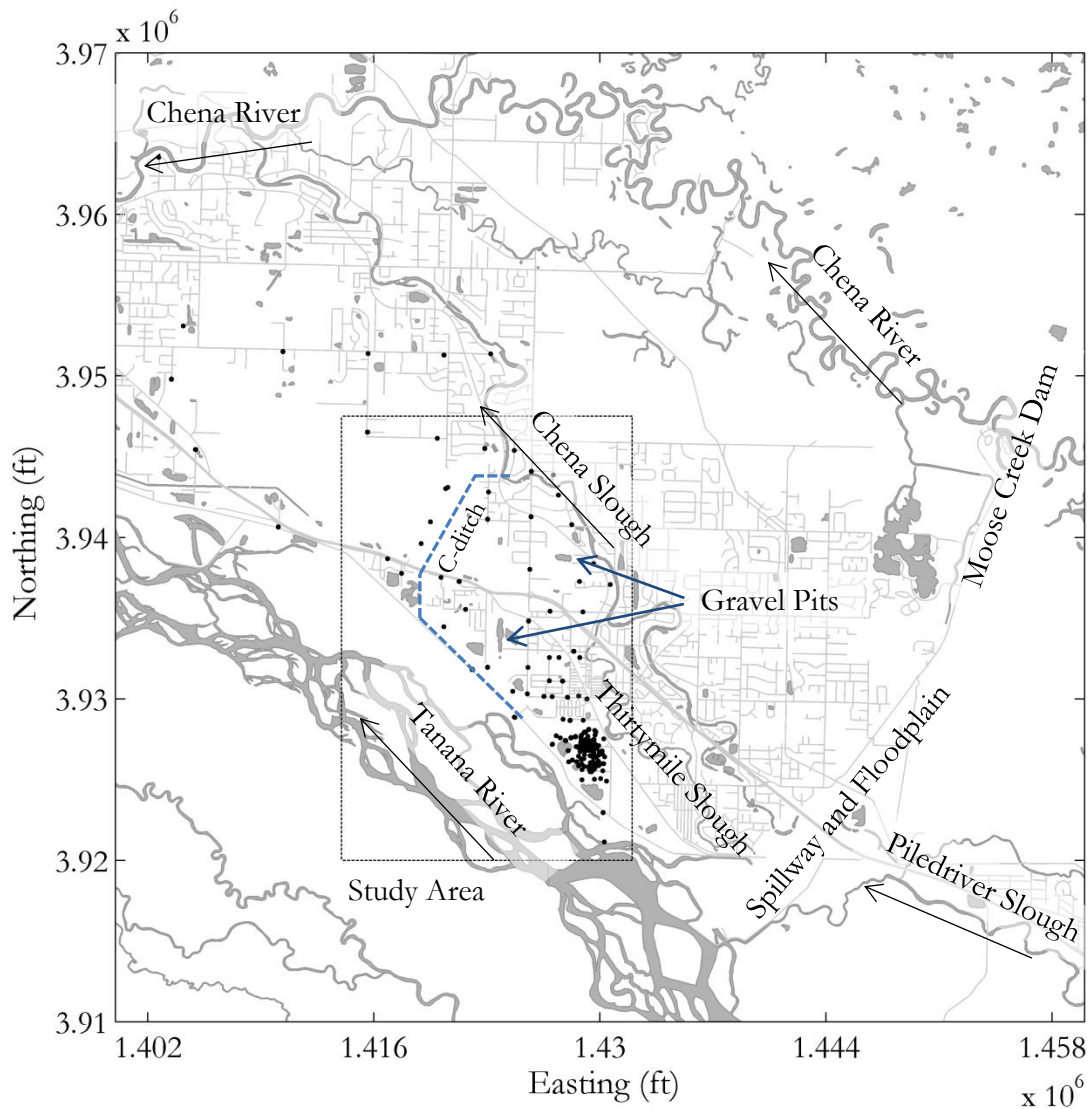


Figure 4. Surface water features relevant to the study area.
Black circles identify monitoring wells.

2.1.4.1 Aquifer Recharge and Properties

Recharge for the alluvial-plain aquifer comes from both the Tanana and Chena Rivers (Glass et al., 1970) depending on river elevation. The majority of recharge of the aquifer supra-permafrost aquifer and at least the upper portion of the sub-permafrost aquifer in the study area is from the Tanana River. The Chena River acts as a sink for groundwater during the majority of the year (Hinzman, Wegner, et al., 2000). Heavy precipitation may result groundwater recharge from the Chena River for short periods of time, resulting in groundwater generally moving northwest from the Tanana River to the Chena River (Glass et al., 1996; Arcadis, 2013).

It is unclear if the recharge of the deep portion of the aquifer comes from the Tanana or if recharge for this portion of the aquifer originates at higher elevations such as the Alaska Range. Sub-permafrost groundwater can also flow into the supra-permafrost portion of the aquifer through taliks. This flow pattern occurs when confined sub-permafrost groundwater, with a static-pressure-head above ground surface, moves upward (Williams, 1970) through a discontinuity between the unconfined supra-permafrost groundwater (Glass et al., 1996). Similarly, groundwater from upper portions of the aquifer can flow into the sub-permafrost portion of the aquifer as previously discussed and illustrated in Figure 1.

Yielding between 1,000 and 3,000 gallons per minute (Anderson, 1970) due to supra-permafrost groundwater recharge and transmissive properties, the aquifer in this region is favorable for development of large groundwater supplies. Both discontinuities and the sub-permafrost portion of the aquifer have an enormous capacity to store water (Williams, 1970). Groundwater has the potential to move quickly through the alluvial aquifer, attributable to the aquifer being generally composed of highly transmissive materials (Glass et al., 1996). Reported transmissivity of the alluvium was in the hundreds of thousands of gallons per foot per day (Williams, 1970). The rapid

advective transport rate of contaminants in this aquifer is due to the high storage capacity and transmissive properties of the aquifer.

2.1.4.2 Tanana River

The Tanana River, a major tributary of the Yukon River, is a large braided river that borders the study area along the southeastern side. The river has a mean annual discharge of 20,200 cubic feet per second (cfs) (Glass et al., 1996) or 44,000 cfs with a drainage area of approximately 44,300 square miles (Kraemer and Brabets, 2012). The United States Geological Survey (USGS) reports drainage area at Nenana, Alaska to be 25,600 square miles. The Tanana River generally has four annual phases: (1) winter base flow, (2) spring breakup, (3) summer, and (4) fall recession (Figure 5). Glacially fed rivers like the Tanana (Wooller et al., 2012; Kraemer and Brabets, 2012) have hydrographs different from those of non-glacial rivers, like the Chena River. Non-glacial rivers have an initial peak after snow melt and begin to recede, with occasional peaks occurring during rain events; whereas glacial rivers increase after snowmelt and breakup and maintain a high water level up to the onset of freezing temperatures due to glacial melt (Hinzman et al., 2006). Two meltwater events occur each year. One is in early summer when the local snowpack and ice melt. The other is later in the summer, when glacial meltwater contributes. Glacial meltwater and other runoff originate from the Alaska Range (Anderson, 1970). Winter base flow originates from deep, lower-altitude Tanana valley alluvium water (Kraemer and Brabets, 2012). Sub-permafrost groundwater originating from the Alaska Range is another likely base flow source; evidence suggesting this was discussed by Racine and Walters (1994) in relation to groundwater upwelling in the Tanana Flats. Groundwater contribution accounts for approximately a quarter of the annual flow (Brabets and Walwood, 2009).

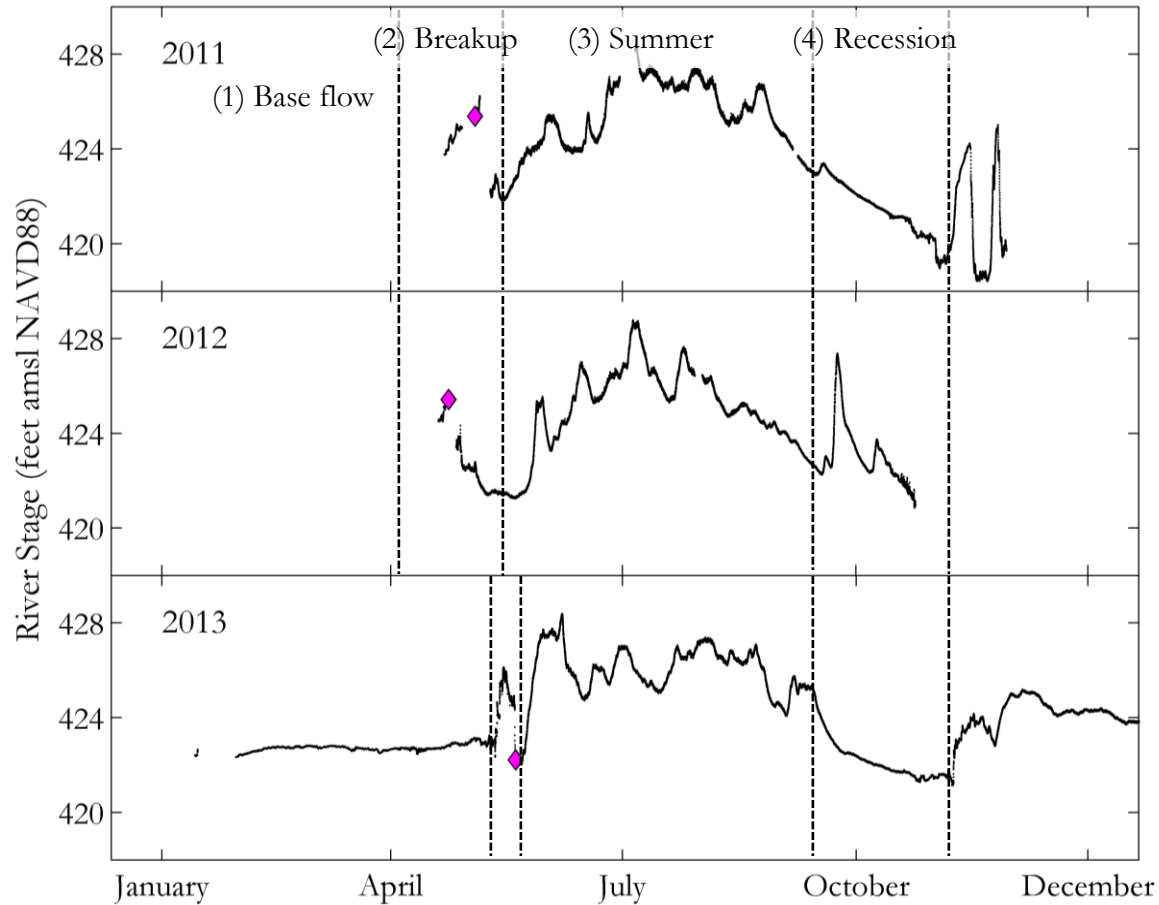


Figure 5. Tanana River stage for 2011 through 2013 (USGS, 2014a).
Magenta diamond – Tanana River break up at Nenana (Nenana Ice Classic, 2014).

2.1.4.3 Chena River

The Chena River, a non-glacial tributary of the Tanana River, is located approximately 7 miles north of the study area. The Chena River flows almost parallel to the Tanana until the two converge approximately 17 miles downstream of the study area. Moose Creek Dam (described subsequently) regulates the flow of the Chena River. Mean annual discharge of the Chena River is 972 cfs (Glass et al., 1996) with a basin area of 1,995 square miles (USGS, 2014b). Snowmelt contributes to spring discharge; during the summer, rain and evaporative influences are the dominating components (Douglas et al., 2014; Wooller et al., 2012).

2.1.4.4 Moose Creek Dam

The US Army Corps of Engineers built Moose Creek Dam in 1979 to prevent the flooding of downtown Fairbanks. During periods of high flow on the Chena River, water builds up behind the dam reducing flow in the reach that passes through North Pole and Fairbanks. The accumulated water is released into the Tanana River by a spillway. Water that builds up behind the dam influences regional groundwater flow by creating a pressure head upgradient of North Pole. Resulting in rising groundwater levels which is evidenced by flooded basements and poorly draining septic leach fields directly downgradient of the dam.

2.1.4.5 Sloughs

Chena Slough and Thirtymile Slough are within the study area; Piledriver Slough is outside the study area. Almost parallel to the Tanana River, Chena Slough borders the northeastern portion of the study area and ends at the Chena River. Prior to 1979, the Chena Slough and Piledriver Slough connected the Tanana and Chena Rivers. However, all connections were severed by development of the Moose Creek Dam and floodway. Prior to construction of the Moose Creek Dam, the Chena Slough had greater flow capacity. Now groundwater maintains it. The length of Chena Slough is approximately 10 miles in a northwest direction. Thirtymile Slough is a smaller slough that converges with Chena Slough (near MW-171), and little to no data is available regarding it. Surface streams like these probably had alternating gaining and losing reaches due to the proximity of the water table (Anderson, 1970).

2.1.4.6 C-ditch and Gravel Pits

Other notable surface water features in the study area are several gravel pits and the C-ditch (Channel C). Gravel pits of varying size are distributed throughout the study area. Groundwater fills these pits that result from gravel excavation. Groundwater flowing into gravel pits subsequently re-

enters the aquifer down-gradient of the entry point, hence gravel pits do not have a major impact on groundwater flow unless they are receiving surface water from runoff or snowmelt that increases the water level in the pit over that of the adjacent groundwater. In addition, reduction of the water surface elevation in a gravel pit by pumping or by evaporation would cause radial flow of groundwater toward the gravel pit influencing the groundwater gradient in the area of the pit.

The C-ditch originates along the Tanana River levee and converges with Chena Slough (Figure 4). Information regarding the C-ditch is limited; but it is likely that, similar to sloughs, C-ditch is groundwater fed. The C-ditch is not in any of the thesis figures since it was not included in the Fairbanks North Star Borough (FNSB) GIS water bodies shapefile.

3 NATURAL TRACERS AND TRENDS IN GROUNDWATER ELEVATIONS

Groundwater scientists commonly use natural tracers and trends in water elevations in groundwater studies to delineate different recharge zones, help interpret flow paths, sources, and quantify recharge. This chapter discusses the principles of using groundwater elevations and two common tracers, stable isotopes (^2H and ^{18}O) and groundwater temperature, in groundwater studies. This chapter also discusses the use of these tracers to identify discontinuities in permafrost. The work presented in this thesis represents the first time a difference in stable isotopes concentrations has been identified between the supra- and sub-permafrost groundwater. It is also the first time this difference has been used to identify areas of interaction between these two portions of the aquifer.

3.1 Groundwater Elevations

Hydraulic head (expressed as groundwater elevation) is necessary for determining groundwater flow direction. Flow directions are complex in discontinuous permafrost aquifers. Often groundwater flow direction will be upward or downward through discontinuities in permafrost, as previously described. Sub-permafrost water moving upward through discontinuities cause increases in pressure head and related changes in supra-permafrost flow direction. Hence, a comparison of groundwater elevation trends in areas of discontinuities will indicate flow of sub-permafrost groundwater into the supra-permafrost portion of the aquifer.

Groundwater elevations reflect recharge and discharge influences of precipitation, surface water or pumping, as well as influence from active layer freezing. Trends in groundwater elevations were used in this study to identify spatial similarities between monitoring wells. Connection between groundwater and surface water features will be apparent in similarities between groundwater levels to river stage. Vertical movement can be calculated using groundwater elevations at numerous depths (Abriola and Pinder, 1982). Vertical gradients in permafrost aquifers indicate upward or

downward flow through a discontinuity. Using vertical gradients, Kane and Slaughter (1973) and Carlson and Barnes (2011) determined upward flow from the sub-permafrost.

3.2 Groundwater Temperatures

Similar to how temperatures can be used to determine groundwater – surface water interactions (Kalbus et al., 2006), groundwater temperature profiles can be used to identify discontinuities where interactions between supra- and sub-permafrost groundwater occur. In a typical aquifer (not impacted by permafrost), water temperatures increase with depth and stay seasonally constant at depth owing to the geothermal gradient as discussed by Anderson (2005). In contrast, the presence of permafrost in discontinuous permafrost aquifers will cool water temperatures to near 0°C close to the frozen soil. Hence, supra-permafrost groundwater that does not freeze will generally have decreasing or constant (close to 0°C) temperature trends with depth from the surface to the top of permafrost.

Groundwater temperature profiles consistent with the geothermal gradient indicate connection with a deep water source that is not seasonally influenced. Beneath permafrost near Fairbanks, groundwater temperatures increased with depth, which is consistent with the expected geothermal gradient, and were constant throughout the year (Williams and van Everdingen, 1973). Kane and Slaughter (1973) used increasing-temperature-with-depth, paired with piezometric data, to demonstrate a thawed zone connecting a lake to the sub-permafrost aquifer.

According to Anderson (2005) shallow groundwater in the surficial zone of any aquifer is subject to seasonal temperature fluctuations and is relatively cooler than associated deep groundwater. In permafrost regions, groundwater temperatures at the water table in areas of shallow permafrost are expected to be colder than in areas of permafrost discontinuities.

The shape of the temperature profiles and seasonal well freezing can indicate groundwater recharge or discharge. Convex upward temperature profiles indicate discharge or upward flow of warmer groundwater (Anderson, 2005), sub-permafrost water in this case. Freezing of wells in a discharge zone is prevented by heat transfer, whereas shallow wells in a recharge system freeze due to lower temperatures (Kasenow, 2001). Convex upward temperature profiles and wells that don't freeze indicate upward flow of groundwater through discontinuities. Given these groundwater temperature characteristics in permafrost impacted aquifers it seems reasonable that discontinuous and continuous permafrost areas can be mapped by distinguishing increasing and decreasing temperature profiles, respectively.

3.3 Stable Isotopes

The stable isotopes oxygen-18 (^{18}O) and deuterium (^2H or D) are naturally occurring tracers commonly used for evaluating hydrologic processes. Ratios of both ^{18}O and ^2H to a standard vary by region and are susceptible to fractionation during phase changes such as precipitation, evaporation, and freezing/melting. During precipitation, factors that influence fractionation include temperature, latitude, and elevation (Clark and Fritz, 1997). Given the different fractionation processes impacting the ratios of these two isotopes similarities (or differences) in the sources of water can be determined from isotopic composition. For example, owing to differing recharge zones, isotopic compositions of deep and shallow groundwater should differ (Clark and Fritz, 1997). Furthermore, in many cases different isotopic composition between groundwater and surface water exist.

Researchers have previously used stable isotopes in arctic and subarctic regions to investigate hydrologic processes. Turner et al. (2010) used stable isotopes to characterize the role of hydrological processes on lake water balances in Yukon Territory. Many researchers use stable isotopes to infer seasonal contributions to rivers and streams from precipitation and groundwater

sources in arctic and subarctic regions (Kraemer and Brabets, 2012; Carey et al., 2013; Douglas et al., 2013). Stable isotopes have been used to aid in the evaluation of runoff generation during summer in a discontinuous permafrost alpine catchment (Carey and Quitor, 2005; Boucher and Carey, 2010). Hayashi et al. (2004) combined the stable isotopes and hydrochemistry to understand the hydrologic function of wetlands in regions of discontinuous permafrost. Yoshikawa et al. (2013) used stable isotopes to demonstrate the occurrence of the closed-system freezing process in the Mongot Pingo in Northwestern Mongolia. For a site in the Canadian Shield, Stotler et al. (2009) used differences in isotopic composition of groundwater in and below the base of thick permafrost to develop a conceptual model. However, no published studies have been found that investigate the differences between ^{18}O and ^2H in supra- and sub permafrost groundwater.

4 METHODS

4.1 Data Collection

Groundwater monitoring well clusters throughout the study area provided locations for measurement of groundwater elevations and temperatures and collection of and stable isotope samples. These monitoring well clusters typically consisted of two or more monitoring wells at different depths. The shallowest monitoring wells were located at the water table. Depth of the deepest well of each cluster was determined once either the depth to permafrost or the maximum ability of the drilling equipment (150 feet bgs) was reached. Additional well depths were installed at depths ranging between the shallow and deep wells.

4.1.1 Groundwater Elevations

Hourly groundwater elevations were determined from a series of water level data loggers in the supra-permafrost portion of the aquifer. Appendix B provides a list of monitoring wells with installed water level data loggers (HOBO[®] U20) maintained for this study. Given that the study area was contaminated, all fieldwork was conducted with oversight from the environmental consultants. Field measured depth to water was used to validate calculated depth to water.

4.1.2 Groundwater Temperatures

Groundwater temperatures used in this study were measured in two ways: manually during quarterly groundwater sampling events and continuously by data loggers. Environmental consultants measured and reported groundwater temperatures and other geochemical parameters of purged water from each monitoring well on a quarterly basis. Quarterly reports are available at the DEC's webpage (DEC, 2014). Groundwater temperatures were measured in the field by use of a multiprobe analyzer, either YSI ProPlus or YSI 556 MPS, in a flow-through cell attached to the pump discharge line as described in the Revised Sampling and Analysis Plan (Arcadis, 2013). Various

data loggers continuously recorded groundwater temperatures. The majority of water level data loggers recorded hourly groundwater temperatures, at the water table. HOBO® TidbiT v2 Water Temperature Data Loggers (temperature loggers) were installed in ten well nests at approximate depths of the screen midpoints (Appendix B) and were programmed to record groundwater temperature every six hours. Groundwater temperatures recorded by the temperature loggers provided continuous data used to evaluate seasonal changes at depth greater than that of the water table.

Field measured temperatures were ideal for using because there was more data available. TidbiT temperature logger data were primarily used to validate field measurements. Temperatures measured by temperature loggers represent those specific to the screen mid-point depth. Field sampling protocols required purging of three well volumes until measured values were stable prior to reporting temperature. Purging the well results in sampling water surrounding the well screen at different depths and not just the water at the well screen depth. Resulting in temperature representing the average temperature from mixed groundwater at different depths. There was also concern regarding introduction of potential errors through exposure of the purge water to atmospheric conditions. When compared using a paired t-test groundwater temperatures measured manually during sampling and those measured by temperature loggers were statistically different (P-value equal to 0.01). However, for the purpose of this study, specific temperature values were not of interest since temperature profile trends were used for the analysis. A statistical comparison (paired t-test) of the temperature profile trends measured manually and by data loggers indicated that the trends were statistically comparable (P-value equal to 0.96). Hence, identification of increasing and decreasing temperature profiles with manually measured temperatures was valid. Section 4.2.2 further discusses analysis of temperature profile trends. Appendix C summarizes the accuracy and resolution of temperature measurement equipment.

4.1.3 Stable Isotopes

Groundwater and surface water samples were analyzed for the stable isotopes deuterium ($\delta^2\text{H}$) and oxygen-18 ($\delta^{18}\text{O}$). The Alaska Stable Isotope Facility (ASIF) analyzed the water samples for ^2H and ^{18}O using Pyrolysis Elemental Analysis-Isotope Ratio Mass Spectrometry (pyrolysis-EA-IRMS). The values for $\delta^2\text{H}$ and $\delta^{18}\text{O}$ were reported as the average of four replicates in per mil Vienna Standard Mean Ocean Water (‰ VSMOW). For details regarding QA/QC methods and standards, refer to ASIF procedure in Appendix D.

Environmental consultants contracted by either the State of Alaska or Flint Hills Resources (FHR) collected all surface water and groundwater samples. All water samples were collected in plastic bottles with zero headspace and sealed tightly, in accordance with sample collection procedure (Appendix D). The samples were refrigerated until analyzed by the ASIF. Groundwater from monitoring wells was collected during four different seasonal hydrologic periods (Table 2). Groundwater samples were also collected from private sub-permafrost wells for six events during the study (Table 2). For a detailed list of samples collected and dates see Appendix E.

Table 2. Summary of groundwater samples collected for study.

Monitoring wells			
Sampling Event	Dates	Total	Clusters
Early Spring 2013	Mar. – Apr.	36	14
Summer 2013	Jul. – Sep.	135	TBD
Fall 2013	Oct. – Dec.	117 ^A	TBD
Winter 2014	Jan. – Mar.	38	TBD
Private sub-permafrost wells			
Sampling Event	Dates	Sub-permafrost	Shallow Pairs
1 st Quarter 2013	Mar. 11 – Apr. 19	17	1
2 nd Quarter 2013	Jun. 4 – Jun. 27	17	2
3 rd Quarter 2013	Sep. 5 – Sep. 26	15	2
4 th Quarter 2013	Oct. 16	1	0
	Nov. 19 – Dec. 17	16	1
1 st Quarter 2014	Mar. 3 – Apr. 3	15	1
2 nd Quarter 2014	May 1, 2014	1 ^B	0

^A - Some wells were sampled twice.

^B - PW-1230 only sampled once

The isotopic composition of surface water was used as an end-member for comparison with groundwater stable isotope results. Stable isotope values for the Tanana River and Chena River are summarized in Appendix F. Surface water samples were collected from both the Tanana River and Chena Slough during the summer of 2013 (Table 3. and Figure 6).

Table 3. Summary of surface water samples collected for stable isotope analysis.

Location	Date	No. of Locations	SW per each	GW per each	Total
Chena Slough	Jun. 21, 2013	3	1	1	6
Tanana River	Aug. 30, 2013	3	3	0	9

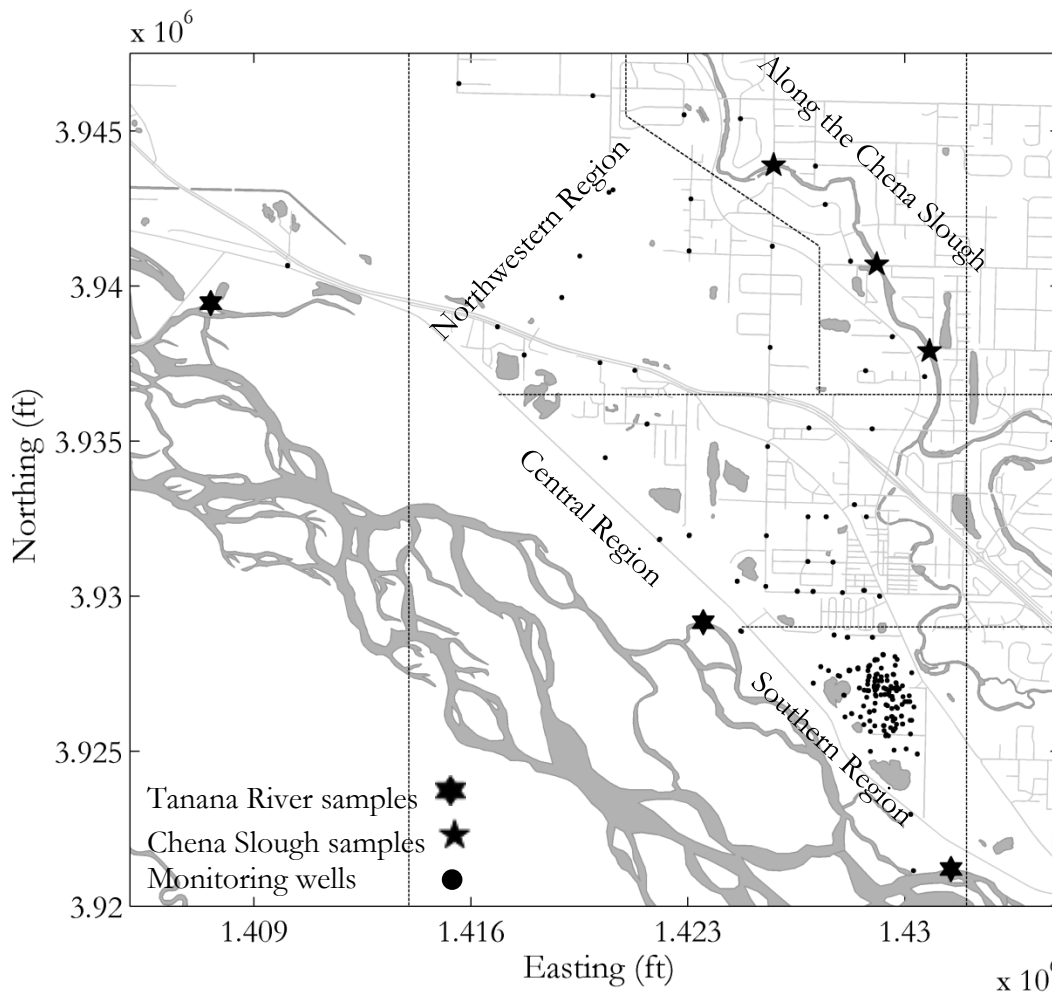


Figure 6. Approximate surface water sample locations for the summer of 2013.

4.2 Data Analysis Procedure

In an effort to identify where permafrost discontinuities occur within the study area, spatial patterns for groundwater elevation trends, temperature profiles, and stable isotopes were compiled, analyzed, and interpreted. Monitoring wells were spatially represented by marker symbols identifying each trend classification. First, spatial evaluation was completed for each parameter independently. Then, combined spatial analysis for selected trends was used to identify general areas of permafrost discontinuity. The following subsections describe trend classifications for each of three parameters.

For the purpose of discussion, the study area was divided into four regions (Figure 3). The coordinate system for the study area was Alaska State Plane 3 NAD83, Zone 3; Northings and Eastings were reported in feet. The water body and roadway shapefiles used as spatial figure backgrounds were obtained from <http://gis.co.fairbanks.ak.us>. Surface water features may vary from those shown. For instance, the gravel pit between MW-164 and MW-190 has grown, and the C-ditch near MW-166 and MW-194 was not shown.

4.2.1 Groundwater Elevation Trends

Monitoring wells were grouped based on the relative similarity between groundwater elevation trends. Groundwater elevation trends were evaluated for monitoring wells screened at the water table with water level data loggers. Groups of similar trends were developed from the comparison of groundwater elevations to the Tanana River and to other monitoring wells. Colored symbols were assigned to each group and used for spatial analysis.

For numerous reasons, groundwater elevations from MW-326-20 (Shannon & Wilson, Inc. (SWI), 2013) were used as a surrogate for the Tanana River stage. The closest gauging station for the Tanana River (USGS 15485500) was located downstream in Fairbanks, Alaska. Tanana River stage was not always continuous; USGS did not report river stage between November and January 2013

likely due to ice cover. Data reported during ice cover are subject to revision due to inaccurate stage measurements as a result of pressure created by ice cover. MW-326-20 was selected because of its close proximity to the river as well as strong similarities between maximum and minimum groundwater elevations to river stage (Figure 7). The groundwater elevations and river stage match especially well during the summer, but deviate between January 2013 and May 2013.

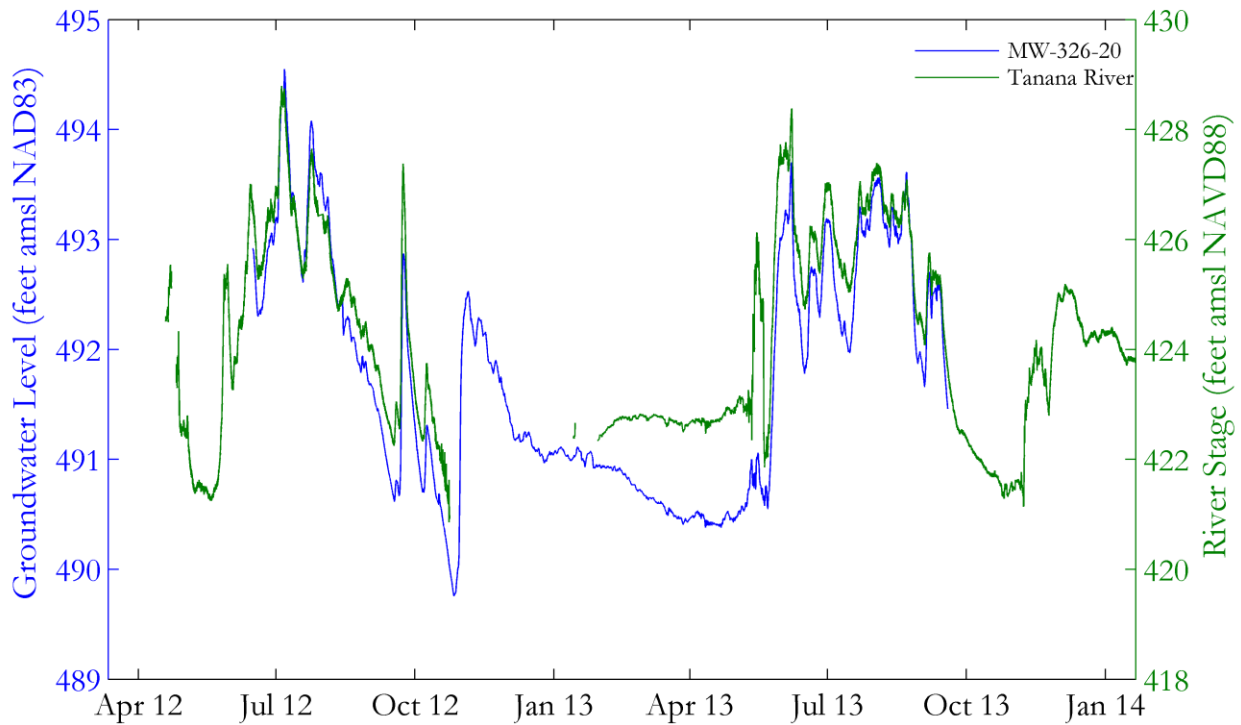


Figure 7. Comparison of MW-326-20 (SWI, 2013) to the Tanana River stage (USGS, 2014a).





4.2.2 Groundwater Temperature Profile Trends

Groundwater temperatures were plotted as a function of depth bgs at the midpoint of the well screens. Two groundwater temperature profile trends were identified: decreasing- and increasing-temperature-with-depth. A temperature profile trend was assigned to each well cluster. These trends were then represented spatially. Profile trends were not determined for well clusters with insufficient data (such as single well clusters, or those with missing data or inconsistent temperature trends).

4.2.3 Stable Isotope Classifications

Stable isotope classifications were developed from isotopic similarities of monitoring wells with the same temperature profile trends. These similarities were identified when $\delta^2\text{H}$ was plotted against $\delta^{18}\text{O}$ and marker symbols identifying either increasing or decreasing-temperatures-with-depth grouped together, or grouped together more than other markers. The plots were divided into four quadrants using threshold values of -170 and -22 for $\delta^2\text{H}$ and $\delta^{18}\text{O}$, respectively. Each quadrant was assigned a stable isotope classification (Table 4): depleted in $\delta^{18}\text{O}$ and $\delta^2\text{H}$, enriched in $\delta^{18}\text{O}$ and $\delta^2\text{H}$, depleted in $\delta^{18}\text{O}$ and enriched in $\delta^2\text{H}$, and enriched in $\delta^{18}\text{O}$ and depleted in $\delta^2\text{H}$.

Table 4. Stable isotope classifications for purpose of this study.

Parameter	$\delta^2\text{H}$	$\delta^{18}\text{O}$	Color
Depleted in $\delta^{18}\text{O}$ and $\delta^2\text{H}$	< -170.5 ‰	< -22 ‰	
Enriched in $\delta^{18}\text{O}$ and $\delta^2\text{H}$	> -170.5 ‰	> -22 ‰	
Depleted in $\delta^{18}\text{O}$ and enriched in $\delta^2\text{H}$	> -170.5 ‰	< -22 ‰	
Enriched in $\delta^{18}\text{O}$ and depleted in $\delta^2\text{H}$	< -170.5 ‰	> -22 ‰	

Groundwater stable isotope data were plotted with surface water data (Appendix G), the global meteoric water line (GMWL), and the regional evaporative line (REL). The GMWL ($\delta^2\text{H} = 4.937 \cdot \delta^{18}\text{O} - 53.04$ (‰) SMOW) represents the relation between $\delta^2\text{H}$ and $\delta^{18}\text{O}$ for surface waters worldwide as determined by Harmon Craig in 1961 (Clark and Fritz, 1997). The REL ($\delta^2\text{H} = 0.8 \cdot \delta^{18}\text{O} + 10$ (‰) SMOW) was fitted and extrapolated by Wooller et al. (2012) using stable isotope data from the Chena River and nearby lakes (i.e., Birch Lake, Harding Lake, Lost Lake, and Quartz Lake). The surface water isotopic values, GMWL, and REL served as points of reference for expected values for this region.

5 RESULTS

5.1 Groundwater Elevation Trends

All groundwater elevations reflected similarities to the Tanana River stage, indicating influence from the river. However, groundwater elevation trends for some monitoring wells were more similar than other monitoring wells. Monitoring wells were separated into eight groups based on these similarities in groundwater elevation trends (Figure 8).

Spatial representation of groundwater elevation trends (Figure 9) reveals spatial similarities within the trend groups. Monitoring wells with groundwater that appears to be increasing during the winter months are located along the Chena Slough (circles). Groundwater elevations that most closely reflect the Tanana River stage are located along the Tanana River (squares). Monitoring wells with groundwater elevations that reflect the Tanana River stage in summer, but appear stable throughout the winter (diamonds) characterize the area between the Tanana River and the Chena River.

Monitoring wells along the C-ditch (MW-165 and MW-191) have very similar groundwater elevations trends relative to one-another, but vary greatly from other groundwater elevation trends (magenta diamonds).

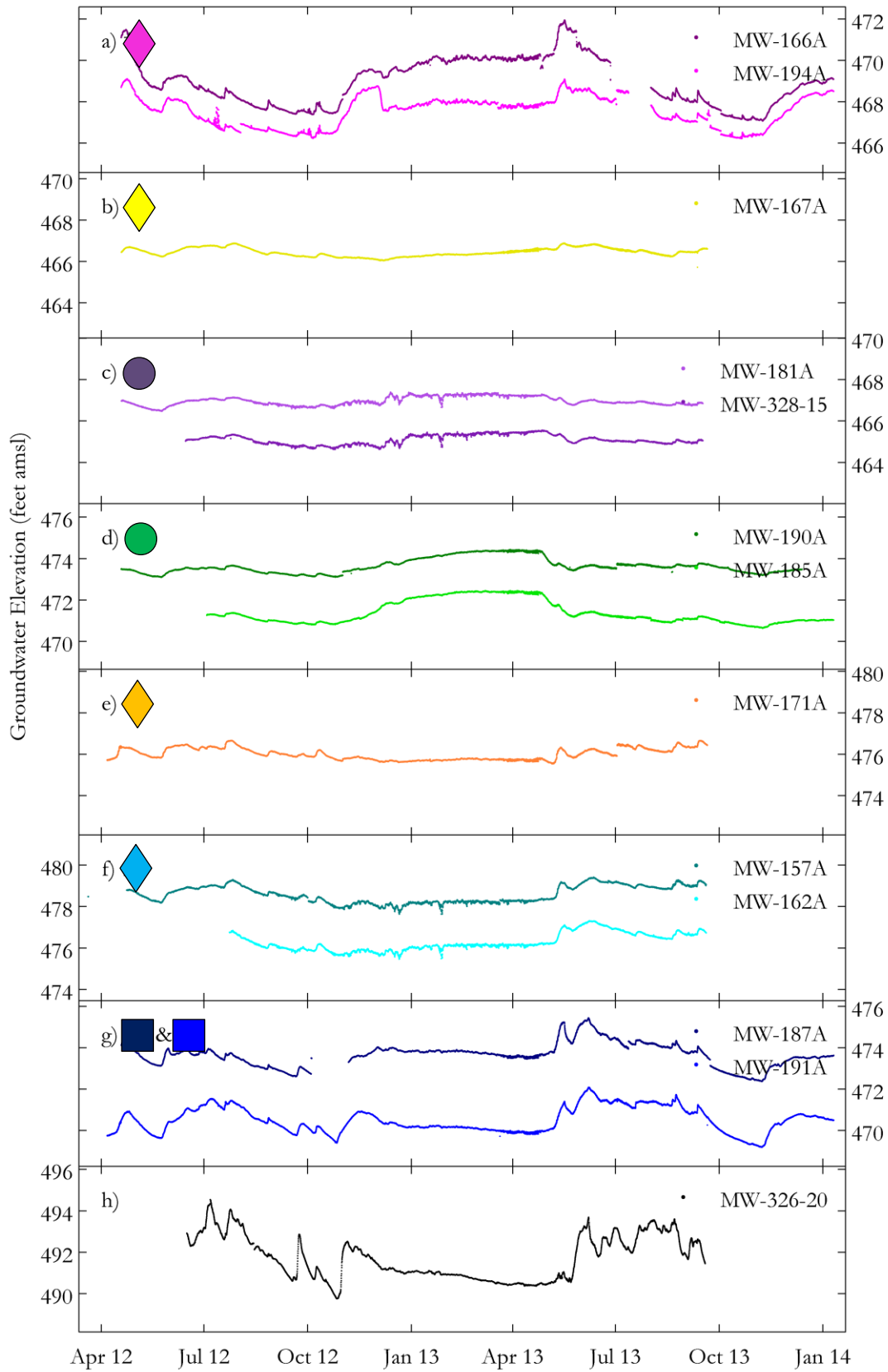


Figure 8. Groundwater elevations grouped by similarities between monitoring wells.

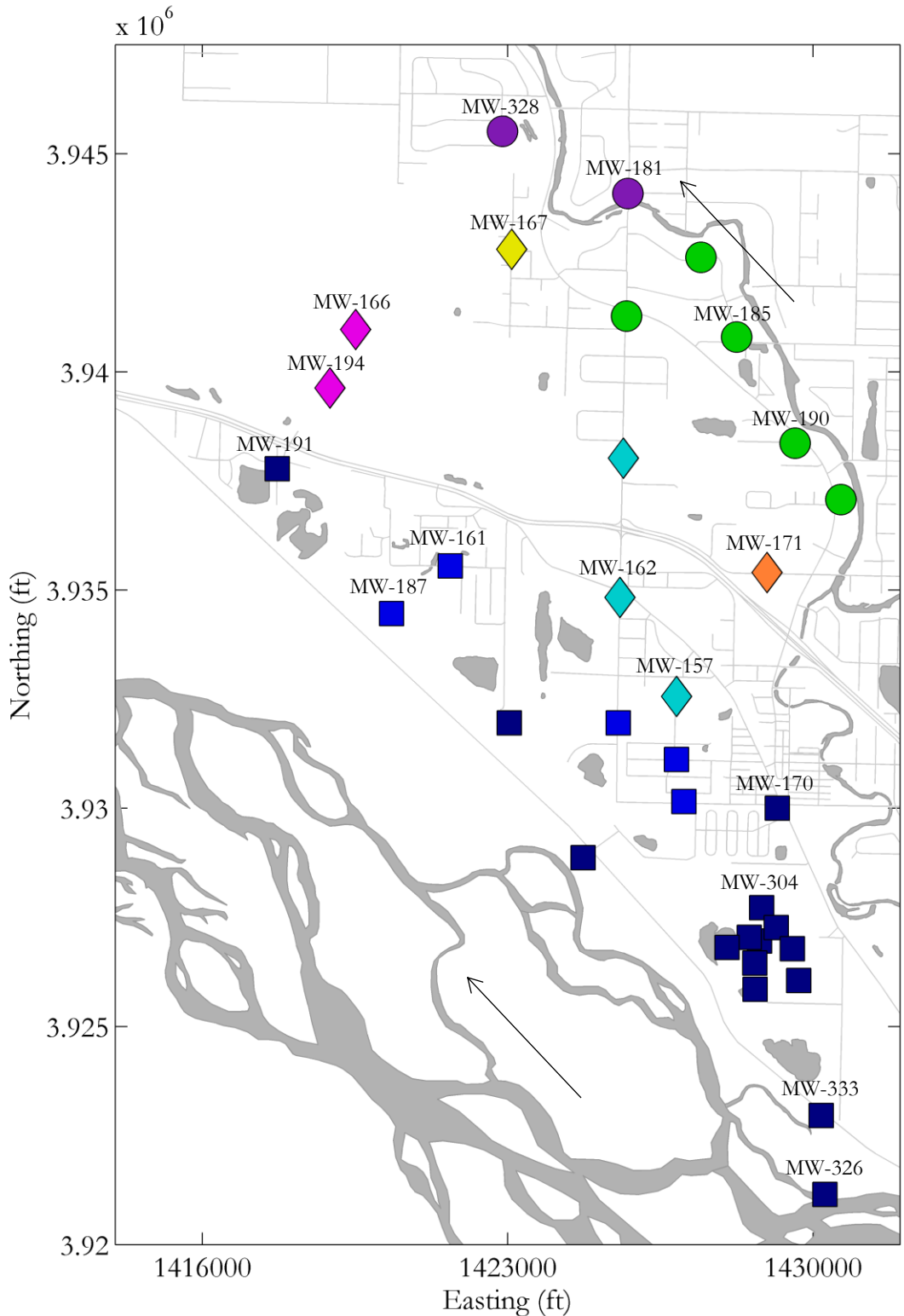


Figure 9. Groundwater elevation trend classifications represented spatially. Groundwater elevation trends indicate areas similarity. Symbols of the same shape indicate that groundwater elevation trends are more closely related relative to other groups, except for the magenta diamonds. Symbols of the same color indicate that monitoring wells are in the same group.

5.2 Groundwater Temperature Profile Trends

Two groundwater temperature profiles were determined: decreasing-temperatures-with-depth (Figure 10a) and increasing-temperatures-with-depth (Figure 10b). A decreasing-temperatures-with-depth profile was assigned to well clusters when groundwater temperatures were warmer in the shallow wells when compared to the deeper wells or when there was no difference in temperature between shallow and deep wells. The increasing-temperatures-with-depth classification was assigned to well clusters when groundwater temperatures of deeper wells were warmer than those of shallow wells. Temperature profiles were consistent throughout the year for groundwater temperatures below the water table. Groundwater temperatures at the water table were subject to seasonal fluctuations and varied by spatial orientation, magnitude, and rate (Appendix F). The following paragraphs discuss general properties specific to each profile trend.

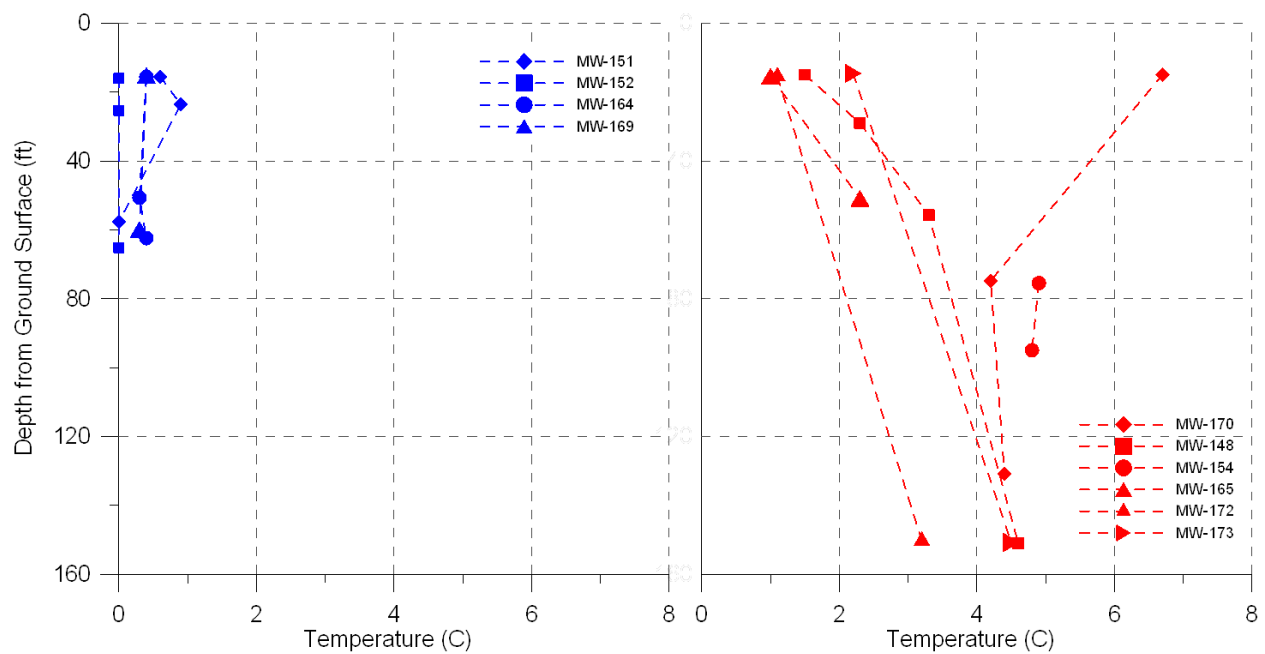


Figure 10. Examples of groundwater temperature profiles.

Groundwater temperature plotted as a function of depth, examples of decreasing-temperatures-with-depth (left) and increasing-temperatures-with-depth (right).

Well depths for monitoring well clusters classified as having decreasing temperatures with depth did not exceed 70 feet bgs; the deepest wells were located just above the permafrost. Groundwater temperatures just above the permafrost were near 0°C and were relatively constant throughout the year. The temperatures at the water table varied seasonally, but generally remained below 3°C.

Well depths for well clusters classified as increasing-temperatures-with-depth typically exceeded 80 feet bgs, except for MW-153, MW-165, and MW-191. The deepest monitoring wells had the highest groundwater temperature of the cluster, except for MW-170. The groundwater temperature at the water table for MW-170 was the highest throughout the year for the cluster; the cause for this is unknown, but possibly due to anthropogenic causes. Groundwater temperatures were generally warmer in well clusters that exhibited increasing-temperatures-with-depth than in well clusters classified as decreasing-temperatures-with-depth. Additionally, concave-downward temperature profiles were apparent in well clusters with three or more screen depths.

Mapped groundwater temperature profiles (Figure 11) indicate spatial similarities for temperature trends. Three different symbols identify the temperature profiles associated with each monitoring well: (a) increasing-temperature-with-depth – upward red triangles, (b) decreasing-temperature-with-depth – downward blue triangles, and (c) temperature profile undetermined – yellow circle.

Decreasing-temperatures-with-depth occurs throughout the central and northwestern region. These areas correspond with shallow depth to permafrost (Figure 3). Increasing-temperatures-with-depth exists in the southern region, at MW-170, and along the Chena Slough. These locations correspond to areas where depth to permafrost was greater than 100 feet bgs or was not encountered at 150 feet bgs. Increasing temperature profiles also occur at the westernmost point of the study area (MW-165 and MW-191); depth to permafrost is unknown. Permafrost was not encountered while drilling MW-165 and MW-191 to depths of 50 and 60 feet bgs, respectively.

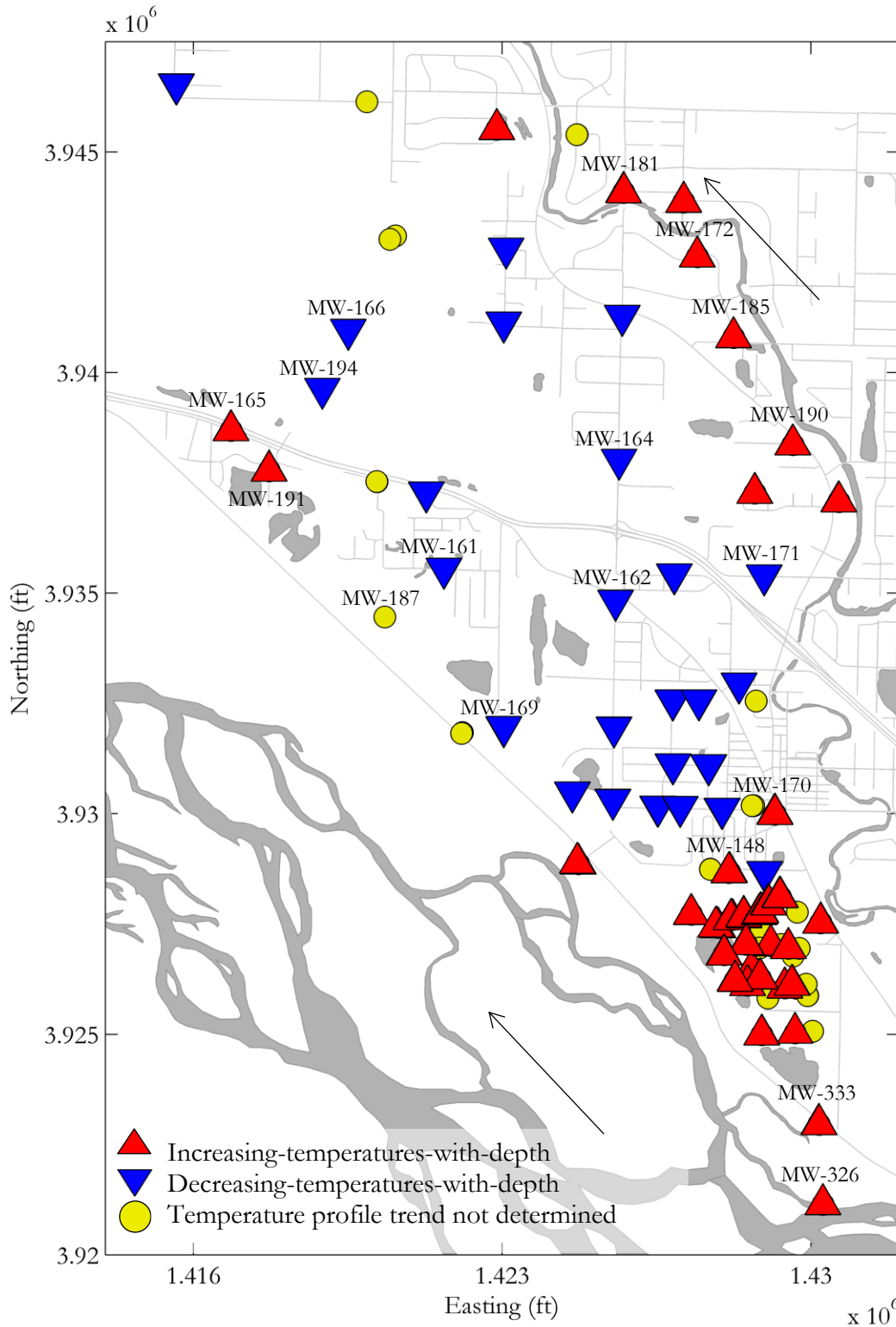








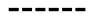
Figure 11. Groundwater temperature profile trends represent spatial similarities. Increasing-temperatures-with-depth exists in the southern region and along the Chena Slough. Decreasing-temperatures-with-depth occurs in the central and northwestern regions.

5.3 Stable Isotope Classifications and Trends

5.3.1 Monitoring well

A comparison of groundwater isotopic composition for the three 2013 sampling events (Figure 12) indicates seasonal variations and a difference in isotopic composition between monitoring wells classified as decreasing and increasing-temperatures-with-depth. Table 5 provides the legend for Figure 12. Additional figures illustrating the relationships between stable isotopes and depth and temperature are included in Appendix H. Classifications determined for the isotopic compositions were used to spatially represent isotopic composition at the water table and below the water table (Figure 13 a-c and d-f, respectively).

Table 5. Figure legend for Figure 12.

Parameter	Marker
Increasing-temperatures-with-depth	
Decreasing-temperatures-with-depth	
Tanana River Surface water	
Chena Slough Surface water	
Chena Slough Groundwater	
Global Meteoric Water Line (GMWL)	
Regional Evaporative Line (REL)	

For spring 2013 samples (Figure 12 a and d), monitoring wells classified as increasing-temperatures-with-depth were more depleted in $\delta^2\text{H}$, while monitoring wells classified as decreasing-temperatures-with-depth were more enriched in $\delta^2\text{H}$. There was no discernible trend for $\delta^{18}\text{O}$; values were evenly distributed over the $\delta^{18}\text{O}$ range. Resulting in not clearly defined spatial trends for the spring 2013 sampling event (Figure 13 a and d). Monitoring wells more depleted in $\delta^2\text{H}$ were located on the southern region and along Chena Slough. Monitoring wells more enriched were located throughout the central and northwestern regions.

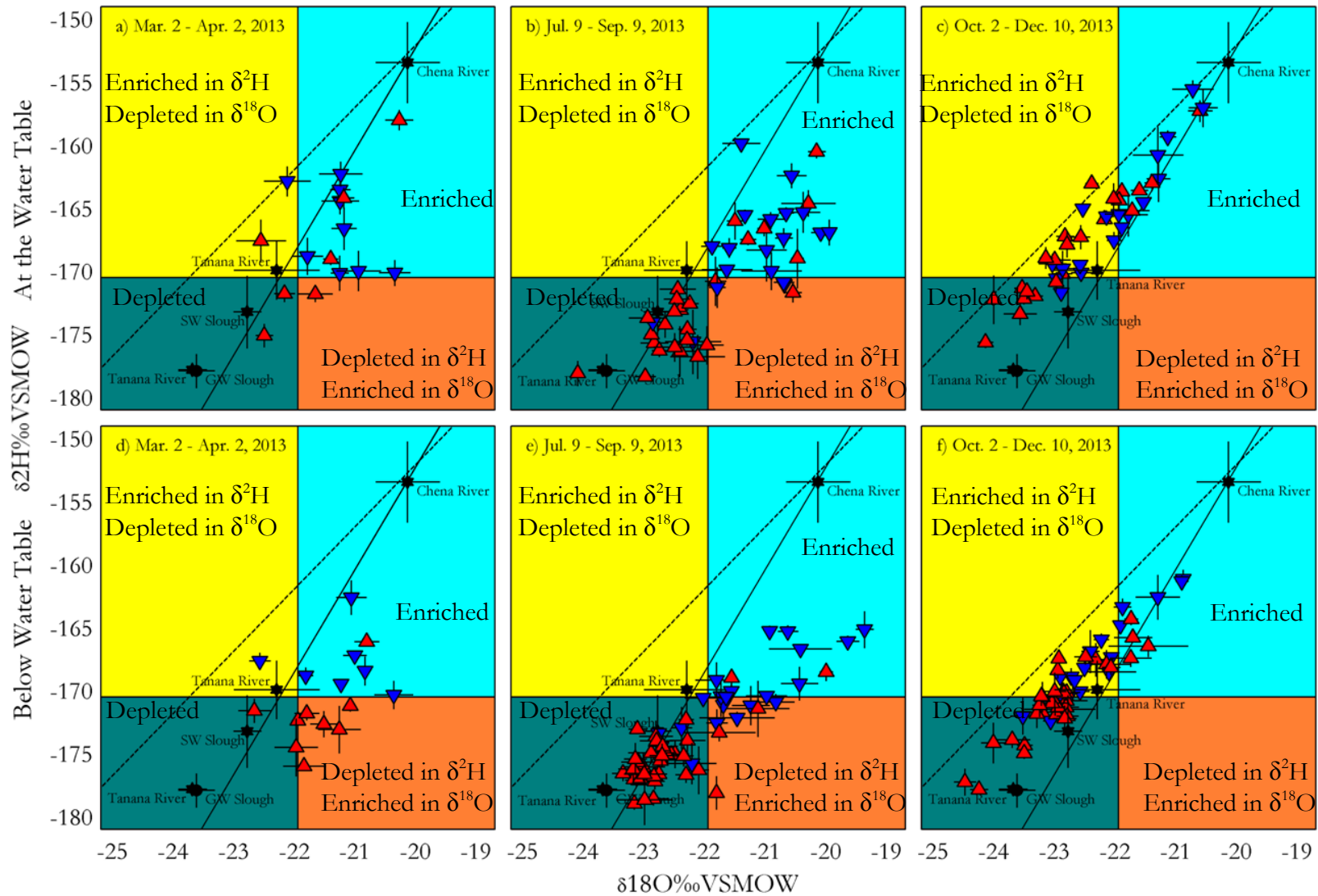


Figure 12. Groundwater stable isotope classifications and trends for three 2013 sampling events.

Groundwater at the water table (a-c) and below the water table (d-f). Temperature trends identified by symbol – increasing (red upward triangle) and decreasing (blue downward triangle). Surface water features identified by black stars or circles. GMWL – solid black line and REL – dashed black line. See Table 5 for legend.

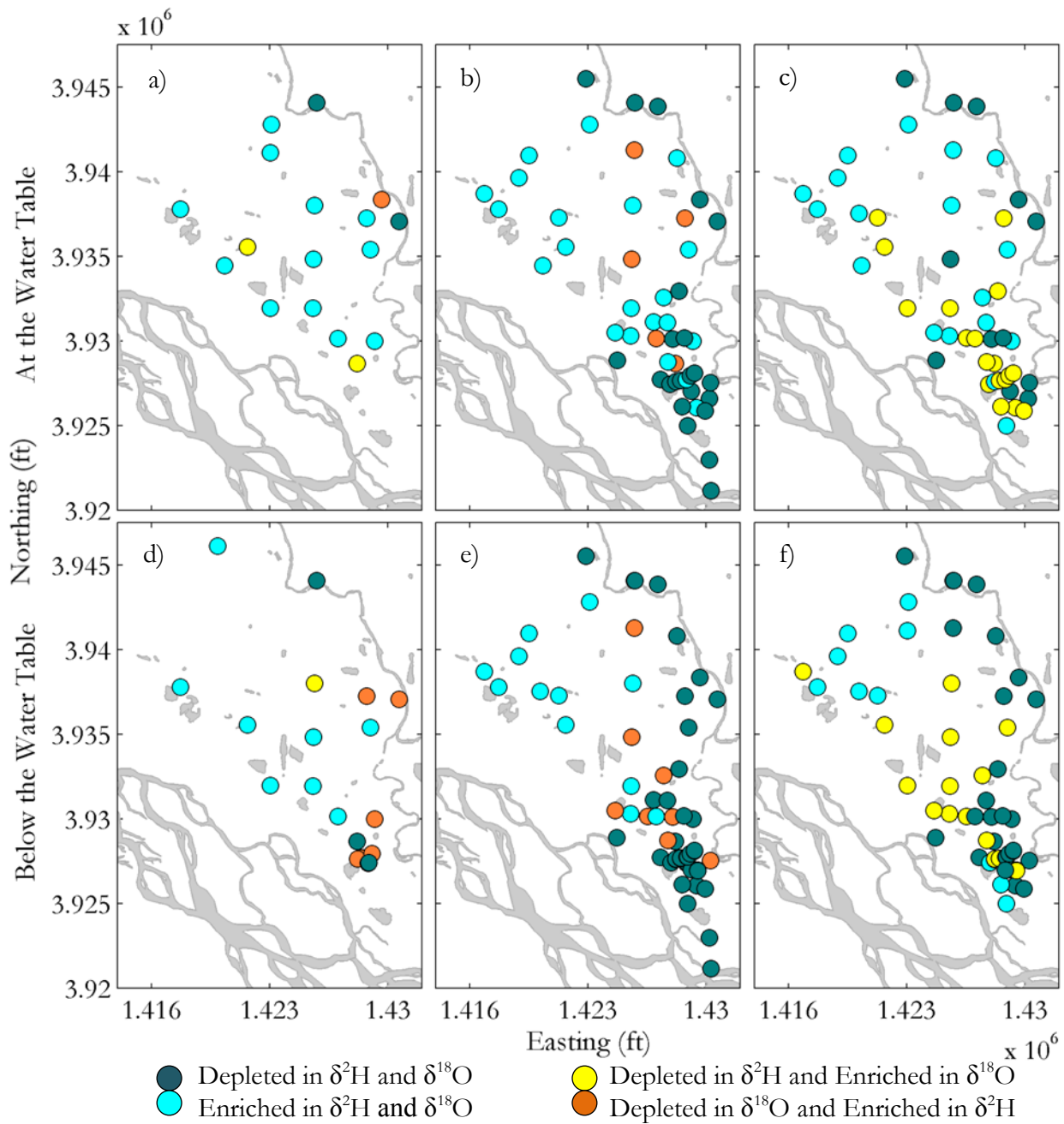


Figure 13. Groundwater stable isotope classifications represented spatially. Groundwater at the water table (a-c) and below the water table (d-f). Below the water table consists of all monitoring wells with screen depths greater than 20 feet bgs.

A stronger distinction between isotopic signatures was observed for the summer 2013 sampling event (Figure 12 b and e), resulting in more defined spatial trends (Figure 13 b and e). Groundwater depleted in $\delta^{18}\text{O}$ and $\delta^2\text{H}$ was located in the southern region and along the Chena Slough and Thirtymile Slough. Groundwater enriched in $\delta^{18}\text{O}$ and $\delta^2\text{H}$ was found in the central and northwestern regions. Groundwater depleted in $\delta^2\text{H}$ and more enriched in $\delta^{18}\text{O}$ was located north of the refinery and along the centerline of the study area. Isotope classifications at the water table compared to those below it were different for some well clusters.

A shift in stable isotope values was observed for the fall 2013 sampling event (Figure 12 c and f): values for each classification were generally more enriched in $\delta^{18}\text{O}$ and $\delta^2\text{H}$ and were bounded by the GMWL, REL, Tanana River, and Chena River. Groundwater isotopic composition was not well-separated based on temperature profiles. Samples from the fall 2013 event fell under three trend classifications: (1) depleted in $\delta^{18}\text{O}$ and $\delta^2\text{H}$, (2) depleted in $\delta^{18}\text{O}$ and enriched in $\delta^2\text{H}$, and (3) enriched in $\delta^{18}\text{O}$ and $\delta^2\text{H}$. These three classifications were distributed throughout the study area (Figure 13 c and f). Groundwater along Chena Slough was still (1), depleted in $\delta^{18}\text{O}$ and $\delta^2\text{H}$. The isotopic composition of groundwater at the water table was dominated by (2), depleted in $\delta^{18}\text{O}$ and enriched in $\delta^2\text{H}$ or by (3), enriched in $\delta^{18}\text{O}$ and $\delta^2\text{H}$, with a few samples (1), depleted both $\delta^{18}\text{O}$ and $\delta^2\text{H}$. Below the water table, depleted signatures dominated with a lesser contribution of (3), enriched in $\delta^{18}\text{O}$ and $\delta^2\text{H}$.

5.3.2 Private Sub-permafrost Wells

The groundwater isotopic compositions from private sub-permafrost wells are represented in Figure 14. The stable isotopes follow the same seasonal shifts as the monitoring well samples. However, values for the isotopic composition for private sub-permafrost groundwater were not as depleted or tightly clustered as expected. This may have occurred for several reasons. Decreased well integrity of

old wells or varying thicknesses of permafrost. There is the potential for short-circuiting of supra-permafrost groundwater around the well casing during pumping to occur. The efficiency of the type of pump used at each private well may have varied, possibly introducing oxygen into the system and resulting in fractionation. Thickness of permafrost at each residential well varied. Some wells might not be in the sub-permafrost portion of the aquifer; they could just have been installed beneath a lens of permafrost or frozen soil. Wells at the base of the permafrost would be representative of Tanana River water that was forced under the permafrost rather than actually representing deep sub-permafrost groundwater. This flow scenario is discussed in Section 6.5.4. To accurately represent deep sub-permafrost groundwater a sample would have to be collected at a depth beyond the influence of the Tanana River or collected from the south side of the Tanana River.

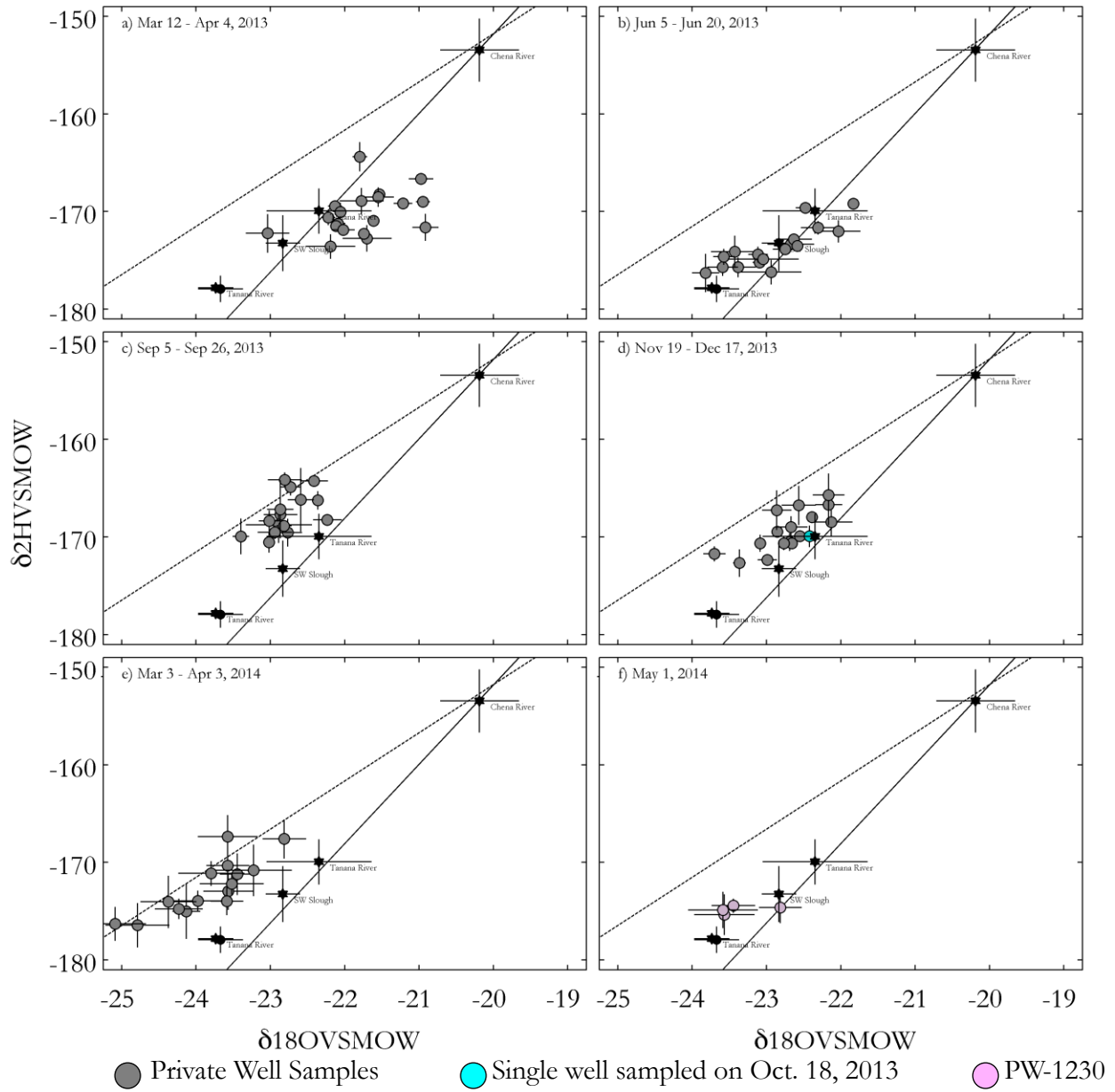


Figure 14. Groundwater isotopic composition for private sub-permafrost wells.

5.4 Combined Spatial Analysis

Spatial similarities between increasing-temperatures-with-depth and stable isotope classifications are shown in Figure 15. The stable isotope classifications used were for monitoring wells below the water table for summer 2013 sampling. Stable isotope classifications for below the water table were used because groundwater conditions there are more stable. Groundwater at the water table is subject to greater variability in both temperature and isotopic composition. Groundwater elevation trends are not included in Figure 15.

Most of the monitoring wells classified by increasing-temperatures-with-depth are also classified as depleted in $\delta^{18}\text{O}$ and $\delta^2\text{H}$. Along the Chena Slough, monitoring wells for which stable isotope data are available are depleted; groundwater elevations in those wells were relatively different from other groundwater elevation trends, and they appeared to be increasing during winter (Figure 8 c and d; and Figure 9). Depleted stable isotopes and increasing-temperatures-with-depth also characterize the monitoring wells in the southern region of the study area. Groundwater elevations closely reflect the Tanana River stage in the southern region as well as at MW-165 and MW-191. However, MW-165 and MW-191 have an isotopic composition classified as enriched in $\delta^{18}\text{O}$ and $\delta^2\text{H}$, even though they have increasing temperatures with depth.

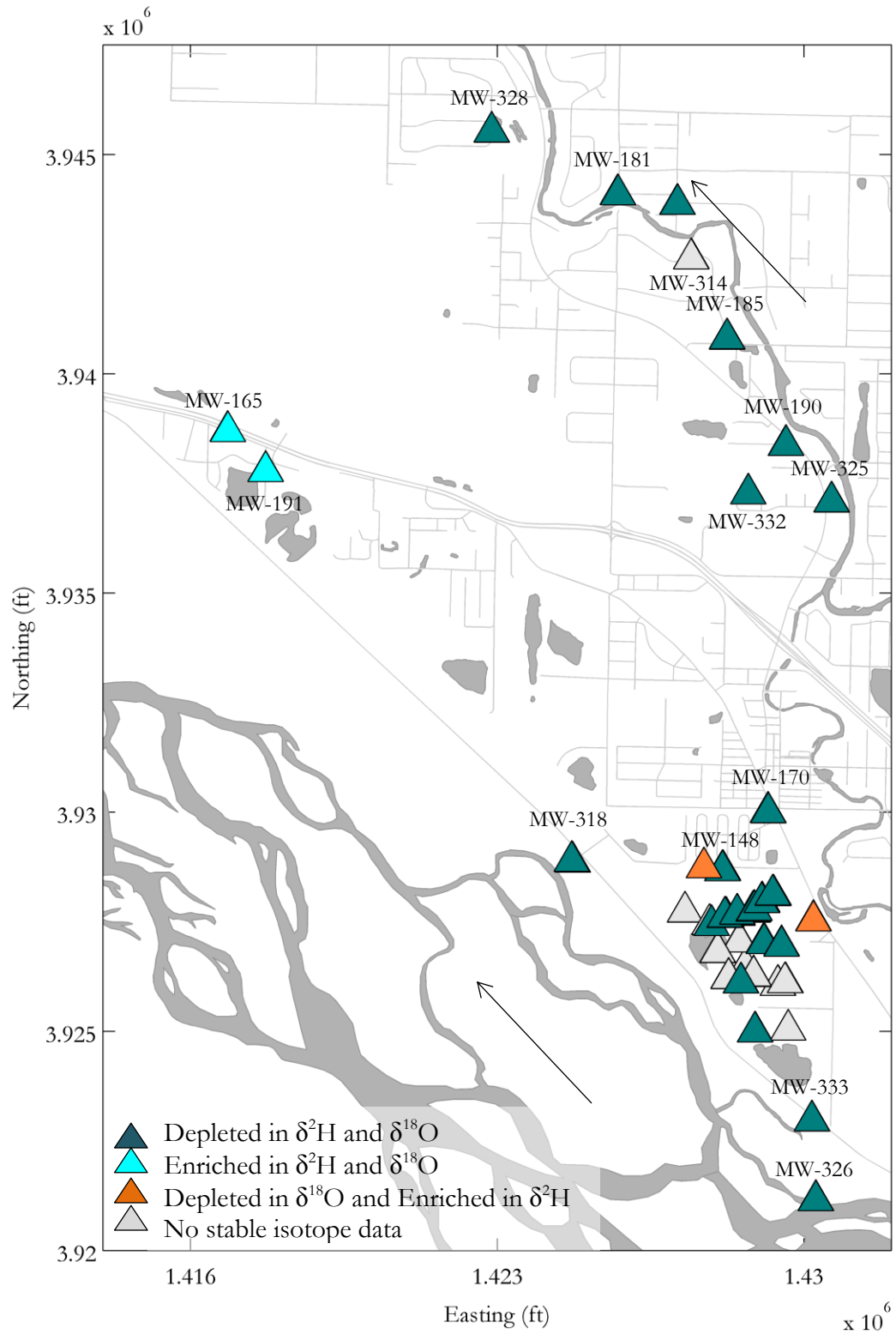


Figure 15. Increasing-temperatures-with-depth and associated stable isotope classifications. Summer 2013 stable isotope classifications. Temperature profiles are a strong indicator of discontinuities due to consistent groundwater temperatures below the water table. Stable isotopes are supporting indicators of discontinuities, but are subject to seasonal variations.

6 DISCUSSION

6.1 Indicators of Discontinuities

Groundwater characteristics can be used as indicators of permafrost discontinuities. Temperature profiles are the most reliable method for determining a connection between supra- and sub-permafrost groundwater. Increased temperatures with depth are consistent with the geothermal gradient (Anderson, 2005), as well as with the temperature trend beneath permafrost in Fairbanks, Alaska (Williams and van Everdingen, 1973). While temperature is a non-conservative tracer, groundwater temperatures below the water table should be consistent throughout the year. Kane and Slaughter (1973) were the first to use temperature profiles as indicators for discontinuities; they paired this use of temperature profiles with piezometric measurements to demonstrate recharge of a lake from sub-permafrost water.

As with piezometric measurements, groundwater elevation trends can also be a line of evidence for permafrost discontinuities. Deviating from a typical winter recession curve, increased groundwater elevations during base flow conditions may indicate upward flow of sub-permafrost groundwater. However, groundwater elevations need to be evaluated carefully, as increases in groundwater elevation may be an artifact of freezing ground, river ice cover, or domination by surface water. Calculating three-dimensional flow paths could make groundwater elevations a more reliable tool.

Groundwater isotopic composition furthers the reliability of temperature profile methods. Relatively depleted stable isotope values indicated areas where recharge from either sub-permafrost groundwater or Tanana River occur. The difference between isotopic composition of groundwater near discontinuities and in areas of shallow permafrost is discussed in Section 6.4. These three groundwater characteristics cannot be used to delineate the extent of the discontinuity, but they can identify groundwater in areas of discontinuities and further our understanding of aquifer dynamics.

6.2 Locations of Discontinuities

Through-taliks are expected to occur under large lakes and rivers (French, 2007; Wellman et al., 2013), thus a discontinuity was expected under the Tanana River, but in no other particular place in the study area. However, at least three other discontinuities were identified: the southern region, along the Chena Slough, and near MW-165 and MW-191 (Figure 16). Temperature profiles in these areas were shown to have increasing-temperatures-with-depth. In the southern region and along the Chena Slough, the depth to permafrost was generally greater than 100 feet bgs or was not encountered at 150 feet bgs (Figure 3). A third line of evidence for the discontinuity along the Chena Slough was groundwater elevation trends. Neither stable isotopes nor depth to permafrost supports a discontinuity at MW-165 and MW-191. Enriched groundwater composition was likely attributed to gravel pit influence. Also, wells depths were less than 60 feet bgs, permafrost was not encountered during installation, and therefore there is no record of permafrost at depths greater than 60 feet bgs.

A fourth discontinuity may exist under Thirtymile Slough; however, not enough information is known to determine this. Isotopic composition of groundwater near Thirtymile Slough was depleted in $\delta^{18}\text{O}$ and $\delta^2\text{H}$ (Figure 13), but depth to permafrost (Figure 3) and temperature profiles (Figure 11) vary along the reach. Conversely, continuous permafrost likely occurs throughout the central and northwestern regions, as indicated by decreasing temperatures with depth. Continuous permafrost corresponds with shallow permafrost depths determined during well drilling (Figure 3).

Formation of discontinuities is likely due to thermal properties of the associated surface water feature. Due to proximity, the discontinuity in the southern region is likely connected to the hydrothermal talik under the Tanana River. In the southern region, a talik could have formed under an old meandering channel of the braided Tanana River. The talik could have developed from advancing permafrost degradation from the talik under the Tanana River or from the combined

thermal properties of the Thirtymile Slough and the Tanana River. A discontinuity under the Chena Slough most likely developed when flow rate of Chena Slough was greater, prior to construction of Moose Creek Dam. All of these discontinuities are now maintained by the heat supply from upward-moving groundwater (French, 2007).

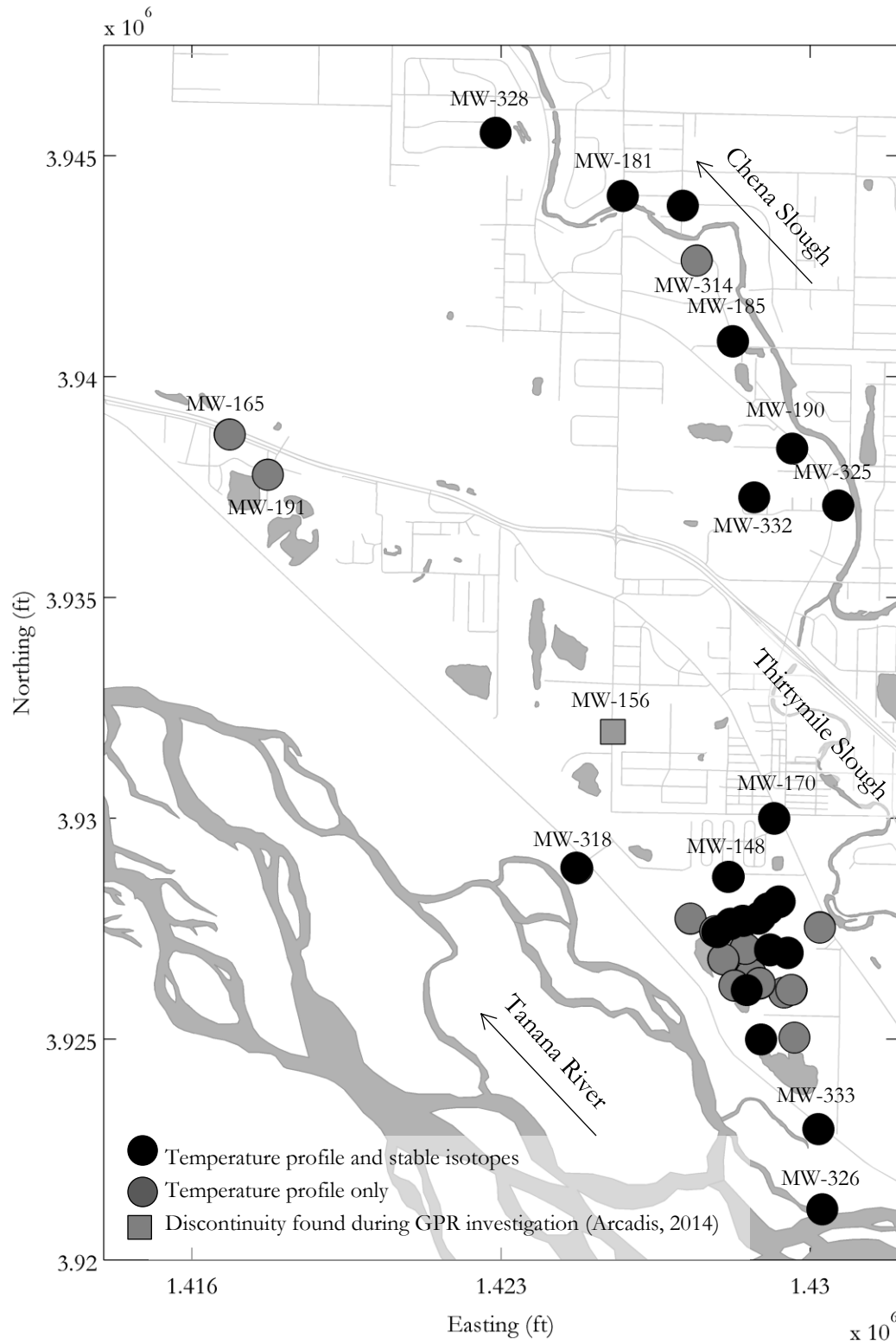


Figure 16. Monitoring wells that exhibit characteristics of discontinuities. Discontinuities in southern region, at MW-170, and along the Chena Slough are confirmed. Isotopes do not confirm a potential discontinuity near MW-165 and MW-191. Discontinuity at MW-156 was determined from GPR (Arcadis, 2014), but was not found using natural tracers.

Discontinuities previously mentioned are limited to the boundaries of the study area; however, it is likely that discontinuities occur beyond these boundaries, especially downstream on the Chena Slough or Tanana River. Evaluation beyond study area boundaries is limited by data scarcity. There is only one monitoring well (MW-313) along the Chena Slough between the bounds of the study area and the connection with the Chena River. Increasing-temperature-with-depth in this monitoring well and depleted stable isotopes indicate a discontinuity in the area (Appendix I), a discontinuity that may extend the length of the Chena Slough to the Chena River. But a discontinuity under the full length of the Chena Slough cannot be confirmed with the available data. A discontinuity is also likely to exist under the Chena River, as indicated by an increasing-temperatures-with-depth at MW-320. However, the isotopic composition of Chena River is more enriched than the glacially fed Tanana River (Appendix I) and representative of meteoric water (Douglas et al., 2014; Wooller et al., 2012), this is attributed to influence from rainfall and evaporation. West of the study area boundary, MW-322 is characterized by increasing-temperatures-with-depth and depleted stable isotopes, which suggests a discontinuity downstream on the Tanana River. Discontinuities at all three of these locations are further indicated by depth to permafrost greater than 150 feet bgs.

6.3 Ground Penetrating Radar

After the initial findings of the spring 2013 stable isotope sampling event, the FHR consultants conducted a ground-penetrating-radar (GPR) study to delineate the presence of permafrost. The three-dimensional permafrost model developed from GPR results (Arcadis, 2013) coincides with the findings of this thesis, confirming the presence of discontinuities in the study area: in the southern region and along the Chena Slough. The permafrost model also shows that permafrost borders the Tanana River, except where a non-permafrost area under a portion of the C-ditch. A discontinuity under a portion of the C-ditch would explain increasing-temperatures-with-depth at MW-165 and MW-191. Thirtymile Slough was not represented on the permafrost model, but a discontinuity may

exist in that area. There is insufficient data, however, to make this determination. The permafrost model shows an isolated permafrost-mass in a thawed zone above a deep layer of permafrost approximately where MW-170 is located.

GPR detected a discontinuity near MW-156 (Figure 16). This discontinuity was small and not connected to surface water. This discontinuity was likely not detected by methods used in this research for many reasons. The groundwater elevations were unique and varied from other wells, but were not included due to a short period of record. Groundwater temperature profiles could be decreasing near a discontinuity if monitoring wells were located over shallow permafrost, or even possibly directly over a discontinuity. Carlson and Barnes (2011) observed decreasing-temperature-with-depth in the area of a discontinuity. While sub-permafrost groundwater is warmer than supra-permafrost groundwater, heat would have dissipated while moving upward through a talik surrounded by permafrost. The isotopic composition of groundwater near MW-156 was more enriched than would be expected with a sub-permafrost source; the isotopic composition may have reflected mixing between the sub-permafrost source and the supra-permafrost enriched groundwater. Depth to permafrost would only indicate greater depths if monitoring well placement was exactly over the discontinuity. Both these responses are also observed in MW-153 over shallow permafrost but near a discontinuity.

6.4 Differences in Isotopic Signatures

There are a number of factors that contribute to depleted stable isotope values for $\delta^{18}\text{O}$ and $\delta^2\text{H}$. Snowmelt and glacial melt have depleted stable isotope compositions. Depletion increases with vertical elevation gain as well as colder climate conditions. These effects likely caused depleted deep groundwater in Aleppo basin (Al-Charideh, 2012). Because of these factors depleted isotope compositions were expected for sub-permafrost groundwater and Tanana River. Sub-permafrost

water is likely recharged at higher elevations. Limited fractionation should occur once this recharge enters the sub-permafrost system. Snowmelt contributes to the Tanana River in early summer, and rainfall and glacial melt contribute later in the summer (Kramer and Brabets, 2012). Wooller et al. (2012) found the Tanana River isotopic composition consistent with glacial melt.

Depleted isotope signatures throughout supra-permafrost groundwater were possible due to the recharge-sources with depleted isotope signatures, Tanana River during the summer and sub-permafrost groundwater during the winter. However, depleted signatures were only found for supra-permafrost groundwater near discontinuities, while groundwater in areas of shallow permafrost was more enriched. Seasonal shifts and differences are discussed in Section 6.5.

Similar trends between $\delta^{18}\text{O}$ and $\delta^2\text{H}$ were found in the Canadian Shield by Stotler et al. (2009) and in the Aleppo basin by Al-Charideh (2012), where shallow water isotopic composition was more enriched and deviated linearly from the tight cluster of deep water isotopic composition. Stotler et al. (2009) attribute the linear deviation of permafrost water from the sub-permafrost waters to the mixing of introduced surface waters with natural permafrost waters and the effects of freezing. Al-Charideh (2012) attributes enrichment of the shallow water to evaporation because the data fit an evaporation line. Clark and Fritz (1997) discuss the processes that lead to evaporative enrichment of shallow groundwater by infiltration of summer rain.

Enriched stable isotope values can be explained for groundwater in areas of shallow permafrost by isotope enrichment by fractionation or mixing processes. Shallow groundwater within the study area is dynamic and is influenced by Tanana River, gravel pits, sloughs, infiltration, and evaporation.

Gravel pits directly interact with shallow groundwater and are subject to evaporation, rainfall, and freeze-thaw – all processes that change isotopic composition. This interaction or contribution from gravel pits influences the groundwater's isotopic composition. Similarly, enrichment of the Tanana

River by evaporation and infiltration would change the groundwater isotopic composition. Isotopic composition of shallow groundwater can also change due to fractionation of the groundwater.

Fractionation between water and vapor is highest at 0°C and decreases as temperature increases (Clark and Fritz, 1997). Groundwater temperatures in the study area range from near 0°C to greater than 6°C, ideal for fractionation. The relation between temperature and stable isotopes (Appendix F) indicates depleted isotope signatures are associated with warmer sub-permafrost water, while enriched isotope signatures are associated with cooler supra-permafrost groundwater. Some evaporation from the water table may also occur.

The isotopic composition of the supra-permafrost groundwater was expected to be depleted based on source waters. Depleted isotope signatures were seen in areas of discontinuities where the connection to the subpermafrost was direct. However, at the water table and in areas of continuous permafrost, more enriched isotope compositions were found. Evaporative enrichment is the likely cause for the change in isotopic composition of source water. Any combination of the factors previously mentioned could account for evaporative enrichment at the water table and in areas of shallow permafrost.

6.5 Improved Understanding of Aquifer Dynamics

Using groundwater elevations, temperature profiles, and stable isotopes furthered our understanding of areas of recharge, flow direction, recharge-sources, and aquifer seasonality within the study area.

The largest area where water enters the supra-permafrost groundwater within the study area is along the Tanana River, in the southern region, and along the Chena Slough. Enrichment of stable isotopes indicates supra-permafrost groundwater movement away from those areas. An increased value of both $\delta^{18}\text{O}$ and $\delta^2\text{H}$ is an indication that groundwater was subjected to enrichment processes, longer than groundwater only enriched in either $\delta^{18}\text{O}$ or $\delta^2\text{H}$. The following three

subsections are an interpretation of groundwater isotopic composition in relation to recharge-sources and aquifer seasonality for the 2013 sampling events. The fourth subsection discusses the recharge-sources for the supra-permafrost groundwater.

6.5.1 Spring 2013

Relatively homogenous groundwater isotopic composition was expected during base flow conditions prior to breakup. During base flow conditions, the supra-permafrost is recharged by sub-permafrost groundwater and Tanana River. No influences on the groundwater isotopic composition from evaporation or infiltration would occur since the Tanana River, gravel ponds, and ground are frozen and snow covered. This was the case for ^{18}O ; values evenly distributed over the $\delta^{18}\text{O}$ range indicate the water throughout the aquifer was the same and had not undergone any processes. Conversely, a difference in $\delta^2\text{H}$ values occurred between groundwater at and below the water table. This difference in values between deep and shallow groundwater could be attributed to the natural variation of deuterium. However, the trend of differences is consistent with the summer and fall sampling events: deep groundwater more depleted than shallow groundwater.

6.5.2 Late Summer 2013

The groundwater isotopic composition in late summer fits primarily within either the depleted or the enriched classification. Depleted groundwater is in areas of discontinuities. Enriched groundwater occurs in areas of shallow permafrost and at the water table. Enriched groundwater deviates from the GMWL. Both spatial trends can be attributed to warmer air temperatures; the summer of 2013 was one of the warmest on record for the region. Depleted isotopic composition of groundwater in areas of permafrost discontinuities can be attributed to increased glacial melt. Increased glacial melt is supported by Tanana River stage; river stage for late summer 2013 was relatively greater and more constant than in the previous two years (Figure 5). Linear deviation from the GMWL indicates

evaporative enrichment of shallow groundwater. Evaporative enrichment can reflect infiltration of rain, and evaporation and precipitation influences on gravel ponds and river recharge. It is also possible that some evaporation from the water table may occur.

6.5.3 Fall 2013

The isotopic composition of groundwater during the fall is more consistent with expected meteoric water, as indicated by stable isotope values more aligned with the GMWL and bounded by the REL. The isotopic composition of groundwater consistent with meteoric water must have occurred from seasonal changes in the Tanana River and gravel ponds. The precipitation input proportion to the Tanana River becomes relatively more significant during recession when less glacial melt contribution attributed to lower air temperatures. A similar shift in fall 2005 stable isotope values for the Tanana River is presented in Wooller et al. (2012). Infiltration of precipitation into the shallow groundwater is another way precipitation could have influenced isotope enrichment; likely suggesting that recharge in the area is somewhat significant. The influence of evaporative enrichment would be reduced due to lower air temperatures.

6.5.4 Supra-permafrost Groundwater Recharge

The Tanana River and sub-permafrost groundwater are two main recharge-sources for supra-permafrost groundwater. Historically, the Tanana River has been accepted as a source of recharge for the alluvial aquifer (Glass et al., 1996; Williams, 1970; Anderson, 1970). This is evident in groundwater flow directions outward from the river within the study area. However, no previous discussions exist in regards to sub-permafrost groundwater as a recharge-source. Recharge scenarios at two different locations, where the relative contributions of recharge-source vary seasonally, are discussed in the following two paragraphs.

Along the Tanana River, supra-permafrost groundwater is recharged from the Tanana River. During the summer, the Tanana River is composed of snow and glacial melt, and precipitation. During the winter, the Tanana River likely receives recharge from Alaska Range subpermafrost groundwater (Racine and Walters, 1994), from deep Tanana Valley alluvium, and from major tributaries (Kraemer and Brabets, 2012). These sources are likely present during the summer, but contribute less when compared to snow and glacial melt, and precipitation.

At the Chena Slough discontinuity, sub-permafrost groundwater moving upward through the discontinuity is a recharge-source. The deep sub-permafrost groundwater is likely composed of recharge from the Alaska Range and from deep Tanana Valley alluvium. However, shallow sub-permafrost groundwater is composed of Tanana River water. Preliminary analysis of hydraulic head profiles (not included in this thesis) indicated splitting of the flow between the supra- and sub-permafrost at the permafrost interface. The sub-permafrost groundwater that recharges the supra-permafrost groundwater is likely a mixture of the Tanana River water and deep sub-permafrost groundwater.

6.6 Contaminant Transport

An understanding of groundwater dynamics is vital to characterization of contaminant transport in any region. Discontinuities in permafrost influence contaminant transport in four ways. First, through-taliks provide pathways for contaminants to be transported into the sub-permafrost groundwater. Second, clean, uncontaminated supra-permafrost groundwater migration downward through a talik could dilute a sub-permafrost plume. Third, upward flow through discontinuities can provide clean, uncontaminated sub-permafrost groundwater, which can dilute and/or redirect the plume. Fourth, upward flow of contaminated sub-permafrost groundwater can reintroduce contaminants to the supra-permafrost portion of the aquifer. Characterizing groundwater

contamination and designing remediation strategies in a discontinuous permafrost aquifer requires an understanding of the transport mechanisms associated with through-taliks.

The contaminated aquifer used for this study was chosen because of evidence of sulfolane in both the supra- and sub-permafrost groundwater. Sulfolane serves as a conservative tracer, identifying groundwater movement. Contaminated groundwater originates from the southern region. Sulfolane was detected throughout the supra-permafrost groundwater as well as in the sub-permafrost groundwater. Groundwater contaminated with sulfolane likely migrated into the sub-permafrost at the permafrost interface, where the flow is divided between the supra- and sub-permafrost, just north of the refinery boundary.

Groundwater from monitoring wells along Chena Slough was primarily non-detect or below the analytical limit for sulfolane (Appendix A). In this area it is likely that uncontaminated sub-permafrost groundwater is flowing upward and diluting or redirecting plume movement. Carlson and Barnes (2011) observed redirection of a contaminate plume by upward flow of sub-permafrost groundwater in Fairbanks, Alaska. This may also occur near MW-165 and MW-191. High concentrations of sulfolane are found parallel to the Tanana River, but no sulfolane has been detected in either MW-165 or MW-191. However, sulfolane concentrations are increasing in MW-166 and MW-194 (Arcadis, 2014) along the C-ditch. Upward flow at MW-165 and MW-194 may have redirected the sulfolane plume; the C-ditch may also be of influence. Sulfolane concentration data are limited for the undeveloped land north of MW-161 and east of MW-166 and MW-194.

Sulfolane-contaminated sub-permafrost groundwater has the potential to contaminate supra-permafrost groundwater where upward flow occurs. Evidence of this occurs at MW-332. At this particular well cluster, increasing sulfolane concentrations were detected at 150 feet bgs; while shallow wells at 15 feet bgs have lower sulfolane concentrations (Arcadis, 2014). Increasing sulfolane

concentrations were also found in private wells on the south side of Chena Slough near MW-181, where the slough is oriented east to west (Arcadis, 2013). The highest concentrations of sulfolane have been found in the sub-permafrost, but the sub-permafrost is not as well delineated and the bottom morphology of permafrost is highly variable. Understanding where the sulfolane contamination might enter the supra-permafrost portion is important in regulatory and cleanup decisions.

In addition to the influence of permafrost discontinuities on contaminant transport, channelization of contaminants by permafrost is also a concern (Hinzman, Johnson, et al., 2000; Carlson and Barnes, 2011). Isotope enrichment can be used as groundwater tracer to identify groundwater movement away from depleted recharge zones. By interpreting these flow paths, it may be possible to identify areas where channelization might occur. Between MW-156 and MW-161 channelization may occur, corresponding with an old slough or swale stringer (Péwé, et al., 1976). The highest concentrations of sulfolane in the supra-permafrost groundwater were detected in these two monitoring wells. Channelization may also occur between MW-162, MW-164, and MW-168, where a thaw bulb beneath Peridot Road is a possible explanation for it. This cannot be confirmed without additional monitoring wells. Inferring transport pathways for sulfolane is limited to the available data. Most monitoring wells are located along main roads and spatial gaps exist, primarily in undeveloped areas.

6.7 Other Applications

In addition to interpreting groundwater movement, surface water interaction, and their influence on contaminants, using available data groundwater characteristics can be used to identify discontinuities for other applications such as developing water resources, investigating permafrost degradation, identifying source contributions, and selecting building locations. Seasonally constant temperature

and water quality make sub-permafrost groundwater more desirable for drinking water purposes (Williams and van Everdingen, 1973); however, installing a well through the permafrost can be expensive. Using available temperature data could result in selecting an optimal well location at or near a discontinuity, which means better drinking water quality and reduced construction costs. For permafrost degradation investigations, using the methods presented in this thesis research could determine the presence or absence of permafrost or changes in the presence or absence over time. Another application of these methods could be used to select building locations or evaluate their impacts on the environment, for example, sulfolane contamination may have been limited to the supra-permafrost groundwater if the North Pole Refinery has been located over continuous permafrost rather than a talik.

6.8 Groundwater Temperature Profiles Used for Indicators of Taliks

Developing temperature profiles is a simple way of determining whether groundwater is in an area of discontinuity or located over permafrost. Groundwater temperature is a commonly measured field parameter captured during groundwater studies. However, there are some limitations to the application of temperature profiles. Determining which temperature profile trend gets assigned to each well cluster can be challenging, depending on the number of screen depths. Well clusters with three or more screen depths are easier to assign temperature profiles; water temperatures below the water table are consistent throughout the year. Well clusters with only two screen depths showed a linear relationship due to limited data points. Due to surficial temperature fluctuations, monitoring wells with only two screen depths were best evaluated for decreasing-temperatures-with-depth during the summer. They were best evaluated during the winter for increasing-temperature-with-depth profiles. Also, detecting a discontinuity using temperature profiles may be dependent on the size of the discontinuity; the heat from warm sub-permafrost water may be depleted while moving upward through a small area surrounded by permafrost, as seen by Carlson and Barnes (2011), or as

possibly seen at MW-156 by GPR study (Arcadis, 2013). Using temperature profiles, with an understanding of their limitations, can be helpful when identifying discontinuities and understanding aquifer dynamics.

6.9 Future Work

The work presented in this thesis is only a portion of that which could be done to investigate groundwater dynamics in degrading, discontinuous permafrost. Related studies for future consideration include:

- Extending the boundaries of the study area. Investigating groundwater dynamics beyond the study area was not within the scope of this project, but it would be valuable to the understanding of contaminant transport.
- Evaluating temperature profiles and isotopic composition of groundwater on the south side of the Tanana River, up-gradient from the study area, and from the sub-permafrost portion of the aquifer.
- Further analyzing groundwater elevation trends and three-dimensional flow calculations would provide more information regarding recharge-sources and flow paths.
- Seasonally dating surface water and groundwater to confirm recharge-sources and processes.
- Continuing to identify end-members for stable isotopes to better interpret groundwater sources and movement.
- Developing the local evaporation line (LEL) and local meteoric water line (LMWL) from the isotopic composition of gravel pits and precipitation, respectively, would strengthen the interpretation of seasonal changes in groundwater isotopic composition.
- Further evaluating seasonal stable isotopes trends, LEL and REL to define recharge-source changes or fractionation processes.

- Investigating ^{18}O and ^2H relations to other stable or unstable isotopes.
- Installing sub-permafrost monitoring wells (at the same depths) to calculate flow direction and allow for sampling and data collection.
- Calculating upward (or downward) flux using temperatures recorded by fiber optic cable installed down well casings, and then comparing flux rates to vertical trends in stable isotope values.
- Mapping which monitoring wells have previously frozen to see if they correspond to locations of shallow permafrost.
- Developing conceptual models for sulfolane transport as well as groundwater flow dynamics (e.g., sub-permafrost flow from Alaska Range, Tanana River recharge from the glacial melt and precipitation, supra- and sub-permafrost groundwater recharge from Tanana River, and upward flow from either deep sub-permafrost groundwater or shallow sub-permafrost groundwater).
- Using a Modflow model to determine whether conceptual model is valid and if interpretation of groundwater elevations trends is correct.
- Further investigating MW-170. Groundwater characteristics below the water table indicate a discontinuity in the area. Groundwater at the water table at MW-170 has the highest temperature of the well nest and enriched stable isotope signatures.
- Confirming if a discontinuity is present under Thirtymile Slough.
- Mapping temperature profiles throughout the Tanana River floodplain using temperature data from other contaminated sites to determine where discontinuities may be throughout the area.
- Increasing our understanding of recharge and aquifer dynamics for the Tanana Watershed by incorporating these parameters into future studies to refine longstanding work regarding groundwater (Williams, 1970; Anderson, 1970; Péwé, and Bell, 1975b; Glass et al., 1996).

7 CONCLUSION

The aim of the work presented in this thesis was to use groundwater characteristics to evaluate groundwater dynamics. This study has demonstrated that areas of discontinuity can be determined using groundwater elevation, temperature profiles and stable isotopes. At least three discontinuities were identified within the study area: under the southern region, along the Chena Slough, and near MW-165 and MW-191. Use of groundwater temperature profiles was determined the best method for identifying discontinuities. The same groundwater characteristics were used to understand groundwater dynamics in areas of discontinuity and to trace groundwater flow paths. The dynamics paired with implications of upward-moving groundwater aided in interpretation of sulfolane transport in the aquifer. Consideration of the flow paths, as determined by isotope enrichment, helped in the identification of areas of potential channelization for sulfolane. Stable isotopes were also used to infer seasonal changes in source water in the aquifer. The Tanana River is likely the primary recharge-source for supra-permafrost groundwater during the summer, while sub-permafrost groundwater is likely the primary recharge-source during the winter.

REFERENCES

- Abrióla, L. M., & Pinder, G. F. (1982). Calculation of velocity in three space dimensions from hydraulic head measurements. *Groundwater*, 20(2), 205-213.
- Alaska Climate Research Center. (2014). Alaska Climatology. Retrieved from <http://akclimate.org/Climate>
- Al-Charideh, A. (2012). Geochemical and isotopic characterization of groundwater from shallow and deep limestone aquifers system of Aleppo basin (north Syria). *Environmental Earth Sciences*, 65(4), 1157-1168.
- Anderson, G.S. (1970). Hydrologic reconnaissance of the Tanana Basin, central Alaska: U.S. Geological Survey Hydrologic Investigations Atlas HA-319, 4 sheets.
- Anderson, M. P. (2005). Heat as a ground water tracer. *Groundwater*, 43(6), 951-968.
- Arcadis. (2012). Revised Sampling and Analysis Plan, in Site Characterization. Report prepared for Flint Hills Refinery. Seattle, Washington.
- Arcadis. (2013). Third Quarter 2013 Groundwater Monitoring Report. Report prepared for Flint Hills Refinery. Seattle, Washington.
- Arcadis. (2014). Ground Penetrating Radar Study, in Site Characterization Report. Report prepared for Flint Hills Refinery. Seattle, Washington.
- BARR Engineering Company. (2012). Revised Site Characterization Report: North Pole Refinery Flint Hills Resources Alaska, LLC. Minneapolis, MN.
- Bense, V. F., Ferguson, G., & Kooi, H. (2009). Evolution of shallow groundwater flow systems in areas of degrading permafrost. *Geophysical Research Letters*, 36(22).
- Bolton, W. R. (2006). *Dynamic modeling of the hydrologic processes in areas of discontinuous permafrost* (Doctoral dissertation, University of Alaska Fairbanks).
- Boucher, J., & Carey, S. (2010). Exploring runoff processes using chemical, isotopic and hydrometric data in a discontinuous permafrost catchment.
- Brabets, T. P., & Walvoord, M. A. (2009). Trends in streamflow in the Yukon River Basin from 1944 to 2005 and the influence of the Pacific Decadal Oscillation. *Journal of Hydrology*, 371(1), 108-119.
- Callegary, J. B., Kikuchi, C. P., Koch, J. C., Lilly, M. R., & Leake, S. A. (2013). Review: groundwater in Alaska (USA). *Hydrogeology Journal*, 21(1), 25-39.
- Carey, S. K., & Quinton, W. L. (2005). Evaluating runoff generation during summer using hydrometric, stable isotope and hydrochemical methods in a discontinuous permafrost alpine catchment. *Hydrological Processes*, 19(1), 95-114.

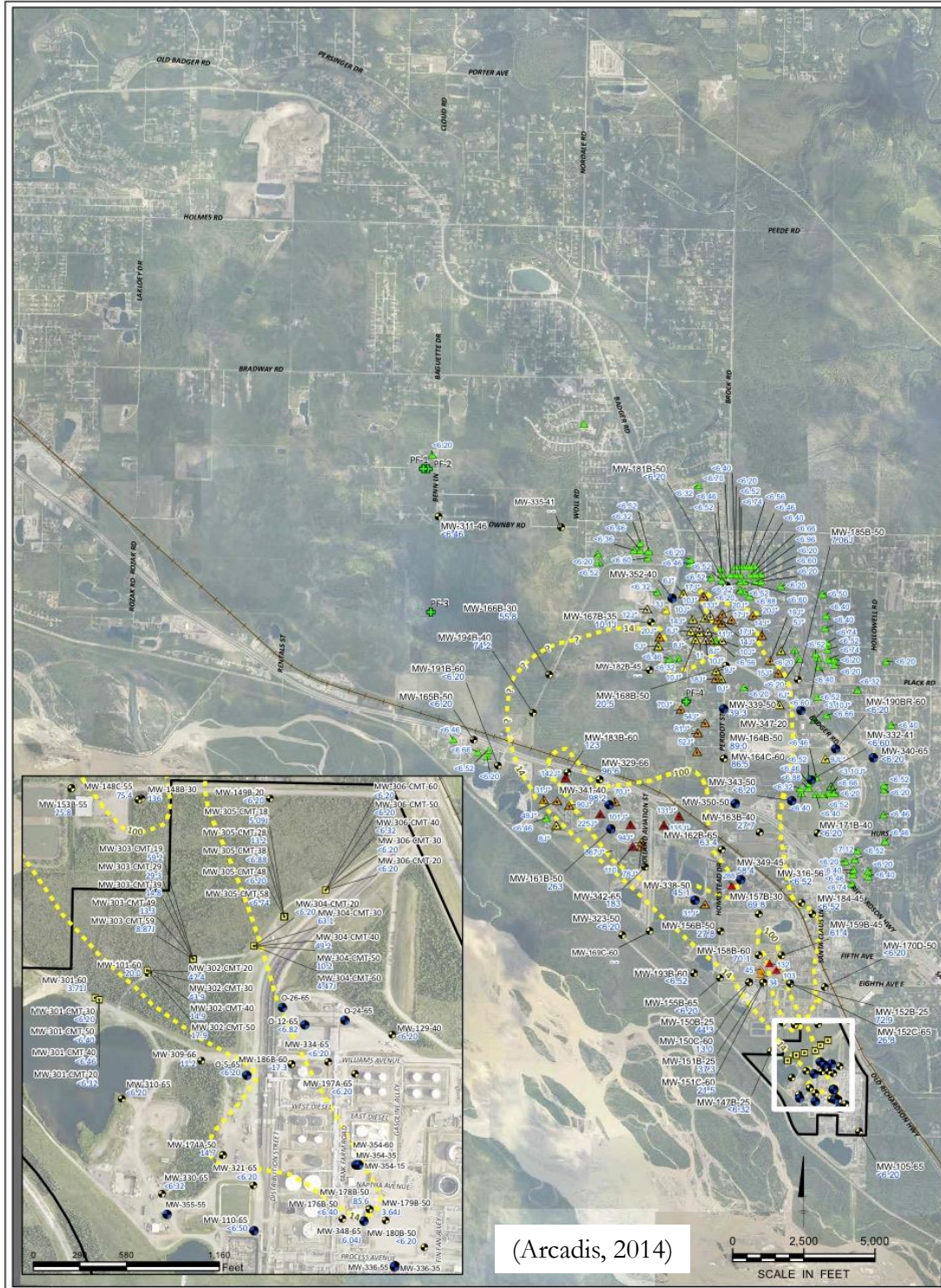
- Carlson, A. E., & Barnes, D. L. (2011). Movement of trichloroethene in a discontinuous permafrost zone. *Journal of contaminant hydrology*, 124(1), 1-13.
- Chapin III, F. S., Hollingsworth, T., Murray, D. F., Viereck, L. A., & Walker, M. D. (2006). *Floristic diversity and vegetation distribution in the Alaskan boreal forest* (pp. 81-99). Oxford University Press, New York.
- Clark, I. D., & Fritz, P. (1997). *Environmental isotopes in hydrogeology*. CRC press.
- Department of Environmental Conservation (DEC), Contaminated Sites Program. (2014). North Pole Refinery Project Home. Retrieved from <http://dec.alaska.gov/spar/csp/sites/north-pole-refinery/maps.htm>
- Deprez, P. P., Arens, M., & Locher, H. (1999). Identification and assessment of contaminated sites at Casey Station, Wilkes Land, Antarctica. *Polar Record*, 35(195), 299-316.
- Douglas, T. A., Blum, J. D., Guo, L., Keller, K., & Gleason, J. D. (2013). Hydrogeochemistry of seasonal flow regimes in the Chena River, a subarctic watershed draining discontinuous permafrost in interior Alaska (USA). *Chemical Geology*, 335, 48-62.
- Evengard, B., Berner, J., Brubaker, M., Mulvad, G., & Revich, B. (2011). Climate change and water security with a focus on the Arctic. *Global health action*, 4.
- Ferrians Jr., O.J. (1965). Permafrost Map of Alaska. US Geological Survey Miscellaneous Geologic Investigations Map I-445, Scale 1:2,500,000.
- French, H. M. (2007). *The periglacial environment*. John Wiley & Sons.
- Geomega, Inc. (2013). Interim Remedial Action Plan Addendum, Appendix A, Source History. Retrieved from https://dec.alaska.gov/spar/csp/sites/north-pole-refinery/docs/npr-irapadd13-appA-source_history.pdf
- Glass, R.L., Lilly, M.R., & Meyer, D.F., 1996, Groundwater levels in an alluvial plain between the Tanana and Chena Rivers near Fairbanks, Alaska, 1986-93: US Geological Survey Water-Resources Investigation Report 96-4060, 39 P. + Appendices.
- Green, T. R., Taniguchi, M., Kooi, H., Gurdak, J. J., Allen, D. M., Hiscock, K. M., ... & Aureli, A. (2011). Beneath the surface of global change: Impacts of climate change on groundwater. *Journal of Hydrology*, 405(3), 532-560.
- Hayashi, M., Quinton, W. L., Pietroniro, A., & Gibson, J. J. (2004). Hydrologic functions of wetlands in a discontinuous permafrost basin indicated by isotopic and chemical signatures. *Journal of Hydrology*, 296(1), 81-97.
- Haldorsen, S., Heim, M. & van der Ploeg, M. (2011). Impacts of climate change on groundwater in permafrost areas: case study from Svalbard, Norway Treidel, H., Martin-Bordes, J. L., & Gurdak, J. J. (Eds.). In, *Climate change effects on groundwater resources: A global synthesis of findings and recommendations* (pp. 326-327). CRC Press.

- Hinzman, L. D., Johnson, R. A., Kane, D. L., Farris, A. M., & Light, G. J. (2000). Measurements and modeling of benzene transport in a discontinuous permafrost region. *Contaminant Hydrology: Cold Regions Modeling*, Alex Iskandar and Steven Grant (Eds.), Lewis Publishers, 175-237.
- Hinzman, L. D., Wegner, M., & Lilly, M. R. (2000). Hydrologic investigations of groundwater and surface-water interactions in subarctic Alaska. *Nordic hydrology*, 31(4), 339-356.
- Hinzman, L. D., Bettez, N. D., Bolton, W. R., Chapin, F. S., Dyurgerov, M. B., Fastie, C. L., ... & Yoshikawa, K. (2005). Evidence and implications of recent climate change in northern Alaska and other arctic regions. *Climatic Change*, 72(3), 251-298.
- Hinzman, L. D., Jones, J. B., Bolton, W. R., Adams, P. C., & Petrone, K. C. (2005). Watershed hydrology and chemistry in the Alaskan boreal forest: The central role of permafrost. *Alaska's changing boreal forest*, 269.
- Hinzman, L. D., Viereck, L. A., Adams, P. C., Romanovsky, V. E., & Yoshikawa, K. (2006). Climate and permafrost dynamics of the Alaskan boreal forest. *Alaska's Changing Boreal Forest*, 39-61.
- Iwakun, O., Biggar, K., Van Stempvoort, D., Bickerton, G., & Voralek, J. (2008). Fuel contamination characterization in permafrost fractured bedrock at the Colomac mine site. *Cold Regions Science and Technology*, 53(1), 56-74.
- Jorgenson, M. T., Shur, Y. L., & Pullman, E. R. (2006). Abrupt increase in permafrost degradation in Arctic Alaska. *Geophysical Research Letters*, 33(2).
- Jorgenson, M. T., Racine, C. H., Walters, J. C., & Osterkamp, T. E. (2001). Permafrost degradation and ecological changes associated with a warming climate in central Alaska. *Climatic change*, 48(4), 551-579.
- Kalbus, E., Reinstorf, F., & Schirmer, M. (2006). Measuring methods for groundwater–surface water interactions: a review. *Hydrology and Earth System Sciences*, 10(6), 873-887.
- Kane, D.L. and Slaughter, C.W. (1973). Recharge of a Central Alaska Lake by Subpermafrost Groundwater, In *Permafrost North American Contribution 2nd International Permafrost Conference, Yakutsk, USST. National Academy of Sciences, Washington, DC* (pp. 458-462).
- Kasenow, M. (2001). *Applied ground-water hydrology and well hydraulics*. Water Resources Publication.
- Kraemer, T. F., & Brabets, T. P. (2012). Uranium isotopes ($^{234}\text{U}/^{238}\text{U}$) in rivers of the Yukon Basin (Alaska and Canada) as an aid in identifying water sources, with implications for monitoring hydrologic change in arctic regions. *Hydrogeology Journal*, 20(3), 469-481.
- Muskett, R. R., & Romanovsky, V. E. (2011). Alaskan permafrost groundwater storage changes derived from GRACE and ground measurements. *Remote Sensing*, 3(2), 378-397.
- Nenana Ice Classic. (2014). Nenana Ice Classic Brochure. Retrieved from <http://www.nenanaakiceclassic.com/brochures.htm>

- Osterkamp, T. E. (2007). Causes of warming and thawing permafrost in Alaska. *Eos, Transactions American Geophysical Union*, 88(48), 522-523.
- Osterkamp, T. E., & Romanovsky, V. E. (1999). Evidence for warming and thawing of discontinuous permafrost in Alaska. *Permafrost and Periglacial Processes*, 10(1), 17-37.
- Osterkamp, T. E., Jorgenson, M. T., Schuur, E. A. G., Shur, Y. L., Kanevskiy, M. Z., Vogel, J. G., & Tumskey, V. E. (2009). Physical and ecological changes associated with warming permafrost and thermokarst in interior Alaska. *Permafrost and Periglacial Processes*, 20(3), 235-256.
- Péwé, T. L., & Bell, J. W. (1975a). Map showing distribution of permafrost in the Fairbanks D-1 SW Quadrangle, Alaska: U.S. Geol. Survey Misc. Field Studies Map MF-671-A, scale: 1:24,000.
- Péwé, T. L., & Bell, J. W. (1975a). Map showing ground-water conditions in the Fairbanks D-1 SW Quadrangle, Alaska: U.S. Geol. Survey Misc. Field Studies Map MF 671-B, scale: 1:24,000.
- Péwé, T. L.; Bell, J. W.; Williams, J. R.; Paige, R. A. (1976). Geologic map of the Fairbanks D-1 SW Quadrangle, Alaska: U.S. Geol. Survey Misc. IMAP: 949, scale: 1:24,000.
- Prowse, T. D., Wrona, F. J., Reist, J. D., Gibson, J. J., Hobbie, J. E., Lévesque, L. M., & Vincent, W. F. (2006). Climate change effects on hydroecology of Arctic freshwater ecosystems. *AMBIO: A Journal of the Human Environment*, 35(7), 347-358.
- Racine, C. H., & Walters, J. C. (1994). Groundwater-discharge fens in the Tanana Lowlands, interior Alaska, USA. *Arctic and Alpine Research*, 418-426.
- Roach, J., Griffith, B., Verbyla, D., & Jones, J. (2011). Mechanisms influencing changes in lake area in Alaskan boreal forest. *Global Change Biology*, 17(8), 2567-2583.
- Rouse, W. R., Douglas, M. S., Hecky, R. E., Hershey, A. E., Kling, G. W., Lesack, L., ... & Smol, J. P. (1997). Effects of climate change on the freshwaters of arctic and subarctic North America. *Hydrological Processes*, 11(8), 873-902.
- Shannon & Wilson, Inc. (2013). NPR – Data Sharing Website. Retrieved October 11, 2013 from <http://npr-data.azurewebsites.net>
- Shur, Y. L., & Jorgenson, M. T. (2007). Patterns of permafrost formation and degradation in relation to climate and ecosystems. *Permafrost and Periglacial Processes*, 18(1), 7-19.
- Stotler, R. L., Frappe, S. K., Ruskeeniemi, T., Ahonen, L., Onstott, T. C., & Hobbs, M. Y. (2009). Hydrogeochemistry of groundwaters in and below the base of thick permafrost at Lupin, Nunavut, Canada. *Journal of Hydrology*, 373(1), 80-95.
- Turner, K. W., Wolfe, B. B., & Edwards, T. W. (2010). Characterizing the role of hydrological processes on lake water balances in the Old Crow Flats, Yukon Territory, Canada, using water isotope tracers. *Journal of Hydrology*, 386(1), 103-117.

- U.S. Geological Survey. (2014a). National Water Information System data available on the World Wide Web (USGS Water Data for the Nation). Retrieved March 14, 2014 from http://waterdata.usgs.gov/nwis/uv?site_no=15485500
- U.S. Geological Survey. (2014b). National Water Information System data available on the World Wide Web (USGS Water Data for the Nation). Retrieved March 14, 2014 from http://waterdata.usgs.gov/nwis/uv?site_no=15514000
- Wada, T., Chikita, K. A., Kim, Y., & Kudo, I. (2011). Glacial effects on discharge and sediment load in the subarctic Tanana River Basin, Alaska. *Arctic, Antarctic, and Alpine Research*, 43(4), 632-648.
- Walvoord, M. A., & Striegl, R. G. (2007). Increased groundwater to stream discharge from permafrost thawing in the Yukon River basin: Potential impacts on lateral export of carbon and nitrogen. *Geophysical Research Letters*, 34(12).
- Walvoord, M. A., Voss, C. I., & Wellman, T. P. (2012). Influence of permafrost distribution on groundwater flow in the context of climate- driven permafrost thaw: Example from Yukon Flats Basin, Alaska, United States. *Water Resources Research*, 48(7).
- Wellman, T. P., Voss, C. I., & Walvoord, M. A. (2013). Impacts of climate, lake size, and supra-and sub-permafrost groundwater flow on lake-talik evolution, Yukon Flats, Alaska (USA). *Hydrogeology Journal*, 21(1), 281-298.
- Williams, J.R.. (1970). Ground Water in the Permafrost Regions of Alaska: US Govt. Print. Off., US Geological Survey Professional Paper 969, p. 34-39.
- Williams, J. R., & Van Everdingen, R. O. (1973). Groundwater investigations in permafrost regions of North America: a review. In *Permafrost North American Contribution 2nd International Permafrost Conference, Yakutsk, USST. National Academy of Sciences, Washington, DC* (pp. 435-446).
- Woo, M. K., Kane, D. L., Carey, S. K., & Yang, D. (2008). Progress in permafrost hydrology in the new millennium. *Permafrost and Periglacial Processes*, 19(2), 237-254.
- Wooller, M. J., Kurek, J., Gaglioti, B. V., Cwynar, L. C., Bigelow, N., Reuther, J. D., Gelvin-Reymiller, C., & Smol, J. P. (2012). An~ 11,200 year paleolimnological perspective for emerging archaeological findings at Quartz Lake, Alaska. *Journal of Paleolimnology*, 48(1), 83-99.
- Yoshikawa, K., & Hinzman, L. D. (2003). Shrinking thermokarst ponds and groundwater dynamics in discontinuous permafrost near Council, Alaska. *Permafrost and Periglacial Processes*, 14(2), 151-160.
- Yoshikawa, K., Natsagdorj, S., & Anarmaa Sharkhuu, A. (2013). Groundwater Hydrology and Stable Isotope Analysis of an Open-System Pingo in Northwestern Mongolia. *Permafrost and Periglacial Processes*. Published online in Wiley Online Library (wileyonlinelibrary.com) DOI: 10.1002/ppp.1773

Appendix A. Sulfolane concentration maps.



(Arcadis, 2014)

Legend

- Monitoring Well
- Vertical Profile Transect Well
- Point-of-entry treatment system sample collected
- Permafrost Boring (PF-#)
- Phase 8 Wells

Private Well Sulfolane Results

- Not Detected
- 3.1 µg/L - 10 µg/L (J-flagged)
- 10 µg/L - 14 µg/L
- 14 µg/L - 100 µg/L
- 100 µg/L - 500 µg/L
- Greater than 500 µg/L

22.5 Sulfolane Concentration (µg/L)

- J Estimated concentration, detected above the detection level (DL) and below the limit of quantitation (LOQ)
- Result is considered estimated (no direction of bias due to GC failure) (flag applied by SWI)
- < Not detected, detection limit listed
- Not sampled due to well being frozen or obstructed

Notes:

Samples with duplicate data are represented by the greater of the two results.

Sulfolane was analyzed by EPA Method 1631B with iso-dilution.

Sulfolane results for private wells are shown from October 1, 2012 to September 16, 2013.

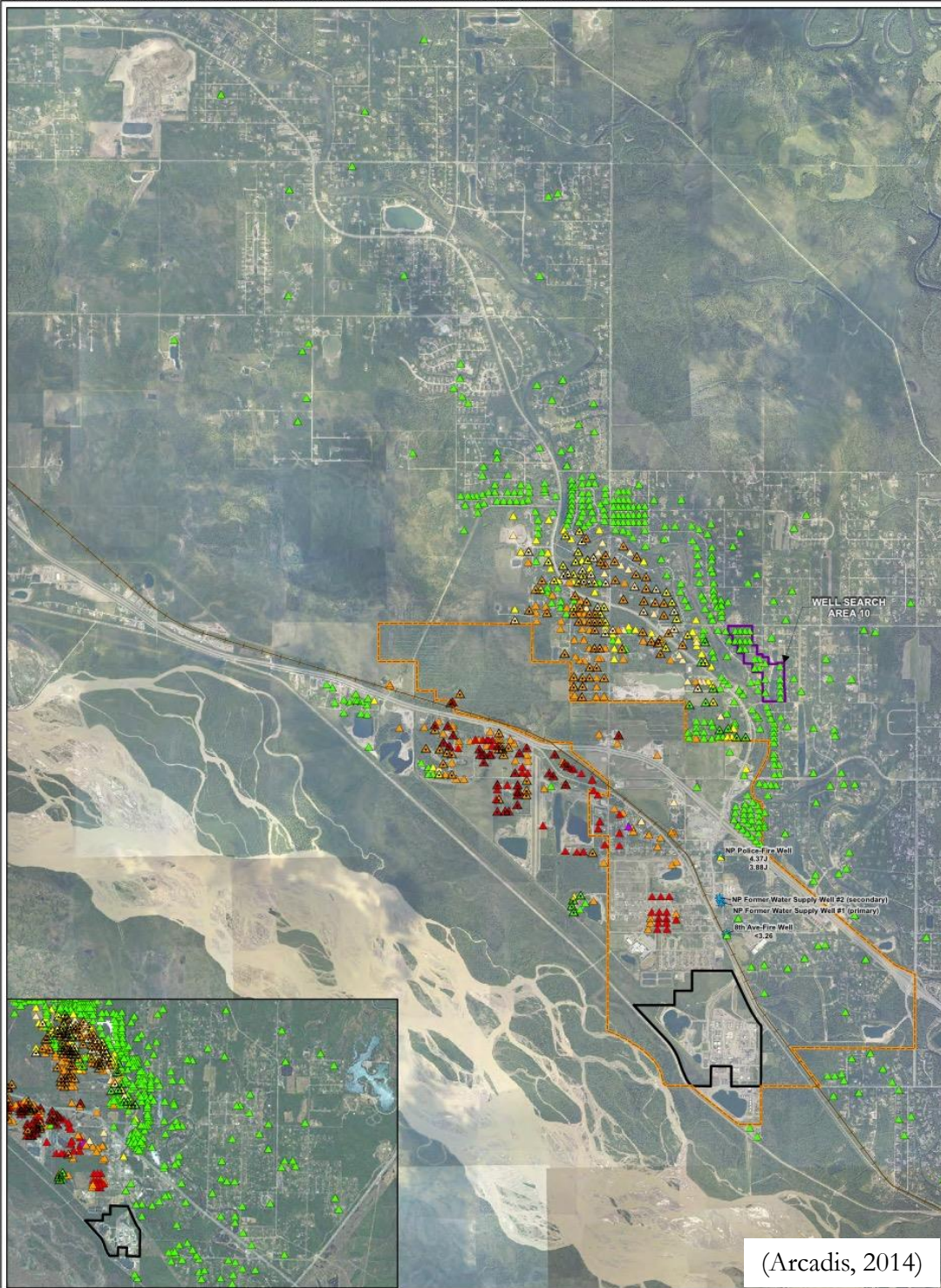
Phase 8 well locations are approximate.

Image provided courtesy of Pictometry International 2012.

FLINT HILLS RESOURCES ALASKA, LLC
 NORTH POLE REFINERY, NORTH POLE, ALASKA
**THIRD QUARTER 2013
 GROUNDWATER MONITORING REPORT**
**ANALYTICAL RESULTS FOR SULFOLANE
 10-55 FEET BELOW WATER TABLE**

FIGURE 4-11

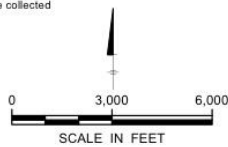
ARCADIS



LEGEND:

- | | |
|----------------------------------|--|
| ▲ Not Detected | ▲ Point-of-entry treatment system sample collected |
| ▲ 3.1 µg/L - 10 µg/L (J-flagged) | ▲ Municipal Wells |
| ▲ 10µg/L - 14 µg/L | ▭ North Pole City Boundary |
| ▲ 14µg/L - 100 µg/L | ▭ FHRA Property Boundary |
| ▲ 100µg/L - 500 µg/L | |
| ▲ Greater than 500 µg/L | |

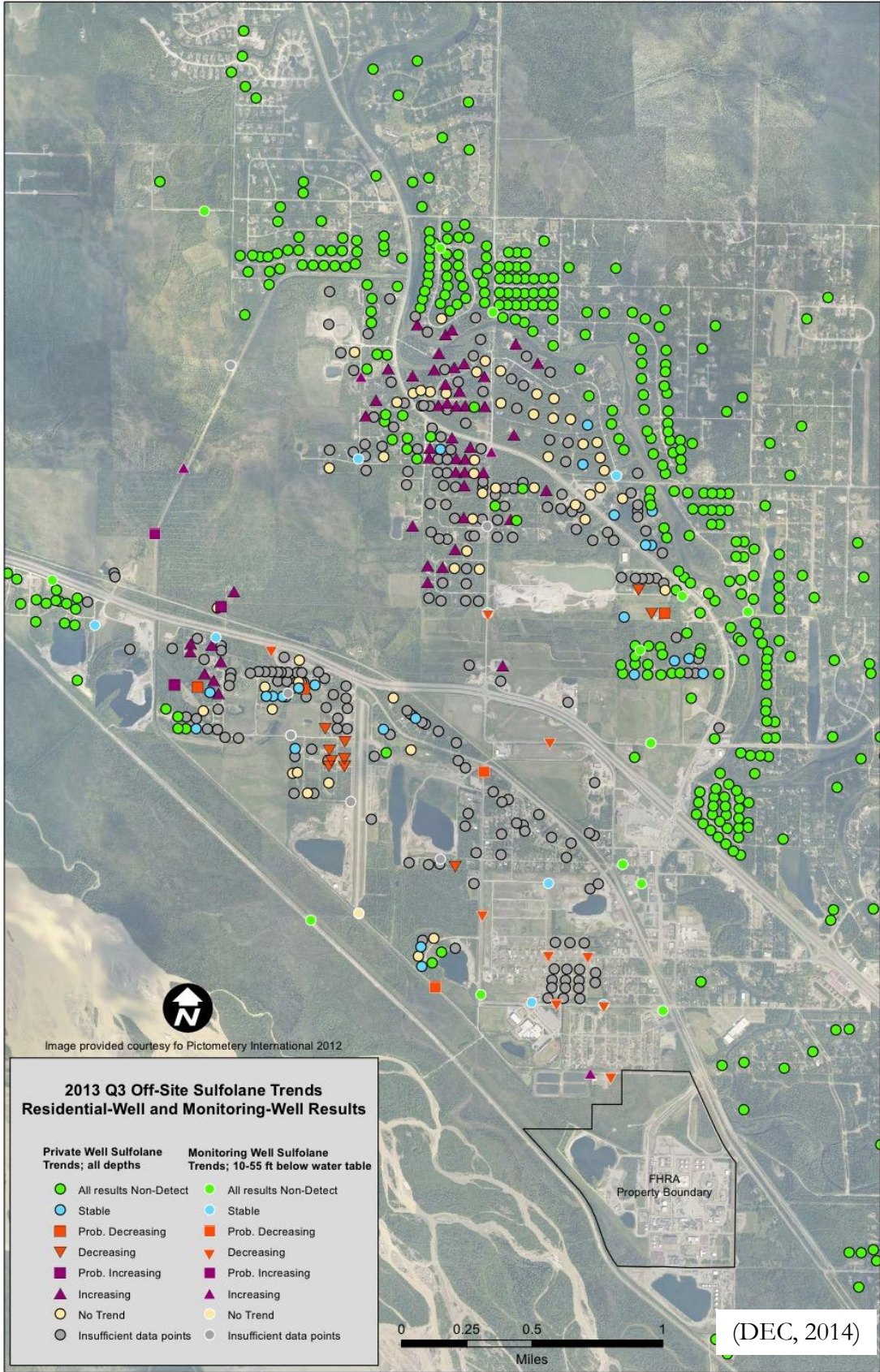
Notes:
 Sulfolane dataset displays the most recent sample collected
 Sample results span the time period between Fourth Quarter 2009 and Third Quarter 2013
 Image provided courtesy of Pictometry International 2012



FLINT HILLS RESOURCES ALASKA, LLC
 NORTH POLE REFINERY, NORTH POLE, ALASKA
THIRD QUARTER 2013
GROUNDWATER MONITORING REPORT
PRIVATE WELL SEARCH AREAS
AND SULFOLANE RESULTS



FIGURE
3-1



Appendix B. List of monitoring wells with data loggers.

Table B-1. Monitoring wells with HOBO U20 Water Level Data Loggers.

Well Id
MW-167A
MW-171A
MW-185A
MW-187
MW-190A
MW-194A
MW-191A
MW-166A
MW-168A
MW-182A
MW-189A

Table B-2. Wells with HOBO TidbiT v2 Temperature Data Loggers.

Well Id	Approximate Cable Length
MW-148A	10 ^A
MW-148D	145 ^A
MW-151A	10
MW-151C	67
MW-156A	10
MW-156B	32
MW-161A	12.5
MW-161B	47
MW-162A	10
MW-162B	62.1
MW-164A	10
MW-164C	55
MW-170A	10
MW-170C	129
MW-170D	45.92
MW-181A	12.6
MW-181C	146.8
MW-191A	10
MW-191B	57
MW-325-150	147
MW-325-18	10
MW-332-15	10
MW-332-150	150

A – measurement not recorded

Appendix C. Comparison of data logger temperature accuracy and resolution.

Table C-1. Comparison of temperature measurement accuracy and resolution from user manuals.

Measurement Device	Accuracy	Range	Resolution
HOBO® TidbiT v2 Water ¹ Temperature Data Loggers	$\pm 0.21^{\circ}\text{C}$	0°C to 50°C	12-bit resolution of 0.02°C at 25°C
HOBO® U20 Water Level ² Data Loggers	$\pm 0.44^{\circ}\text{C}$	0°C to 50°C	0.10°C at 25°C
YSI ProPlus Sensor ³	$\pm 0.2\% \text{ FS } \pm 1$	-10°C to 100 °C	0.1°C
YSI ProPlus Rugged Cables ⁴	$\pm 0.2^{\circ}\text{C}$ $\pm 0.3^{\circ}\text{C}^{\text{A}}$	-5°C to 70°C	NA
YSI 556 MPS ⁵	$\pm 0.15^{\circ}\text{C}$	-5°C to 45°C	0.1°C

A - cables over 45-meters

Additional product specifications can be found on the web.

Appendix D. Stable isotope laboratory procedure and collection procedure.

Collection of Groundwater Samples for Analysis of Stable Isotopes $\delta^{18}\text{O}$ and $\delta^2\text{H}$

Containers and Storage

- 20 mL disposable scintillation vials (provide). Plastic or glass is acceptable.
- No preservation or filtering required for samples.
- Avoid freezing samples.
- Samples can be stored at room temperature or in a cooler.

Collection from Monitoring Wells

- Purge well until groundwater is clear
- Record groundwater temperature
- Fill sample bottle with limited headspace
- Seal bottle tightly
- Label bottle with identification and date

Collection from Private and Public Wells

- Collect sample before any water treatment (eg. water-softening)
- Record groundwater temperature
- Fill sample bottle with limited headspace
- Seal bottle tightly
- Label bottle with identification and date

Pyrolysis Elemental Analysis-Isotope Ratio Mass Spectrometry (pyrolysis-EA-IRMS)

Pyrolysis-EA-IRMS system

$\delta^2\text{H}$ and $\delta^{18}\text{O}$ value are measured using pyrolysis-EA-IRMS. This method utilizes a ThermoScientific high temperature elemental analyzer (TC/EA) and Conflo IV interface with a DeltaV Mass Spectrometer. Prior to November 2013 the system utilized a ThermoScientific high temperature elemental analyzer (TC/EA) and Conflo III interface with a DeltaXP Mass Spectrometer. The pyrolysis reactor consists of a reaction tube packed with glassy carbon/graphite. Other TC/EA conditions are listed in Table 1.

Table D-1. TC/EA conditions.

Pyrolysis tube Temp	1400°C
He Flow rate	120 mL/min
GC column	3 m 5Å mol sieve
GC oven temp	55°C

Water/Liquid Analysis:

0.2 uL of water sample are injected into the TC/EA with a CTC Analytics A200SE liquid autosampler. The sample is pyrolyzed into H_2 and CO gases then separated chromatographically. These gases are then transferred to the IRMS, where the isotopes are measured. $\delta^2\text{H}_{\text{v-smow}}$ and $\delta^{18}\text{O}_{\text{v-smow}}$ values are reported in reference to international isotope standards. Samples are analyzed in a minimum 5 replicates. Values are reported in terms of the last 4 replicates.

Typical Quality Control scheme involves analyzing laboratory working standards every fifteen to twenty five replicate samples. Each sequence batch is calibrated using 4 International certified standards to confirm quality assurance. These calibrations are performed at the beginning, midpoint and end of the sequence. These standards are provided by Elemental Microanalysis Ltd. Standards are analyzed in replicate throughout the sequence.

Laboratory Working Standards

DMW-16May2002: Duckering building Millipore Water collected on 16May2002.

Certified standards:

Elemental Microanalysis Ltd. Okehampton, Devon EX20 1UB UK, Tel +44 1837 54446, microanalysis.co.uk : B2192 (Zero Natural Water), B2193 (Medium Natural Water), B2194 (Low Natural Water).

Alaska Stable Isotope Facility

Appendix E. Sample logs for stable isotopes.

Table E-1. Summary of monitoring well samples collected for stable isotope analysis.

Well Id	Screen Depth (feet bgs)	PF Depth (feet bgs)	Date Collected			
			13Q1	13Q3	13Q4	14Q1
MW-148A	15	—	3/2/13	7/9/13	10/11/13	1/21/14
MW-148C	56	—	NR	7/16/13	10/11/13	NR
MW-148D	151	152	3/2/13	7/9/13	10/11/13	1/21/14
MW-150A	12	—	NR	substituted	10/8/13	NR
MW-150B	24	—	NR	7/10/13	NR	NR
MW-150C	61	64	NR	7/10/13	10/8/13	NR
MW-151A	16	—	3/7/13	9/7/13	10/7/13	1/21/14
MW-151C	58	65	3/7/13	9/7/13	10/7/13	1/21/14
MW-152A	16	—	NR	8/27/13	10/8/13	NR
MW-152C	65	68	NR	8/27/13	10/8/13	NR
				7/10/13		NR
MW-153A	16	—	NR	7/15/13	10/11/13	NR
MW-153B	57	59	NR	7/15/13	10/11/13	NR
					3/1/13	NR
MW-155A	16	—	NR	7/11/13	10/9/13	NR
MW-155B	66	67	NR	7/11/13	10/9/13	NR
MW-156A	16	—	3/9/13	7/12/13	10/7/13	1/29/14
MW-156B	50	52	3/9/13	7/12/13	10/7/13	1/29/14
MW-158A	16	—	NR	7/16/13	S?	NR
MW-158B	61	65	NR	7/16/13	S?	NR
MW-159A	16	—	NR	7/17/13	10/9/13	NR
				9/10/13		NR
MW-159C	72	73	NR	9/10/13	10/9/13	NR
MW-160AR	16	—	NR	7/11/13	10/8/13	NR
MW-160B	91	91	NR	7/11/13	10/8/13	NR
MW-161A	16	—	3/2/13	7/2/13	10/15/13	1/20/14
				7/30/13		
MW-161-30			NR	7/2/13	NR	NR
MW-161B	50	—	3/2/13	7/30/13	10/15/13	1/20/14
MW-162A	16	—	3/1/13	9/11/13	10/9/13	NR
MW-162B	65	68	3/1/13	9/11/13	10/9/13	NR
MW-164A	16	—	3/1/13	7/8/13	10/12/13	1/9/14
					10/21/13	
MW-164B			NR	7/8/13	NR	NR
MW-164C	62	63	3/1/13	7/8/13	10/12/13	1/9/14
					10/21/13	

Well Id	Screen Depth (feet bgs)	PF Depth (feet bgs)	Date Collected			
			13Q1	13Q3	13Q4	14Q1
MW-165A	15	—	NR	9/11/13	10/2/13	NR
MW-165B	51	—	NR	9/11/13	10/2/13	NR
MW-166A	16	—	NS	9/11/13	10/2/13	NR
MW-166-30			NR	NR	10/2/13	NR
MW-166B	32	33	NS	9/11/13	NS	NR
MW-167A	16	—	3/1/13	9/11/13	10/4/13	NR
MW-167B	33	34	NR	9/11/13	10/4/13	NR
MW-168A	16	—	NR	9/5/13	10/8/13	NR
					10/5/13	NR
MW-168B	51	55	NR	9/5/13	10/8/13	NR
					10/5/13	NR
MW-169A	15	—	3/22/13		10/3/13	NR
MW-169C	60	69	3/22/13		10/3/13	NR
MW-170A	15	—	3/21/13	7/9/13	10/9/13	2/6/14
MW-170D	51	—	NR	7/9/13	10/9/13	2/6/14
MW-170B	75	—	NR	7/9/13	10/9/13	2/6/14
MW-170C	131	135	3/21/13	7/9/13	10/9/13	2/6/14
MW-171A	15	—	4/2/13	7/16/13	10/11/13	3/24/14
MW-171B	40	42	4/2/13	7/16/13	10/11/13	3/24/14
MW-181A	15	—	3/2/13	7/2/13	10/4/13	1/22/14
				9/5/13		
MW-181B	51	—	NR	9/5/13	10/4/13	NR
MW-181C	150	—	3/2/13	9/5/13	10/3/13	1/22/14
				7/3/13		
MW-182A	16	—	3/4/13	NS	NS	NR
MW-182B	45	46	NR	NS	10/5/13	NR
MW-183A	16	—	NR	NS	10/3/13	NR
MW-183B	60	59	NR	NS	10/3/13	NR
MW-187	17	—	3/21/13	7/8/13	10/4/13	2/27/14
MW-185A	16	—	NS	8/29/13	10/5/13	1/26/14
MW-185C	121	121	NS	8/29/13	10/5/13	NR
MW-190A	16	—	4/2/13	8/30/13	10/5/13	NR
MW-190BR	61	—	--	8/30/13	10/8/13	NR
				7/15/13		
MW-191A	15	—	3/6/13	8/30/13	10/2/13	2/3/14
MW-191B	60	—	3/6/13	8/30/13	10/2/13	2/3/14
MW-193A			NR	7/3/13	10/4/13	NR
MW-193B			NR	7/11/13	10/4/13	NR

Well Id	Screen Depth (feet bgs)	PF Depth (feet bgs)	Date Collected			
			13Q1	13Q3	13Q4	14Q1
MW-194A	16	—	NR	9/3/13	3/20/13 10/2/13	NR
MW-194B	39	39	NR	9/3/13	3/20/13 10/2/13	NR
MW-312-15	16	—	NR	NS	SD	NR
MW-312-50	50	50	NR	NS	SD	NR
MW-313-15	15	—	NR	8/28/13	12/10/13	NS
MW-313-150	150	—	NR	8/28/13	12/10/13	NS
MW-314-15	16	—	NR	7/3/13	10/3/13	NR
MW-314-150	151	—	NR	7/3/13	10/3/13	NR
MW-315-15	16	—	NR	8/19/13	SD	NR
MW-315-150	151	—	NR	8/19/13	SD	NR
MW-316-15	16	—	NR	7/17/13	10/7/13	NR
MW-316-56	56	57	NR	7/17/13	10/7/13	NR
MW-317-15	16	—	NS	8/27/13	10/11/13	NR
MW-317-71	71	—	NS	8/27/13	10/9/13	NR
MW-318-20	20	—	NR	9/7/13	10/3/13	NR
MW-318-135	135	—	NR	9/7/13	10/3/13	NR
				7/15/13		NR
MW-320-20	20	—	NR	9/1/13		NR
MW-320-130	131	—	NR	9/1/13		NR
MW-322-15	16	—	NR	7/6/13	10/3/13	NR
MW-322-150	151	—	NR	7/16/13	10/3/13	NR
MW-324-15	15	—	NR	8/19/13	12/10/13	NR
MW-324-150	151	—	NR	8/19/13	12/10/13	NR
MW-325-18	19	—	3/10/13	7/9/13	10/12/13	3/25/14
MW-325-150	151	—	3/10/13	7/9/13	10/12/13	3/25/14
MW-326-20	21	—	NR	9/3/13		NR
MW-326-150	151	—	NR	9/3/13		NR
MW-327-15	15	—	NR	9/5/13	SD	NR
MW-327-150	151	—	NR	9/5/203	SD	NR
MW-328-15	16	—	NR	8/30/13	10/3/13	NR
MW-328-151	151	—	NR	8/30/13	10/3/13	NR
MW-329-15	15	—	NR	7/3/13	10/4/13	NR
MW-329-66	66	67	NR	7/3/13	10/4/13	NR
MW-332-15	16	—	3/6/13	7/16/13	10/4/13	1/21/14
MW-332-150	151	—	3/5/13	7/16/13	10/4/13	1/21/14

Well Id	Screen Depth (feet bgs)	PF Depth (feet bgs)	Date Collected			
			13Q1	13Q3	13Q4	14Q1
MW-333-16	16	—	NR	9/3/13	NS	NR
MW-333-150	150	—	NR	9/3/13	NS	NR
MW-335-41	41	43	3/9/13	NS	NS	NR
MW-349-15	15		NR	NR	NR	3/26/14
MW-349-45	45		NR	NR	NR	3/26/14
MW-133	22	—	NR	7/21/13	11/7/13	NR
MW-147A	13	—	NR	7/25/13	NS	NR
MW-147B	26	—	NR	7/25/13	10/28/13	NR
MW-154A	76	—	3/18/13	7/17/13	10/17/13	NR
MW-154B	95	102	3/18/13	7/17/13	10/17/13	NR
MW-173A	15	—	NR	7/18/13	10/29/13	NR
MW-173B	151	—	NR	7/18/13	10/29/13	NR
MW-176A	15	—	NR	8/7/13	11/11/13	NR
MW-176C	90	—	NR	8/7/13	11/27/13	NR
MW-180A	15	—	NR	8/7/13	11/11/13	NR
MW-180C	90	—	NR	8/7/13	11/11/13	NR
MW-186A	15	—	NR	8/20/13	11/5/13	NR
MW-186E	76	—	NR	8/20/13	11/5/13	NR
MW-186D	135	—	NR	8/20/13	11/5/13	NR
MW-192A	15	—	NR	8/23/13	12/10/13	NR
MW-192B	56	—	NR	8/23/13	12/10/13	NR
MW-195A	15	—	NR	8/6/13	10/23/13	NR
MW-195B	150	—	NR	8/6/13	10/23/13	NR
MW-197A	66	—	NR	7/21/13	11/4/13	NR
MW-197B	150	—	NR	7/21/13	11/4/13	NR
MW-301-CMT-20	20	—	NR	7/31/13	10/16/13	NR
MW-301-70	71	72	NR	7/31/13	10/16/13	NR
MW-302-CMT-20	20	—	NR	8/28/13	10/14/13	NR
MW-302-CMT-50	50	—	NR	8/28/13	10/14/13	3/12/14
MW-302-110	110	110	3/22/13	8/28/13	10/14/13	3/13/14
MW-303-CMT-19	19	—	NR	8/8/13	10/15/13	3/13/14
MW-303-CMT-49	49	—	NR	8/8/13	10/15/13	NS
MW-303-130	131	130	3/22/13	8/8/13	10/15/13	3/13/14
MW-304-15	18	—	NR	7/30/13	11/18/13	NR
MW-304-70	71	—	NR	7/30/13	11/18/13	NR
MW-304-150	151	—	NR	7/30/13	11/18/13	NR
MW-305-CMT-18	18	—	NR	7/11/13	11/18/13	3/13/14
MW-305-CMT-38	38	—	NR	7/11/13	NR	3/13/14

Well Id	Screen Depth (feet bgs)	PF Depth (feet bgs)	Date Collected			
			13Q1	13Q3	13Q4	14Q1
MW-305-CMT-48	48	—	NR	substituted	11/18/13	NR
MW-305-CMT-58	50	—	NR	NR	NR	3/13/14
MW-305-100	100	110	3/22/13	7/18/13	11/18/13	3/21/14
MW-306-15	15	—	NR	7/18/13	10/17/13	NR
MW-306-80	81	—	NR	7/18/13	10/17/13	NR
MW-306-150	150	—	NR	7/18/13	10/17/13	NR

NS - Not Sampled

NR - Not Requested

S - Sampled, dates not entered

SD - Sample Damaged

Table E-2. Summary of private sub-permafrost well samples collected for stable isotope analysis.

Location Id	Date Collected				
	13Q1	13Q2	13Q3	13Q4	14Q1
#8	3/11/13	6/5/13	9/5/13	11/19/13	3/10/14
#2	4/4/13	6/19/13	NS	NS	NS
#15A-deep	3/21/13	6/13/13	9/12/13	12/4/13	3/24/14
#15A-shallow	3/21/13	6/13/13	9/12/13	12/4/13	3/24/14
#5	4/19/13	6/20/13	9/24/13	12/16/13	3/17/14
#16	3/25/13	6/12/13	9/10/13	12/9/13	NS
#12A	4/4/13	6/27/13	9/12/13	11/25/13	3/11/14
#12B	3/28/13	6/27/13	9/25/13	12/3/13	3/19/14
#12C	4/18/13	6/12/13	NS	12/16/13	3/11/14
#10	3/18/13	6/12/13	9/11/13	12/3/13	3/19/14
#15B	3/20/13	6/19/13	9/16/13	11/26/13	4/3/14
#13	3/12/13	6/6/13	9/11/13	11/26/13	3/3/14
#1-deep	3/17/13	6/20/13	9/5/13	11/21/13	3/3/14
#1-shallow	NR/NS	6/20/13	9/5/13	NS	NS
#18	3/12/13	6/4/13	9/26/13	12/2/13	3/24/14
#14	3/13/13	6/5/13	9/9/13	12/17/13	3/18/14
#9	3/18/13	6/5/13	9/11/13	11/25/13	3/10/314
#7	3/11/13	6/27/13	9/12/13	12/2/13	3/27/14
#6	3/20/13	6/13/13	9/10/13	11/21/13	3/13/14
PW-1230	NR	NR	NR	NR	5/1/14

NR/NS - Not Requested/Not Sampled

Appendix F. Groundwater temperatures at the water table.

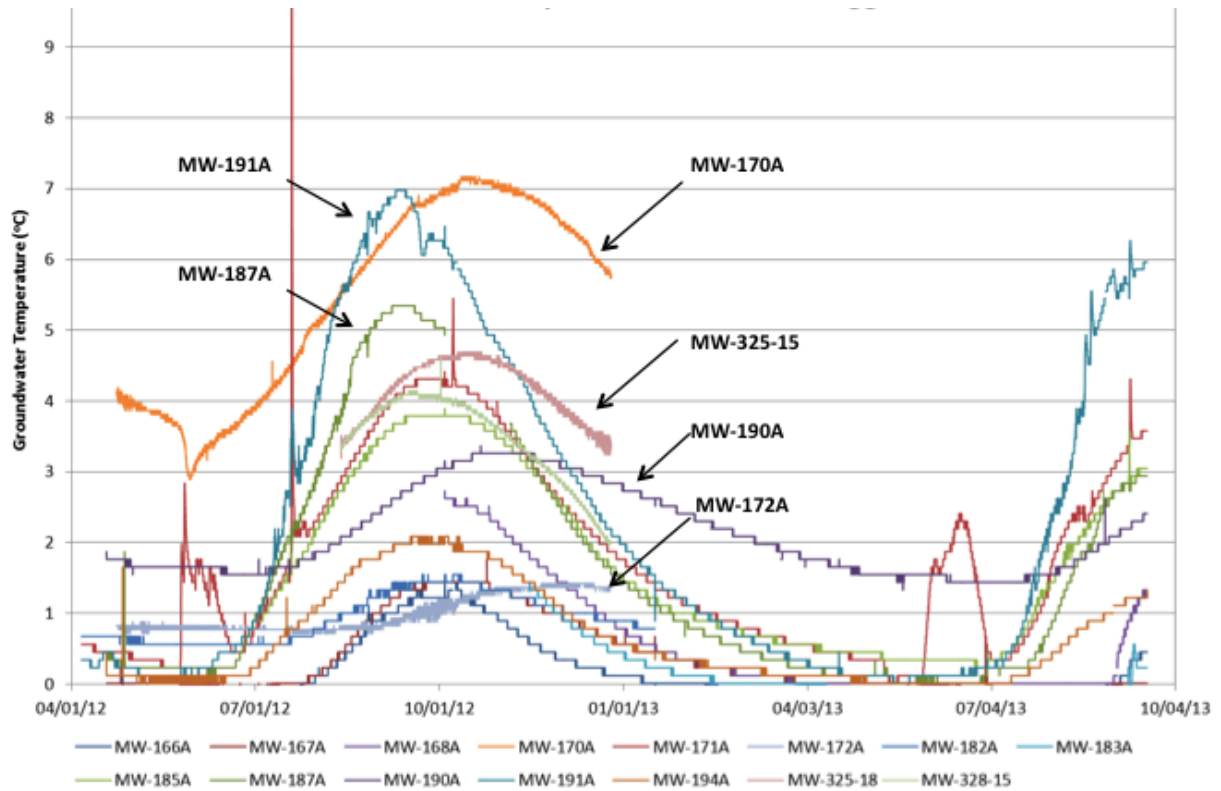


Figure F-1. Time series of groundwater temperatures at the water table. Data loggers recorded the temperatures represented in this figure. The coldest groundwater temperatures occur between May and July. Groundwater temperatures begin to warm up in July. Highest groundwater temperatures are seen between September and October. There appear to be two rates of groundwater temperature increase: rapid and gradual. The monitoring wells where a steeper curve is observed, rapid, typically have groundwater temperatures that peak in September. Groundwater temperatures that have a gradual increase typically have peak temperatures in October and have warmer temperatures through winter. Monitoring wells that have gradual temperature increases are located in areas of discontinuities, e.g., MW-172A, MW-190A, MW-325-15 along the Chena Slough. Monitoring wells that have more rapid increases in temperature are found above shallow permafrost or closer to the Tanana River, e.g., MW-187A and MW-191A.

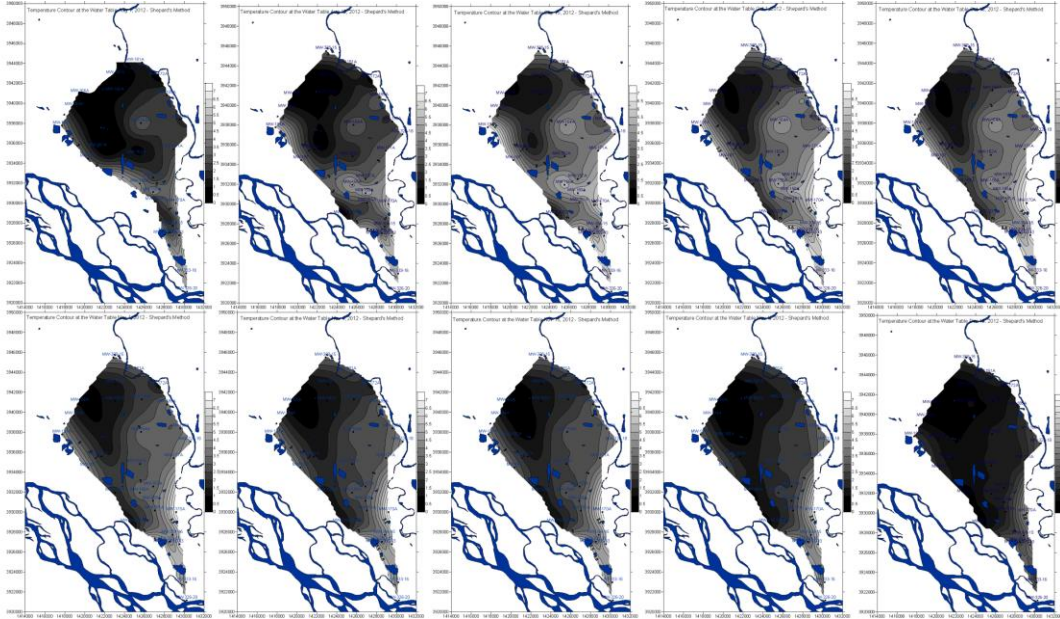


Figure F-2. Groundwater temperature contours at the water table recorded by data loggers. Seasonal trends represented from August 2012 (top left) to December 2012 (bottom right). Contours created using Modified Shepard's Method. Warmer temperatures are found along the Thirtymile and Chena Sloughs, as well as in the southern region near the Tanana River. Colder groundwater temperatures are found throughout the central and northwestern regions, this is consistent with shallow permafrost depths.

Appendix G. Summary of surface water stable isotopic composition.

Data for surface water isotopic composition is compiled in Table G-1. The data compiled was used for plotting and comparing groundwater values.

Table G-1. Stable isotope data for the Tanana and Chena Rivers and the Chena Slough.

Water Source	Isotope	Min	Max	Avg	SDev	n	Source and Year
Chena River at Fairbanks	$\delta^{18}\text{O}$	-23.3	-19.4	-21.6	± 0.83	53	Douglas et al., 2014 (2004-2006, 2008-2009)
	$\delta^2\text{H}$	-164.5	-147.9	-154.2	± 3.51		
Chena River at Fairbanks	$\delta^{18}\text{O}$	-22.05	-19.23	-20.19	± 0.53	152	Wooller et al., 2012 (August 2004-December 2005)
	$\delta^2\text{H}$	-164.87	-147.16	-153.45	± 3.22		
Tanana River at Fairbanks	$\delta^{18}\text{O}$	-24.17	-20.08	-22.35	± 0.71	163	Wooller et al., 2012 (July 2004 - December 2005)
	$\delta^2\text{H}$	-175.35	-158.18	-169.94	± 2.3		
Tanana River at North Pole	$\delta^{18}\text{O}$	-24.24	-23.43	-23.74	± 0.24	9	Data for this study (August 2013)
	$\delta^2\text{H}$	-178.68	-176.91	-177.83	± 0.53		
Chena Slough Surface water	$\delta^{18}\text{O}$	-23.03	-22.58	-22.83	± 0.23	3	Data for this study (July 2013)
	$\delta^2\text{H}$	-176.34	-170.69	-173.24	± 2.87		
Chena Slough Groundwater	$\delta^{18}\text{O}$	-23.89	-23.33	-23.67	± 0.30	3	Data for this study (July 2013)
	$\delta^2\text{H}$	-178.88	176.40	-177.92	± 1.34		

Min = minimum; Max = Maximum; Avg = average; SDev = standard deviation; n = number of times sampled

Appendix H. Supplemental stable isotope plots.

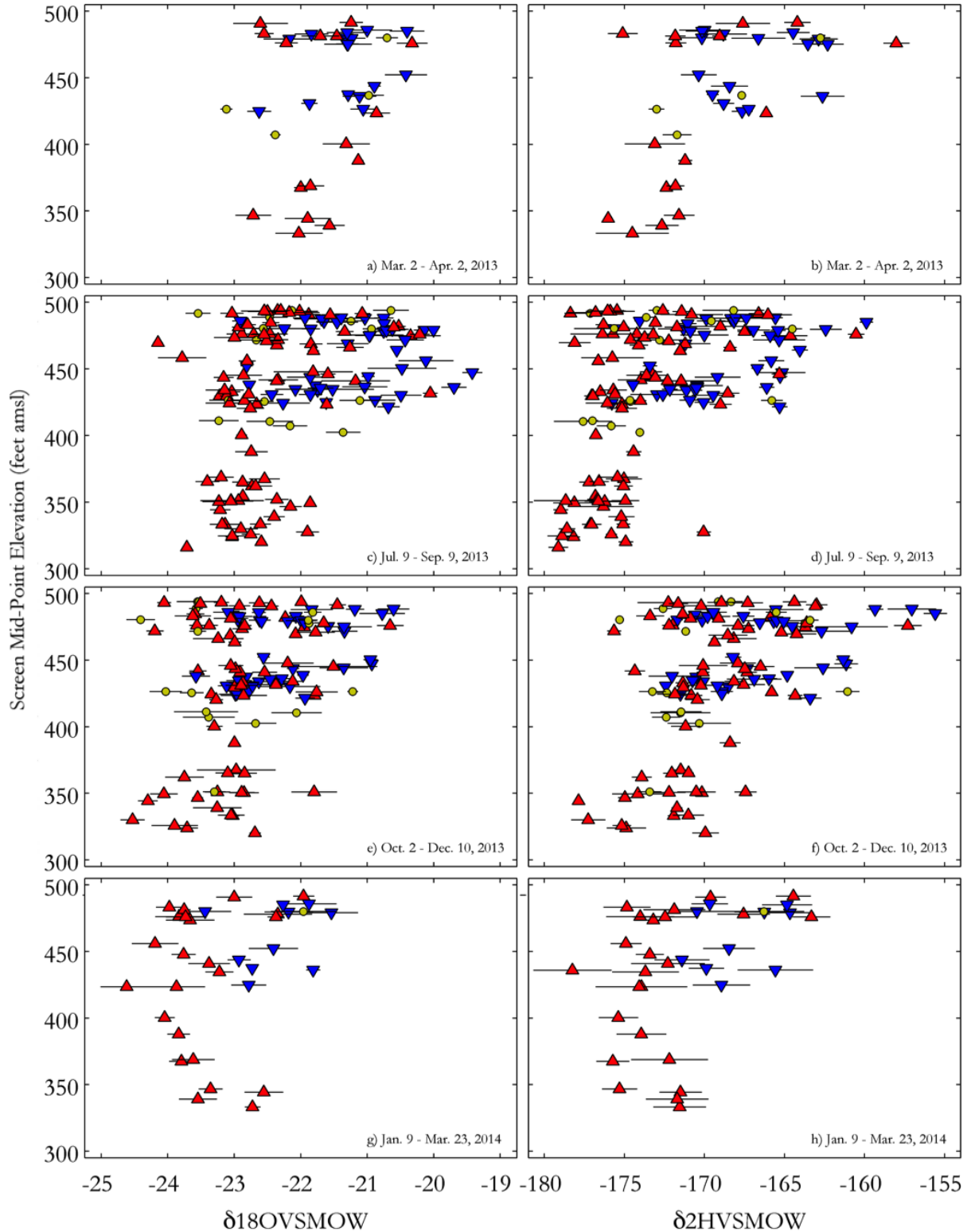
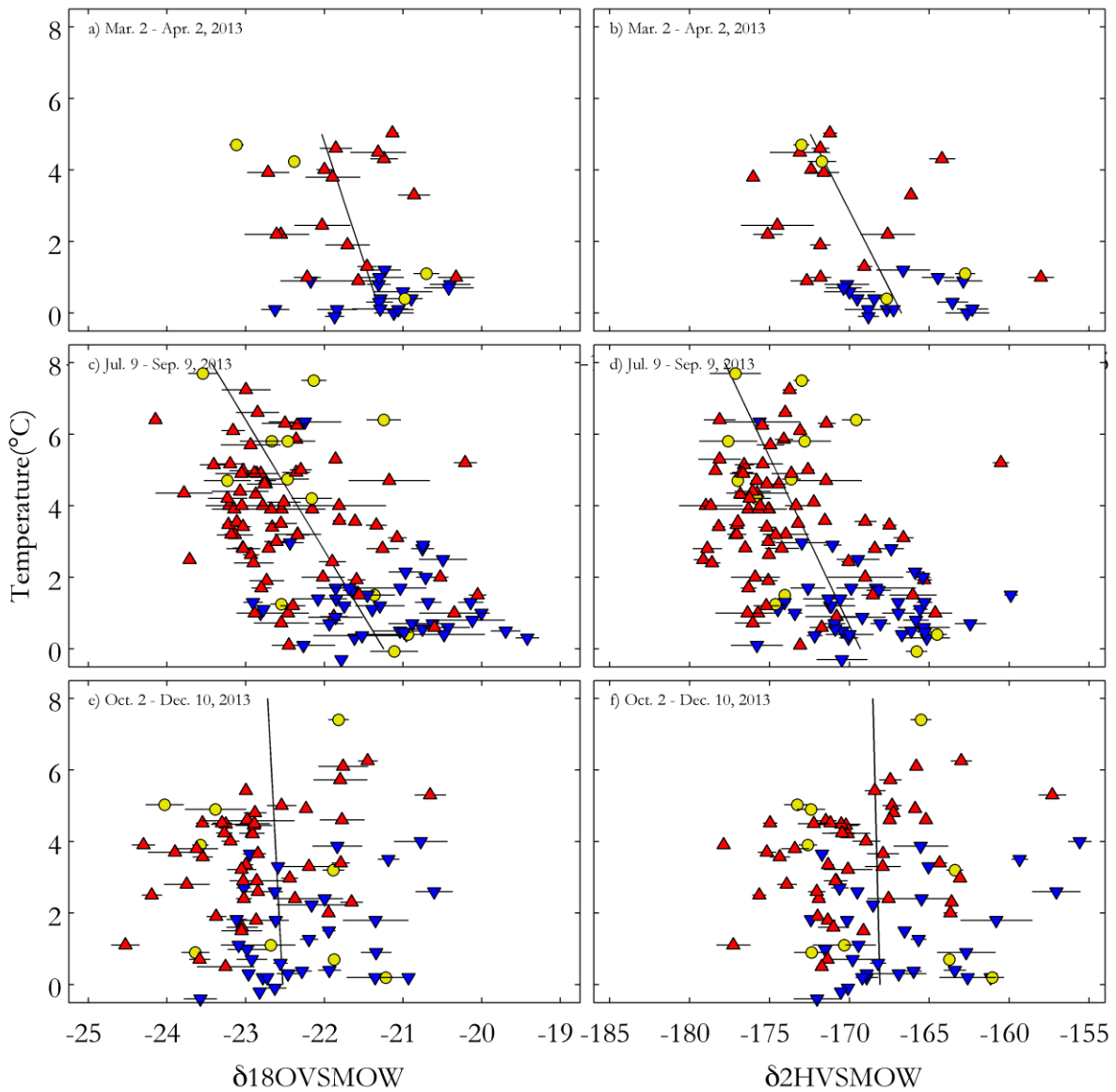


Figure H-1. Groundwater isotopic composition relative to screen-depth. For increasing temperature profiles: groundwater of deepest well is depleted in $\delta^{18}O$ and δ^2H , groundwater at mid-range wells is slightly more depleted, shallow wells span the range of isotope values. Groundwater for decreasing temperature profiles is less depleted in $\delta^{18}O$ and δ^2H for all depths.



- ▲ Increasing temperatures with depth
- ▼ Decreasing temperatures with depth
- Profile not determined

Figure H-2. Groundwater isotopic composition relative to groundwater temperature. The groundwater temperature values shown on this graph are those measured during field sampling. These temperatures are used for determining the general relation between isotopic composition and groundwater temperature. The values may not be accurate as discussed in Section 4.1.2. Generally for the spring and late summer events, more depleted groundwater is warmer and more enriched groundwater is cooler. During the fall event, temperature appears to be evenly distributed. Temperature data was not available for the winter 2014 data set.

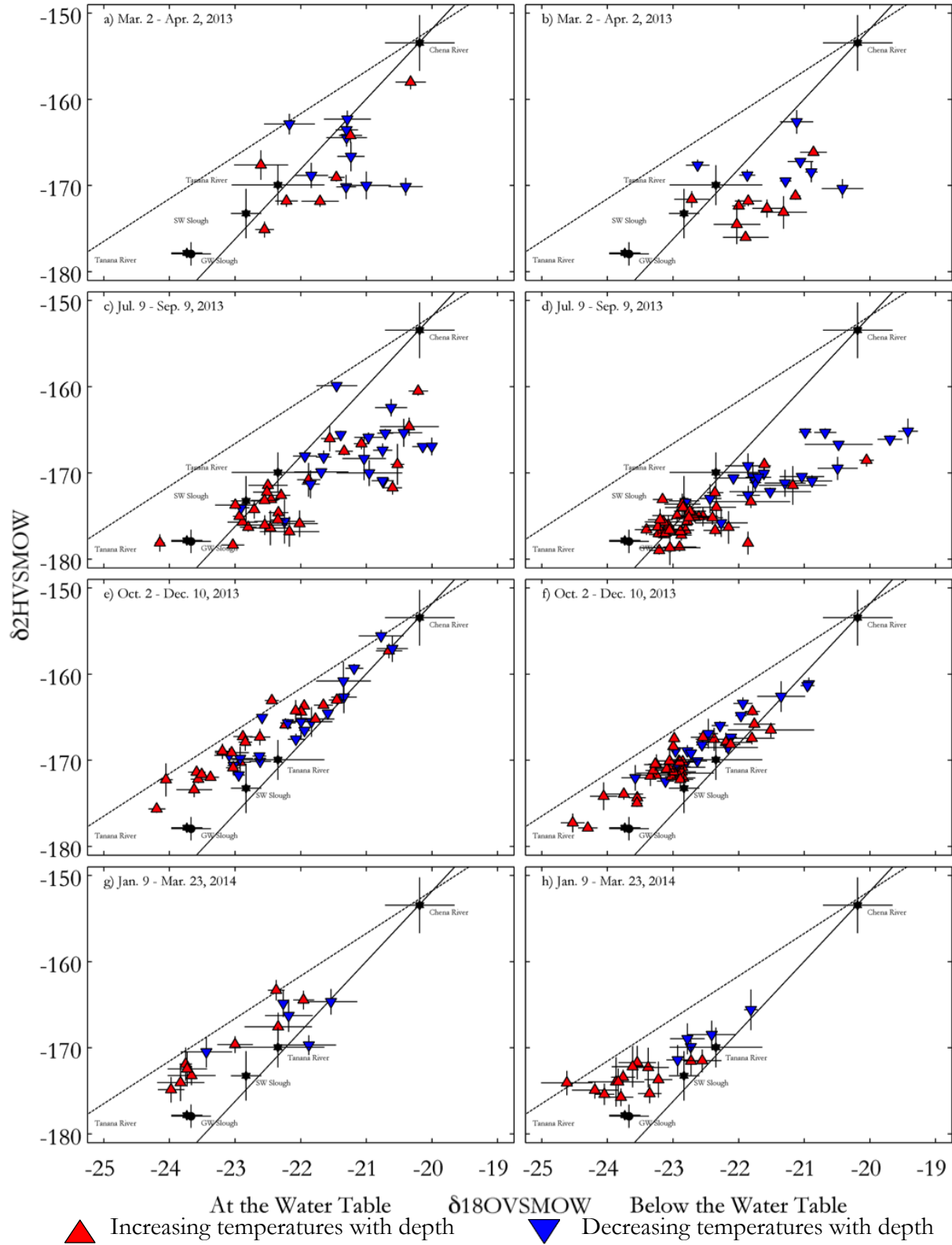


Figure H-3. Groundwater isotopic composition for all four monitoring well sampling periods. Analysis of 2013 sampling events (a-f) results is included in Section 5.3 and 6.5. Analysis of winter 2014 sampling event (g-h) is not included in thesis.

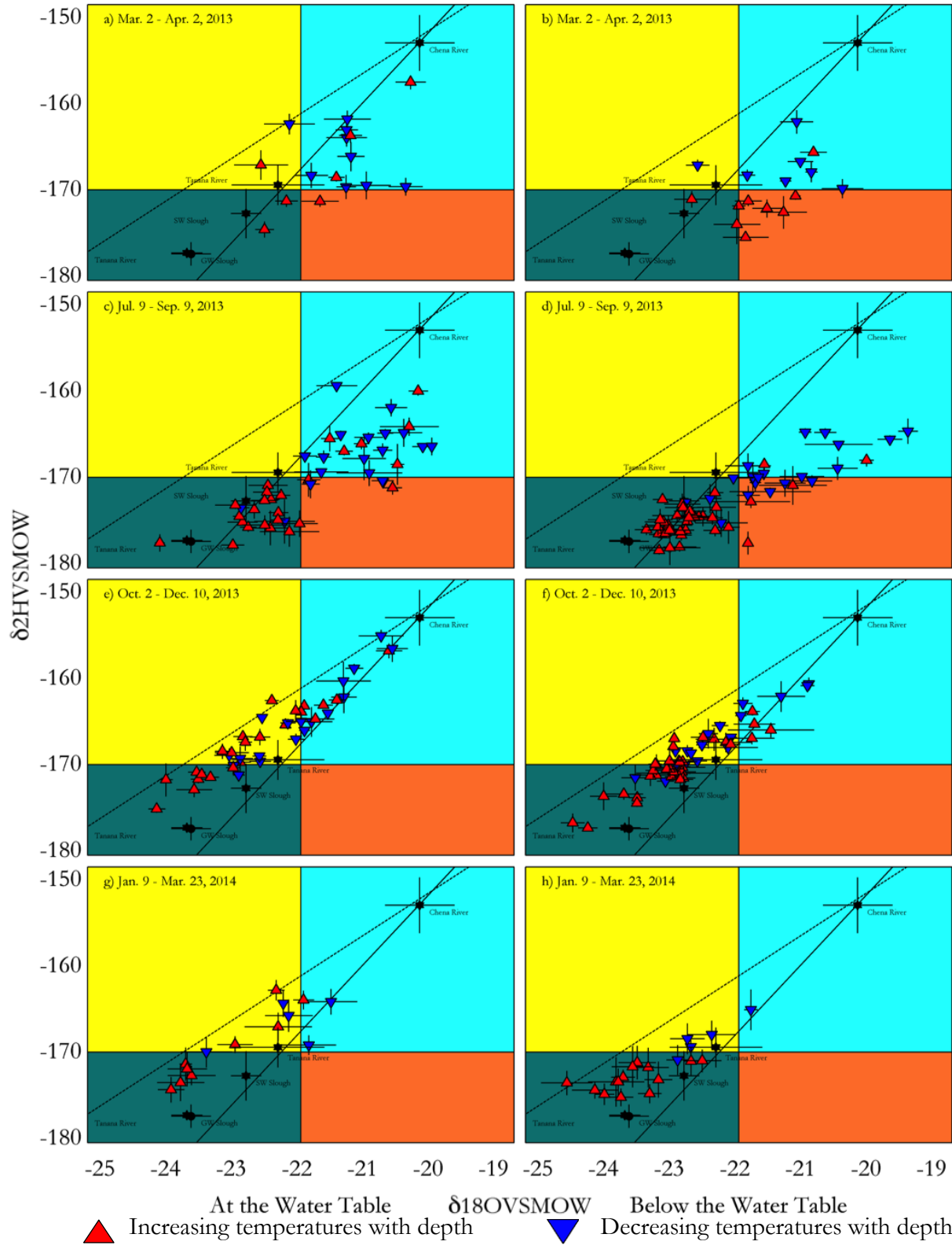


Figure H-4. Groundwater stable isotope trends for all four monitoring well sampling periods. Analysis of 2013 sampling events (a-f) results is included in Section 5.3 and 6.5. Analysis of winter 2014 sampling event (g-h) is not included in thesis.

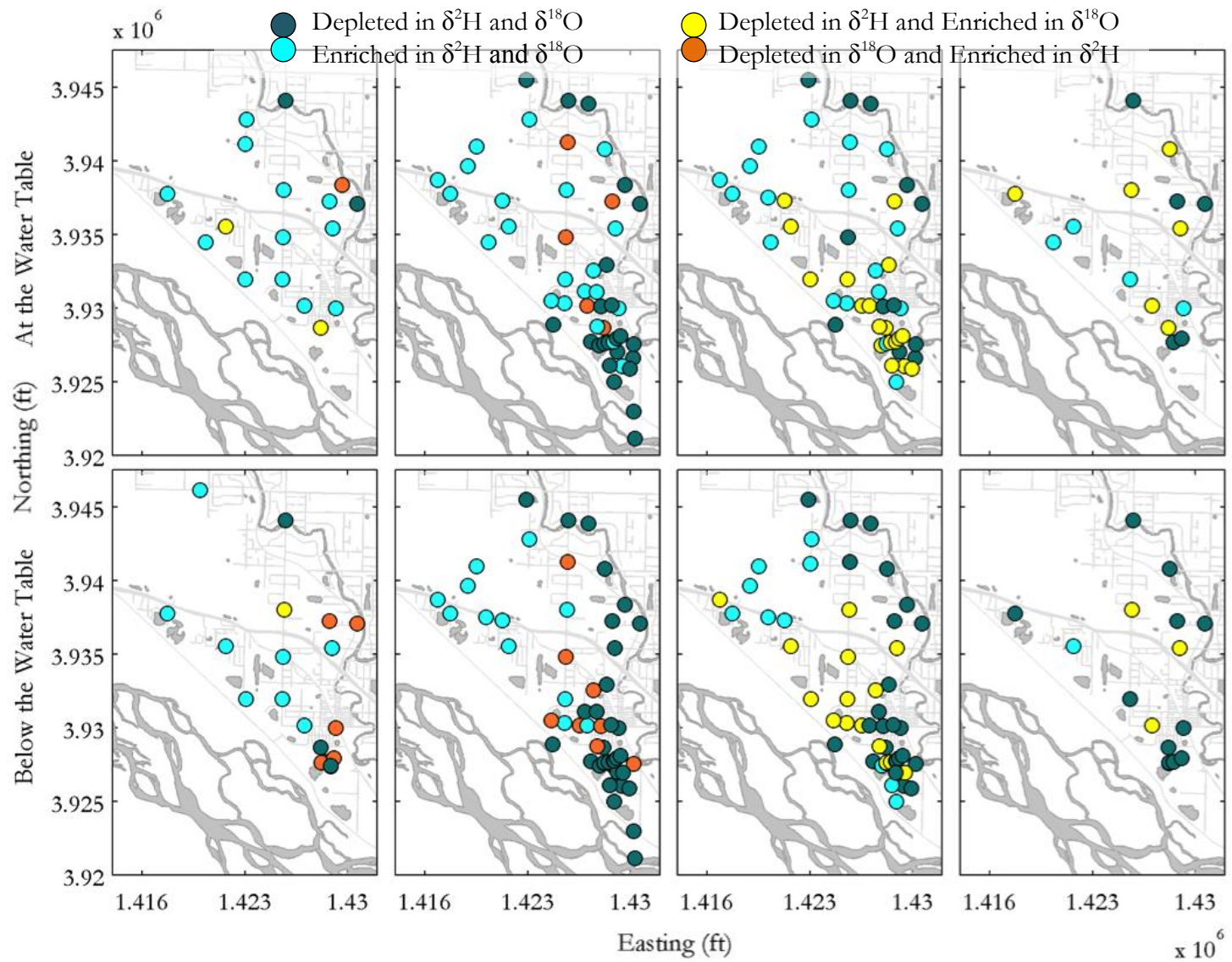


Figure H-5. Groundwater isotopic composition represented spatially for all for sampling events.
See Section 5.3 and 6.5 for discussion of spatial relations.

Appendix I. Extended study area figures for temperature profiles and stable isotopes.

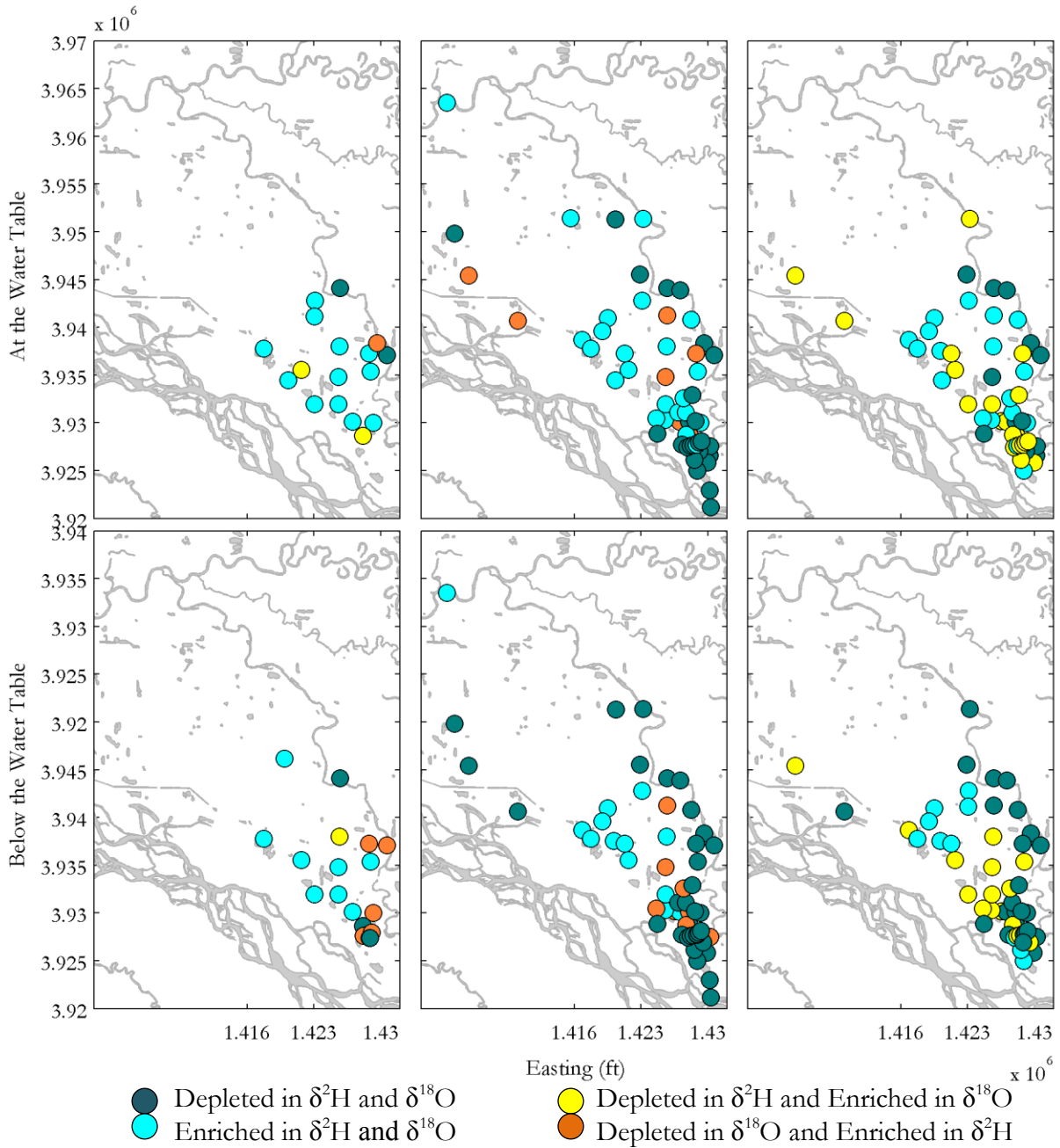


Figure I-1. Stable isotope trends for the extended study area, at and below the water table. Only 2013 sampling events considered. Depleted groundwater, below the water table, along the Chena Slough support temperature profile for a discontinuity. Chena River sample is consistent with surface water subject to meteoric influences. See Section 6.2 for further discussion.

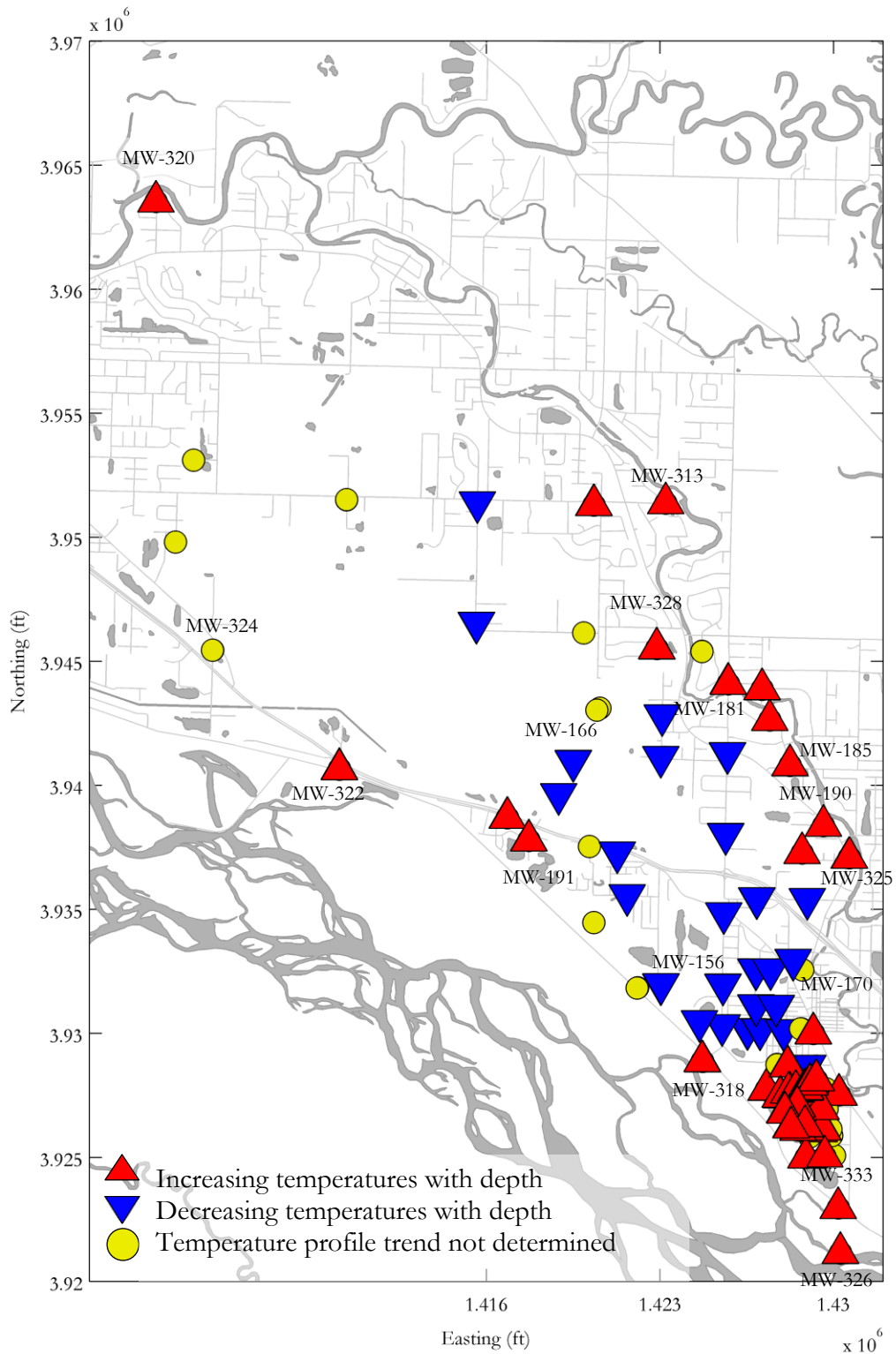


Figure I-2. Temperature profiles for the extended study area. Increasing temperature profiles are found downstream on Chena Slough and downstream on Tanana River, as well as on the Chena River. Increasing temperatures with depth indicate discontinuities in those areas. See Section 6.2 for further discussion.